ALMA MATER STUDIORUM – UNIVERSITÀ DI BOLOGNA

SCUOLA DI SCIENZE

A.A. 2020/2021

Corso di Laurea Magistrale in Analisi e Gestione dell'Ambiente

TESI DI LAUREA

in

Biocarburanti e Bioraffinerie

New path for thermochemical-biological conversion with a power-to-material approach

CANDIDATO

Andrea Facchin

RELATORE

Prof. Cristian Torri

CONTRORELATRICE

Prof. Francesca Soavi

Table of Contents

Abstract

Thermochemical-biological systems are based on the ability of thermochemical process to break down macromolecule to yield smaller ones, while bacteria can convert also complex substrates into valuable chemicals. In this thesis the possibility of a direct couple between pyrolysis and anaerobic digestion has been investigated for the purpose to produce Volatile Fatty Acids (VFA), considering also the possibility to provide extra hydrogen to enrich the value of the products. Firstly, a large characterization of the COD yield and chemical composition of pyrolysis products was made, revealing the conversion of more than 50% of biomass's COD into bioavailable chemicals. Secondly, three biotrickling bed reactors were developed with different filling materials, included biochar, and tested with and without hydrogen. Results suggest that biochar acted as a promoter for the biotransformation of pyrolysis products COD into VFAs, yielding 35% of conversion, meanwhile hydrogen had demonstrated the ability to stabilize higher yield of longer chain VFAs.

1 Introduction

1.1 Biorefinery concept

In the last decades, energy and chemical demand and supply increased worldwide, and consequentially, the use of petroleum products increased. Together with the energy and material supply problem, the consumption of fossil resources can be unsustainable in the long term and worsen the environmental issues related to emission greenhouse gas and consequential global warming. A potential candidate that can contribute to solving these problems is biomass, namely a short cycle organic material, suitable to be produced in large renewable amounts to substitute petrochemical derivatives. In this context, a biorefinery is a facility that produces fuels, energy, and chemicals by the conversion of biomass sources [1]. According to *Fernando et Al.* [1] "biomass consists of carbohydrates, lignin, proteins, fats, and to a lesser extent, various other chemicals, such as vitamins, dyes, and flavors" and can, at the end of the biorefinery transformation, give two types of products:

1. Low-Value High Volume (LVHV): products useful to produce energy and meet the energy supply-demand

2. High-Value Low Volume (HVLV): mainly chemicals, produced in small quantity but with a high market value

Accordingly to Van Dyen *et Al.* [2], biorefineries can be categorized into three types:

- Phase I: biorefinery that uses one feedstock and produces a single product (e.g. bioethanol from grain)

- Phase II: biorefinery that uses one feedstock but can produce several products (e.g. wet mill biorefinery)

- Phase III: biorefinery that uses several feedstock types and can produce different products

The capability to convert different feedstock (flexibility) and obtain a large array of products is intimately related to the use of different processes and technology. Also, in the biorefinery concept, the value of each stream must be maximized in order to reduce the production of waste and maximize the recovery of energy [3]. Although the phase III biorefinery is the more complex, it could be more efficient in terms of ability to cover the supply of energy, fuels, and chemicals.

1.2 Pyrolysis of biomass

Many different technologies have been developed in the lasts decades to allows the biorefineries to process a wider number of ores and to maximize the outputs yield, for this they can have biotic processes (as oxic and anoxic processes), abiotic processes, or, more often, both. Thermal treatments are very diffuse and enable the possibility to use a different source of complex biomass to get gas, liquid, and solid products. Pyrolysis is one of the straightest ways to breakdown the complex biomass into the smallest molecules and can be defined as thermal decomposition occurring in absence of oxygen. It can be applied to many different materials, in particular, the pyrolysis of biomass has been widely researched to obtain fuels and chemicals. The products of pyrolysis are:

- Biochar: carbon-rich solid which retains most of the feedstock ashes.
- Pyrolysis liquid, bio-oil, or pyro-oil: water, water-soluble, and water-insoluble condensable compounds

- Non-condensable gases: CH_4, CO_2, CO, H_2, and other light hydrocarbons (C_2-C_4)

The type and yield of products depend on different parameters such as type of biomass, the temperature in which the pyrolysis occurs, heating rate and heat transfer to the biomass, residence time of the gaseous phase in the reactor, or cooling time of the exiting gas [4]. Pyrolysis types can be divided mainly into two categories:

1. Fast pyrolysis (high temperatures, low residence time, high heating rate)
2. Slow pyrolysis (lower temperatures, higher residence time, low heating rate)

Slow pyrolysis enhances the production of biochar while fast pyrolysis allows a higher bio-oil and gas yield and, for this reason, it can be preferred as a method to breakdown the complex polymers of the biomass to produce smaller molecules that can be sent to other processes [5]. Biomass is mainly composed of cellulose/hemicellulose (carbohydrates) and lignin (aromatic polymer) with variable percentages depending on the biomass type. During the pyrolysis process, these macro-molecules are break up into smaller particles that can be further recombined or decomposed. Biochar is formed by rearrangements of the macromolecules into condensed polycyclic aromatics rings, mainly from lignin [6]. Non-condensable gases are formed during primary pyrolysis, charring, and secondary decomposition of larger compounds. The main gaseous components are carbon monoxide, carbon dioxide, methane, and hydrogen, with the minor presence of C_2-C_4 molecules. Pyrolysis liquid is composed of a large number of molecules, namely 14-30 %wt water and 70-86 %wt organic compounds [7]. Pyrolysis liquid includes hundreds of molecules: acids (e.g. Acetic Acid), sugars, anhydro sugars (e.g. levoglucosan), and aldehydes (e.g. hydroxy acetaldehyde) are formed from carbohydrate part; phenols, catechols, guaiacols, and other aromatic ones derive from lignin [8]–[14]. Although pyrolysis was often proposed as a direct method to obtain fuels from biomass, the process produces a liquid that is not suitable for use in actual engines without upgrading. This huge variety of chemical

functionalities in the final pyrolysis liquid represents a challenging issue in terms of analytical characterization and hampers the design of strategies for catalytic upgrading.

The key issue is that most chemical catalysts allow the transformation of reactants with comparable chemical properties into one or more products, whereas the upgrading of pyrolysis products requires the production of one or few defined compounds from reactants characterized by totally different chemical properties.

This task is challenging for chemical catalysis, but it worth noticing that, from a chemical perspective, is exactly what microorganism consortia routinely do in anaerobic environments (e.g. anaerobic digestion of organic matter). This simple deduction suggests a completely new bio-funneling approach for addressing the molecular diversity of pyrolysis products.[15].

1.3 Mixed Microbial Communities (MMC) for anaerobic digestion

The biological processes, in biorefineries, are often carried out by unicellular organisms (bacteria or yeasts) that can be single strains or mixed microbial communities (MMC). The MMC cultures offer some advantages: higher metabolic potential (potential use of mixed substrates), no sterilization required, and higher adaptability through ecological selection[16]. They are usually preferred when the substrate is more complex or slightly toxic, in fact they are commonly used for the commercial-scale fermentation of the biodegradable waste streams to produce valuable energy carriers such as methane [17]. The possibility to convert a complex substrate have, although, some limitation connected to the thermodynamics of fermentation and the biological limits. In a spontaneous reaction, the main driver is the Gibbs free energy (ΔG_r) and the difference between the reagents and the products must be negative. Moreover, even with largely negative ΔG_r , it does not mean that the biological reaction is feasible: the enzymatic pathway can be absent or inhibited, the reaction rate can be too slow or others reactions can compete with the biological catalyzed path [18]. For organic carbon anaerobic systems, the equilibrium is reached when the molecules with the lowest ΔG change per electron are produced, that is

when CH_4 and CO_2 are produced [19]. The elimination of the oxygen allows the production of final molecules that keep part of the initial energy since the oxidation is not completed. However, due to the actual low economic value of methane, in the last years, the attention was focused on the obtainment of other possible final products, especially chemicals [19]. Among the possible pathways in which anaerobic digestion occurs, there is the possibility to control the trend of the fermentation to obtain only a few valuable chemicals. In *Figure 1* (from *Kleerebezem et Al.*) the ΔG $(KJ*mol_e^{-1})$ of the main molecules involved in anaerobic fermentation is presented. Since the variation of free energy must be negative, the molecules with the lowest Gibbs Free energy per electron (at given conditions) are the most favorable products. Alcohols, Volatile Fatty Acids (VFA) are typical spontaneous products of anaerobic fermentation which can have high commercial value. Conversion of wastes into such chemicals allows to increase the profitability of the conversion and to cover a large array of drop-in applications (e.g. advanced biofuels, polymers, chemicals).

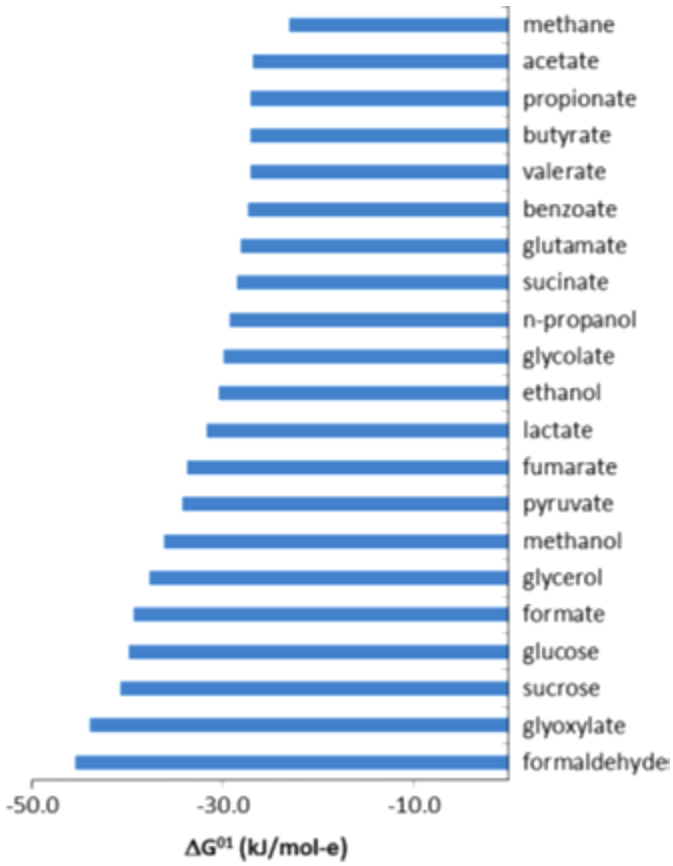

Figure 1. From Kleerebezem et Al. 2015 [19]

Pyrolysis produces a large number of completely different molecules, with the consequential high cost for the purification. Therefore a new alternative strategy for thermal-microbial conversion of biomass wastes was proposed [20]. Different research lines have focused on the toxicity of the bio-oil and some have tried to biologically treat the pyrolysis product or similar mixtures [21]–[25]. Two different approaches seem to outcrop: direct coupling of pyrolysis and MMC capable to address pyrolysis products (e.g. able to address toxicity and degrade pyrogenic compounds), or increasing selectivity of pyrolysis in order to enhance the fermentable fraction and avoid the high levels of toxic compounds. Given the complexity of pre-treatment and conditions required to increase the selectivity of pyrolysis (e.g. de-mineralization for an increase of anhydro sugars yield), the first pyrolysis "as-it-is" approach using a partially inhibited "*pyrotrophic consortium*" able to funnel pyrolysis product into

specific chemicals or intermediates, could be a relatively straight path for flexible biomass conversion system, as well as an extremely interesting new field of research

1.4 Effect of additional hydrogen supply on MMC

Recently hydrogen has attracted many interests as a possible source of clean energy, not only for fuels. Renewable electricity can be used to reduce hydrogen from water, obtaining molecular hydrogen which can be considered as a stock of the initial clean energy. Hydrogen, then, can be used in anaerobic digestion, as an easy way to provide clean energy and produce valuable chemicals and materials. For the carboxylic anaerobic digestion, hydrogen seems to favor the reversed ß-oxidation [26], [27], with an increased yield of longer VFAs. Also, it's possible to couple pyrolysis product digestion with an addition of hydrogen as an extra electron source, with the aim of a more easily degradation of the pyrolysis products more difficult to digest.

1.5 Chemical Oxygen Demand (COD) as a measure of chemical energy: definitions and rationale.

Understanding of hybrid thermochemical-biological processes requires a steep change in the view of pyrolysis processes. Since most pyrolyses studies aim to directly obtain a fuel, they are usually characterized in terms of average fuel proprieties (e.g. elemental analysis, HHV), neglecting details on molecular structures or bioavailability features.

The ambitious scope of this thesis is to obtain information necessary to provide some direct measurements required for design thermochemical-biological processes. To facilitate the connection of relatively distant research areas (as biology and chemistry), it is helpful to use a common unit of measure of chemical energy that should be easily applicable in both aqueous biological systems and thermochemical processes. The most widely used unit of measure of chemical energy is the tons of oil equivalent (toe) which corresponds to 41.85 GJ, which is used to compare oil, biomass fuels, and power sources in energy systems. Although helpful, such measure is

intrinsically "built around oil" and requires analysis (namely higher heating value or elemental analysis) that are difficult to perform in aqueous solutions, and this hampers its use for the abovementioned purposes. Borrowing approaches from the other fields, Chemical oxygen demand (COD) or theoretical oxygen demand, which is commonly used in wastewater treatment and monitoring of biological systems, is a direct and useful measurement of chemical energy in biomass or solutions (as COD concentration). 1 kg of COD (otherwise named 1 kgO) corresponds to a certain amount of organic matter that needs 1 kg of oxygen to be completely oxidized. From the theory, COD is proportional to the number of electrons that are transferred from water to organic molecules during biomass photosynthetic production. Due to the stoichiometry of redox reactions, 1 kg of COD corresponds, by definition, to 0.125 kmol of electrons packed into the energy-rich bonds of organic compounds by photosynthesis.[19] Both COD (due to stoichiometry) and higher heating value are linearly correlated to elemental compositions.[28] It follows that 1 kg of natural occurring COD typically contains about 15 MJ of chemical energy and can be transformed into heat, work (with a certain efficiency), or into a maximum of 1 kg of COD of chemicals or materials. The COD of common biomass feedstock ranges between 1 and 4 $kgO/kg_{feedstock}$ (COD of H_2 is 8 kgO/kgH_2) which are easily memorized. If a chemical or biological process produces a 100% COD yield, this means that the process is perfectly efficient. More in general, according to thermodynamic principles, biocatalysts allow to exploit paths that are within the limits of two fundamental rules, which can be summarized as follows:

1) The COD of reactants should be equal to the COD of products. Given that oxidant has negative COD (e.g. COD of oxygen = -1 gO/g, by definition) this assumption is valid in both anaerobic and aerobic systems.

2) In a thermodynamically closed system, namely in absence of energy input (e.g. light, electrical current), MMC catalyzes reactions towards thermodynamic equilibrium. The state of thermodynamic equilibrium for organic compound conversions is achieved when the compound with the lowest Gibbs energy is

produced. Since electrons are proportional to COD by definition, the most favorable "COD pathways" are those that foresee the largest Gibbs energy decrease per g of COD converted.[16] It is interesting to notice that almost all Pyrolysis products (apart elemental carbon and methane, which is the most thermodynamically stable product of fermentation) have enough negative $\Delta G_{COD ox}$ to allow the production of interesting chemicals like ethanol, butanol, or short-chain fatty acids. More specifically, the mixture of bioavailable condensable constituents (gas and water-soluble products) has a weighted average ΔG_{CODox} in the range between -14.3 kJ/gCOD and -15 kJ/gCOD. This value is more negative than those of most target fermentation products, like combined acetogenesis products (e.g. H_2 and acetic acid), butanoic or longer fatty acids, ethanol (-13.7 kJ/gCOD), and butanol (-13.4 kJ/gCOD). PyP can be transformed into products when Gibbs energy per gCOD decreases by more than 0.5 kJ/gCOD. This is valid with most of known PyP, which means that, on average, PyP have more energy-rich bonds than biological intermediates or most of MMC targeted chemicals

1.6 Aim of the Thesis

This research has the purpose to implement an experimental system suitable to investigate new thermochemical-biological pathways for conversion of biomass, waste, and renewable hydrogen to valuable intermediates.

Thermochemical-biological systems, in which biomass is pretreated through pyrolysis and thereafter digested in anaerobic conditions with hydrogen from hydrolysis of water, were investigated with the aim to obtain Volatile Fatty Acids, which represents a versatile biological building block, that can be used (biologically or chemically) to obtain valuable chemicals or materials (*Figure 2*).

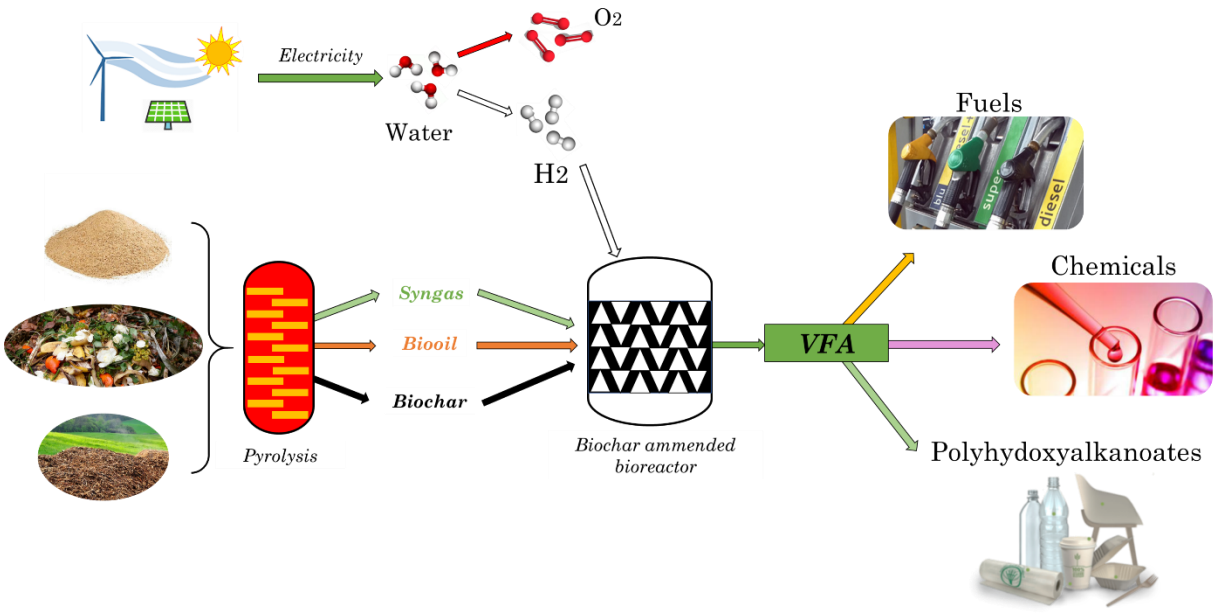

Figure 2

In this wide aim, three specific targets of this thesis were:

- To establish, with a newly developed analytical procedure, the exact partition of chemical energy into different pyrolysis products, namely gas, water-soluble substances, water-insoluble substances, and char. Shortly, the first aim of this thesis is to answer the question: "how much of feedstock chemical energy is converted fo bioavailable constituents?"
- Design, validate and test an experimental system for the study of anaerobic biodegradation of pyrolysis products in presence of hydrogen produced by electrolysis. This means a controlled system that can be feed with pyrolysis products (gas and liquid) and hydrogen and with acceptable COD closure (no leaks or losses)
- Use the validated experimental system to evaluate (in preliminary experiments) the bioavailability of different biodegradable fractions produced from pyrolysis and the effect of hydrogen supply on anaerobic conversion.

2 Methods

2.1 Analytical methods

In this chapter, all the methods used for this thesis are presented. The names of each analysis here reported are thereafter used as a reference to indicate the method further described.

2.1.1 Elemental analysis

Approximately 1 mg of solid sample was weighted inside a silver vial and analyzed in a Thermo Fisher Elemental Analyzer (Flash 2000), configured for solid samples with a copper/copper oxide column (flash combustion method). The instrument analyzes carbon, hydrogen, nitrogen, and sulfur percentage. Oxygen was determined by difference.

2.1.2 Gas analysis

10 mL of gas sample were collected with a syringe and injected in a GC-TCD 7820A using three packed columns placed in series (HAYASEP 80e100 mesh HAYASEP 0 80e100 mesh, and MOL SIEVE 5A 60e100mesh, from Agilent Technologies) with the following thermal program: 9 min at 50 °C, then 8 °C*min^{-1} to 80. Quantitation was performed using calibration with pure gases.

2.1.3 pH

pH was measured with a SI analytics Lab845 pH-meter.

2.1.4 Total COD

COD was measured by thermal oxidation at 1200 °C with detection of the oxygen consumption using a COD analyzer QuickCODLab (LAR Process Analyzer AG) following the ASTM D6238-98 method. After proper dilution, the sample was injected directly into the reactor where it was completely oxidized at 1200 °C under air/nitrogen flow and continuously analyzed with an O2 detector. The COD was calculated as g O_2 L^{-1} by comparison of signal areas (O2 consumption) with those of known standard solution of glucose. All analysis was performed in duplicate, with a percentual error threshold of 5%. Total COD analysis was performed by direct analysis of 100 µL. For soluble COD determination, 1 mL sample was centrifuged at 5000 RPM for 5 minutes. The soluble part was separated and 100 µL of it was injected in a LAR's COD analyzer QuickCOD calibrated with glucose standard solutions.

2.1.5 Volatile Fatty Acids (VFA) analysis

Volatile fatty acids (VFA) analysis was performed following method from *Ghidotti et Al.* [29] with slight modification. In a GC vial (volume 2mL): 100 µL of sample, 100 µL saturated solution of $KHSO_4$, 100 µL saturated solution of NaCl, 100 µL of 2-ethyl butyric acid at 1000 ppm in deionized water as Internal Standard, 1 mL of dimethyl carbonate (DMC) were added. The solution was hand-shaken and 1 µL of the supernatant was injected at 250 °C in splitless mode in a GC-7820A Agilent Technology coupled with MSD 5977E detector. Column type: DB-FFAP from Agilent Technology. The method starts from 50 °C for 10 minutes then 10°C*min^{-1} up to 250 °C without holding time. Detection was performed by MSD 5977E detector under electron ionization at 70 eV with full scan mode acquisition at 1 scan *s^{-1} in the 29-450m/z range. The response factors (RF) of the VFA were obtained from a standard solution prepared in

laboratory from pure VFA. RF and the concentration of the different analytes were obtained with *Equation 1* and *Equation 2*:

$$gCOD_x/_L = \frac{Area_x}{IS_{area}} * \frac{m_{IS}}{RF_x} * \frac{COD_x}{Sample\ Volume}$$

Equation 1

$$RF_x = \frac{A_x}{A_{IS}} * \frac{m_{IS}}{m_x}$$

Equation 2

When the RF of a substance was not known, a similar compound RF was applied.

2.1.6 Aldehydes

Aldehydes analysis was performed as Busetto *et Al.* [30] adapted to the purpose through liquid-liquid DMC extraction. Briefly, in a GC vial (volume 2mL): 100 µL of sample, 100 µL saturated solution of $KHSO_4$, 100 µL saturated solution of NaCl, 100 µL of 2-ethyl butyric acid at 1000 ppm in deionized water as Internal Standard, 1 mL of dimethyl carbonate (DMC) were added. The solution was mixed, and 0.500 mL of the supernatant was taken and mixed with 0.500 mL of methanol and some Amberlyst® (previously washed under methanol). The mixture was sonicated for 10 minutes and 1 µL was injected at 250 °C in spitless mode in a GC-7820A Agilent Technology with a DB-FFAP column from Agilent Technology. The method starts from 50 °C for 5 minutes then 10°C*min^{-1} up to 250 °C and holds for 10 minutes. Detection was performed by MSD 5977E detector under electron ionization at 70 eV with full scan mode acquisition at 1 scan *s^{-1} in the 29-450m/z range. The RF was determined from a solution of 1 g*L^{-1} of glycolaldehyde dimer from Sigma-

Aldrich. The chromatograms were integrated using TIC integration. RF was obtained with *Equation 1* and *Equation 2*.

2.1.7 Silylation

Aldehydes analysis was performed as Busetto *et Al.* [30]. In a GC vial (volume 2mL): 100 µL of sample were dried under nitrogen. In the vial were then added: 100 µL of N,O-Bis(trimethylsilyl)trifluoro-acetamide with trimethyl-chlorosilane (BSTFA), 100 µL acetonitrile, 50 µL of 3-chlorobenzoic acid as IS at 1000 ppm in acetonitrile, and 10 µL of pyridine. The solution was heated at 75 °C for 1.5 hours. After 0.5 mL of ethyl acetate was added in the vial and 1 µL was injected at 280°C in splitless mode in a GC-6850 Agilent with an HP-5MS column from Agilent Technology. The initial temperature was set at 50 °C for 5 minutes, then 10 °C*min^{-1} up to 325 °C held for 10 minutes. Mass spectra were recorded under electron ionization (70 eV) at a frequency of 1 scan*s^{-1} within the m/z 50–450 range. A standard solution for the main categories was prepared from Sigma-Aldrich pure compounds. RF and the concentration of the different analytes were obtained with *Equation 1* and *Equation 2*

2.1.8 HPLC-SEC

The sample was filtrated with a nylon 6-6 filter at 0.20 µm and 20 µL were injected with an Agilent 1200 series G1328B manual injector into an HPLC composed by an Agilent 1200 series TCC G1316A with PL aquagel-OH-20 column, an Agilent 1200 series DAD G1315D detector, and an Agilent 1260 Infinity II G7162A 1260 RID detector. Different standards of Poly-ethylene Glycol were prepared in water and analyzed to obtain a calibration (200, 400, 1450, and 3500 Da). The data were collected both in RID and DAD detectors.

2.1.9 Ash content

Approximately 1 g of sample was weighted in a calibrated ceramic vessel, previously dried at 550°C for 10 minutes. The sample was left at 550°C for 30 minutes and the residual material was weighted.

2.1.10 Moisture

Approximately 1 g of sample was weighted inside a calibrated ceramic crucible, previously dried at 105°C for 30 minutes, and was left to dry at 105°C for one hour. The sample was then weighted to determine the difference in weight.

2.2 Determination of the Potential Fermentable COD in Pyrolysis Products

Fir sawdust was selected as a model woody feedstock. Elemental analysis, moisture, and Ash content (Paragraphs 4.1, 4.10, and 4.11) were used to characterize the initial biomass. COD was then determined by elemental analysis using *Equation 3*:

$$\frac{gCOD}{g} = \frac{C}{12} * 32 + \frac{H}{2} * 16 - O$$

Equation 3

Where:

- *C*: is the %wt of carbon
- *H*: is the %wt of hydrogen
- *O*: is the %wt of oxygen

Different carriers (N_2 and CO_2) and pyrolysis chambers, namely 20 mm diameter (D20) and 50 mm (D50) were investigated. The functional scheme of the experimental apparatus and a short description of the components are shown in *Figure 3* and *Table 1* :

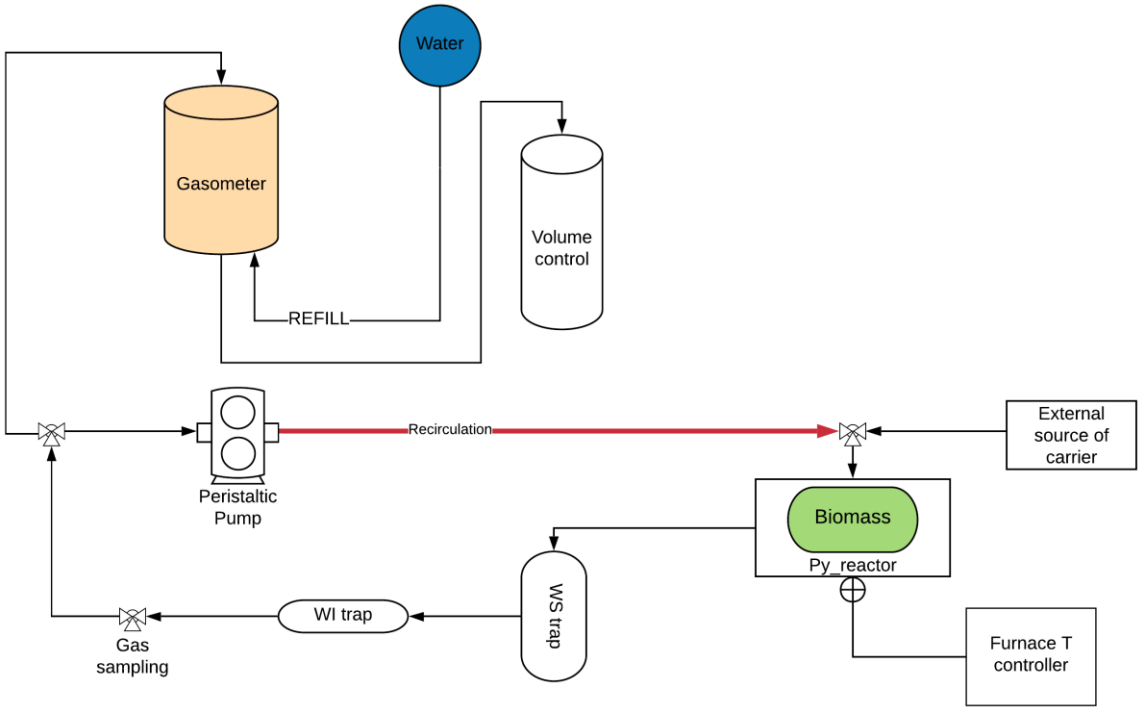

Figure 3. Experimental set up to obtain the pyrolysis COD yield

Table 1. Description of the pyrolysis experimental components

Component	Details
External source of carrier	N_2 99% or pure CO_2 source
Furnace T controller	Carbolite HST 12/300
Py reactor	Tubular quartz pyrolizer
WS trap	Quartz bubbler with 50 mL of distilled water at environmental temperature
WI trap	Quartz pipe with pressed cotton in one end
Gas sampling	Pierceable septum
Peristaltic pump	Watson Marlow, 100 series cased pump

Gasometer	Upside-down bottle used to collect the extra gas from the pyrolysis
Volume control	Graduated cylinder
Water	Tap water used to fill the gasometer bottle

The two pyrolizers used were:

- fixed bed quartz tubular reactor (TR) able to carry up to 5 g of biomass in an internal quartz vessel (D50)
- Fixed bed quartz tubular reactor with an internal quartz cylinder able to carry around 2.5/3.0 g of biomass (D20)

Both pyrolizers were externally heated by an electrical furnace (*Figure 4*). The pyrolysis procedure is here described:

1. Weighted biomass was placed in the sample holder (in the pyrolizer), then the system was closed.
2. Traps for Water-soluble and Water-Insoluble were prepared and connected
3. All the sealed system was preliminarily filled with 2 L (1 L/min for 2 min) of carrier gas, using an external source, leaving opened the gas sampling cap.
4. The system was switch to recirculation mode (no dilution) and a peristaltic pump was used for the gas recirculation, with a flow of 0.1 $L*min^{-1}$.
5. The sample was inserted in the hot zone and there left for the length of the experiment.
6. After the experiment, the sample was withdrawn from the hot zone and cooled. A gas sample was immediately taken for the GC-TCD analysis.
7. Once cooled down, biochar was weighted.
8. The solution in the WS trap (typically a turbid orange/yellowish solution) was drawn and used to wash the WI trap, this allows to filter the particles in solution from WS trap. The tubular reactor was washed with distilled water

and collected together with the WS solution, after filtration. The filtered solution obtained was defined as WS pyrolysis products

9. Acetone was used to wash the heavies WI in the glass walls (WS trap, pyrolizer, and pipes) and WI trap (cotton filter), thus allowed to obtain a dark brown solution which was evaporated overnight under N_2, yielding WI.

With the same procedure, different conditions were investigated:

1. Two steps, one hour each: starting at 350 °C for one hour then 13°C*min^{-1} up to 550 °C until the second hour (only with the larger pyrolizer)
2. One hour at 550°C (with both D20 and D50 different carrier gases)

Figure 4. On the right: larger fixed-bed quartz tubular reactor (D50); on the left: smaller fixed bad quarts tubular reactor (D20)

The gas produced was collected by means of a water displacement gasometer as those shown in *Figure 5, Figure 6,* and *Figure 7*.

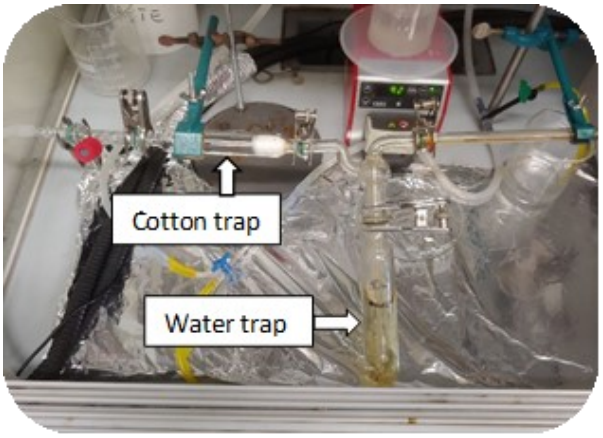

Figure 5. Water-soluble and water-insoluble traps

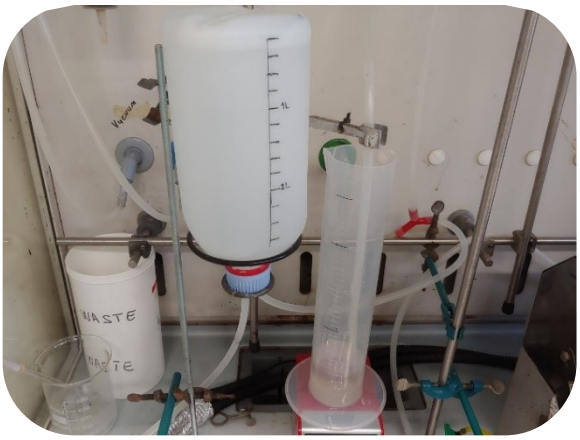

Figure 6. Hydraulic gasometer

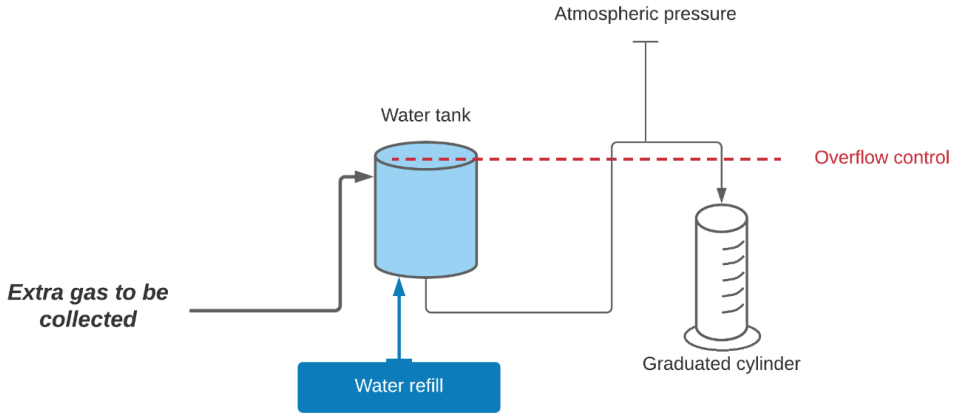

Figure 7. Scheme of the hydraulic gasometer

A U-shape pipe was used to retain water inside the gasometer maintained at atmospheric pressure. The gas produced was collected at the top of the gasometer, with the consequent spill of an equal amount of water in a graduated cylinder. Immediately after the pyrolysis, the gas analysis was performed to determine H_2, CH_4, CO_2, and CO. The COD of the mixture was calculated using *Equation 4* and *Equation 5*.

$$COD_{py\ gases} = \sum_{i=1}^{n} gCOD_{gas_i}$$

Equation 4

$$COD_{gas_i} = \%_{V\ gas_i}\ x\ V_{(reactors+gasbag)}\ x\ {}^{gCOD_i}/_{L}$$

Equation 5

Biochar was collected and weighted. The COD was determined with *Equation 6* using the average COD obtained from elemental analysis:

$$\%\ COD\ Yield_{Biochar} = \frac{m_{Biochar} * COD_{Biochar}}{m_{Biomass} * COD_{Biomass}}$$

Equation 6

WS yield of COD was determined with *Equation 7*.

$$\%\ COD\ Yield_{Water-Soluble} = \frac{Vol_{Final\ solution} * \frac{gCOD_{\ Water-Soluble}}{L}}{m_{Biomass} * COD_{Biomass}}$$

Equation 7

WI yield was determined with Equation 8:

$$\%\ COD\ Yield_{Water-Insoluble} = \frac{m_{Water-Insoluble} * COD_{Water-Insoluble}}{m_{Biomass} * COD_{Biomass}}$$

Equation 8

The yield of the fermentable compound was calculated with *Equation 9*:

$$\%COD_{fermentables} = \%COD_{WS} + \%COD_{WI} + \%COD_{H_2} + \%COD_{CO}$$

Equation 9

The analyses made are summarized in *Figure 8*. All the analysis methods can be found in *Chapter 2.1*.

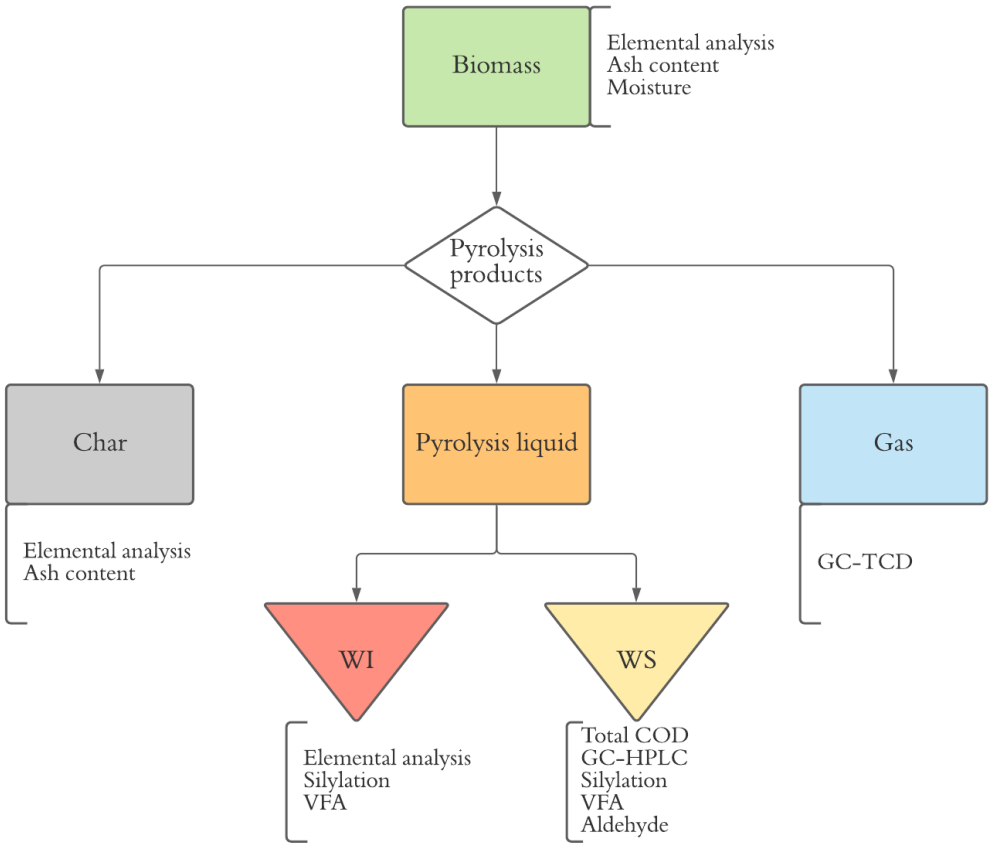

Figure 8. Scheme of the analysis for the pyrolysis products characterization

2.3 Anaerobic digestion of pyrolysis products and Hydrogen

From preliminary tests (Annex 5.1), Water-Insoluble component was not considered for the degradation tests. Biotrickling bed reactor was selected for the gas and liquid fermentation. Three reactors were built from a 0.5L Pyrex bottle, each with a cap built with four smaller tight pipe holder's caps (*Figure 9*). Two exits were used for the liquid recirculation and liquid sampling, one for the gas inputs and one for the gas sampling. Different filling materials were used for the reactors.

Figure 9. Four tight pipes holder cap

Liquid recirculation was made with a 220 L h^{-1} electrical centrifugal pump. The liquid was drawn from the bottom through a reinforced multi-layer pipe and pumped, through another multi-layer pipe, at the top of the reactor, where branched tees were used to sprinkle the liquid onto all fixed bed top surface. To minimize gas leaks, all multi-layer pipes were made with silicone pipe coaxially placed around the aluminum foil and polyamide pipe, as shown by *Figure 10*. Such pipe, as well as all fast-joint pneumatic valves used, were leak tested prior to the utilization. Leak tests were performed using hydrogen as test gas. The pipes were filled with the gas and the initial amount of hydrogen was detected by GC-TCD analysis. After one day the gas concentration inside the pipes was again analyzed to evaluate the leaks.

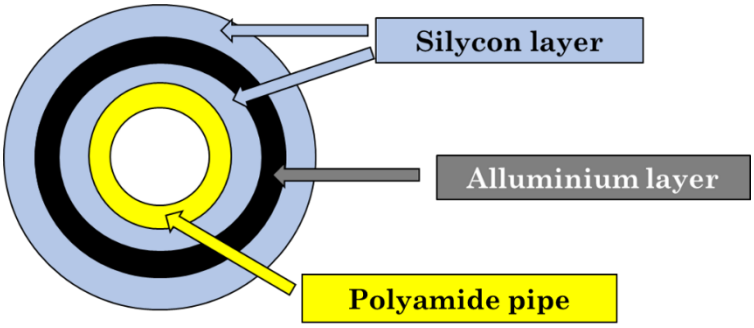

Figure 10. Section of the polyamide pipe upgraded to guarantee the tightness

Table 2 shows the effect of a multi-layer structure on the leaks of manufactured pipe, highlighting the large improvement obtained with the definitive configuration.

Table 2. Results of the leak test with different types of polyamide pipes

Info	***Delta time***	***Volume***	***H_2 variation***	***Air variation***	***H_2 leaks***	***Air input***
	h	*mL*	*%*	*%*	*mL/h*	*mL/h*
Simple pipe	16	6,2	-37,2%	29,6%	-0,1441	0,1147
Pipe upgraded	23,5	6,2	0,8%	-1,9%	0,0020	-0,0050

The temperature was controlled through a digital thermostat temperature controller (XD-W2308, DC 12V, accuracy: ±0.1°C), coupled with two electrical pads attached to the reactor glass wall. For the gas amount control and record, three digital gasometers were developed with Arduino Mega and an Ultrasonic Sensor HC-SR04, designed with *AutoCAD 3D®*, then printed in ABS with a *WASP 3D* printer (*Figure 11, Script in Chapter 5.2*).

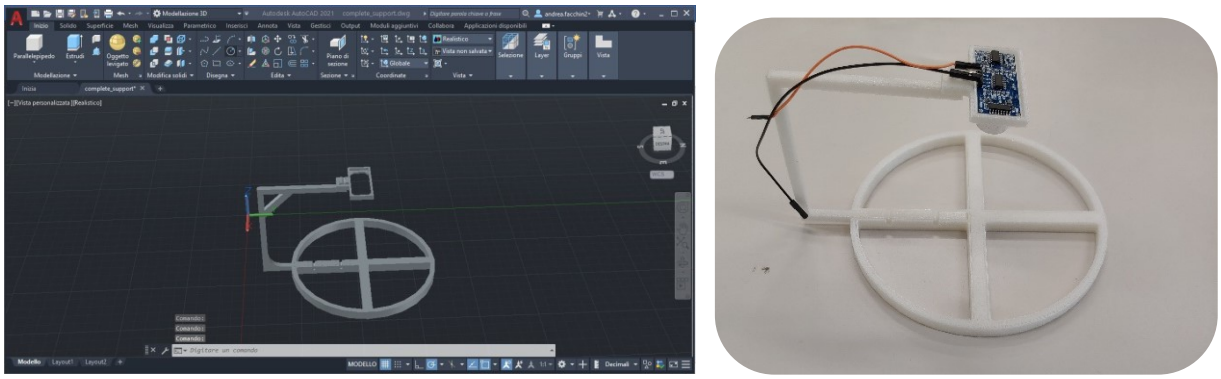

Figure 11. Digital gasometer developed with WASP 3D printer

Digital gasometers were calibrated up to 600 mL (*Figure 12*).

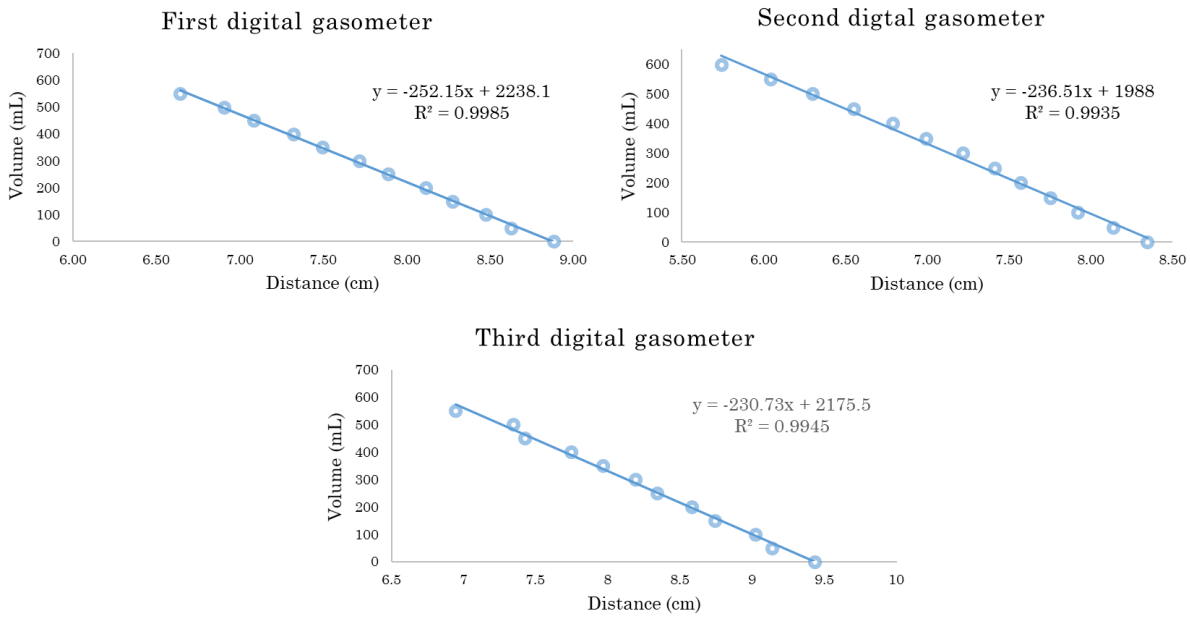

Figure 12. Calibrations of the digital gasometers

The final design of the reactor and the final disposition are shown in *Figure 13* and *Figure 14*. Due to the four caps configuration, the reactors were named "Tetrapods".

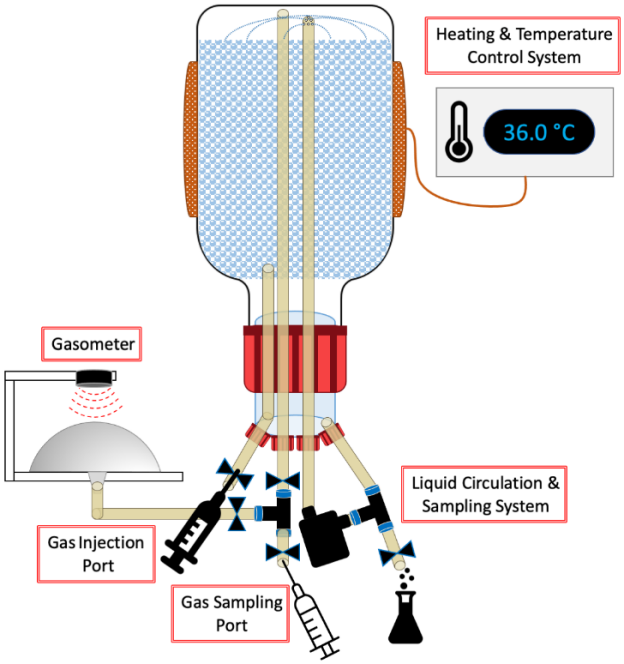

Figure 13. Final design of the "Tetrapod" reactor (From Yusuf Küçükağa)

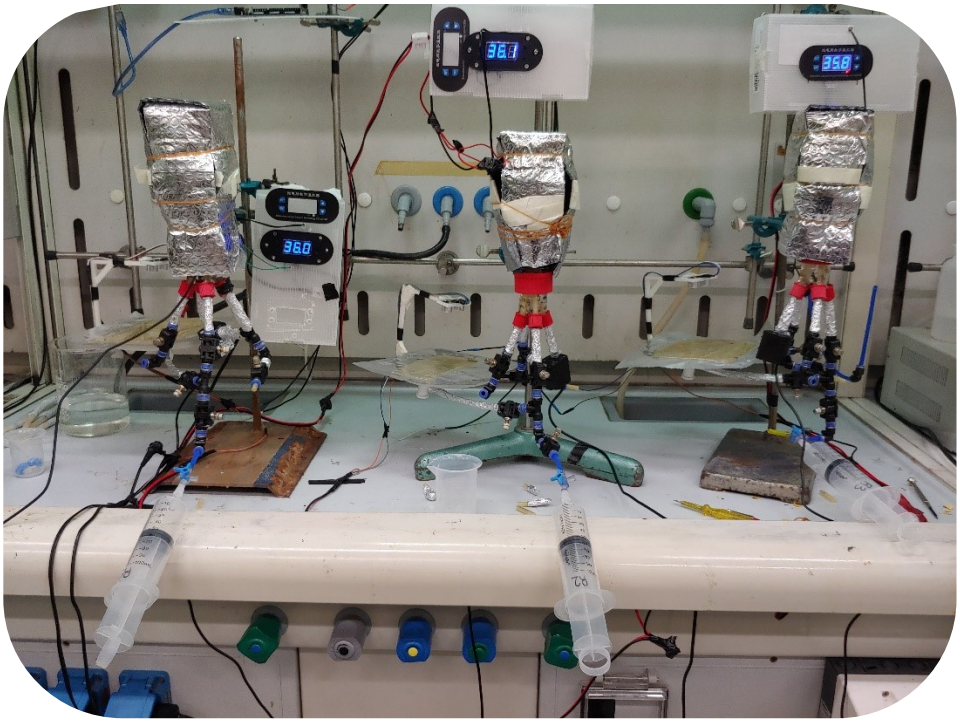

Figure 14. Final configuration of the Tetrapods

To leak test the reactors, they were filled with hydrogen (70% from initial analysis) and were left operating overnight, to evaluate the leaks. After one day the gas was analyzed, reviling the absence of leaks. The possibility to operate three reactors allowed to organize different experiments in different condition. The experiments carried are summarized in *Table 3*:

Table 3. Experimental design of the "Tetrapods". Glu=Glucose; Py=Water-Soluble and Syngas from pyrolysis; H_2 = Hydrogen addition; WS=Water-Soluble from pyrolysis.

Set	*Reactor 1*	*Reactor 2*	*Reactor 3*	*Conditions*
1	Py, 20 gCOD*L^{-1} + H_2	Py, 20 gCOD*L^{-1}	Glu, 20 gCOD*L^{-1}	*pH and methanogens not daily controlled*
Automatic Feeding system				
2	Py, 20 gCOD*L^{-1} + Biochar	Glu, 20 gCOD*L^{-1} + H_2 +Biochar	Glu, 20 gCOD*L^{-1} + H_2	*pH and methanogens daily controlled*
3	WS, 10 gCOD*L^{-1} + Biochar	Glu, 20 gCOD*L^{-1} + Biochar	Glu, 20 gCOD*L^{-1}	*pH and methanogens daily controlled*

For Set 1, the selected parameters for all the reactor are presented in *Table 4*:

Table 4. Set 1 Experimental Set-Up Parameters

Reactor Total Volume	621	*mL*
Glassball Bed Volume	288.4	*mL*
Total Number of Glassballs	1097	#
Total Surface Area of Glassballs Bed	2176.5	cm^2
Total Liquid Vol. in the System	200	*mL*
Total Headspace in the reactor	130	*mL*
Temperature target	36	*°C*

Digestion of pyrolysis products (Water-soluble and pyrolysis gas) was evaluated without daily control of methanogenesis and pH. Initially, the inoculum was thermically pretreated at 85°C for 60 minutes. The third reactor was fed with glucose, as a control. The target COD was 20 $gCOD*L^{-1}$ for all three bioreactors, with a total liquid amount of 200 mL for each reactor, weekly checked. Initially, all three reactors were fed with glucose to enrich the biomass inside. In R1 and R2 glucose was used as only feed for 6 days, then in five days a progressive quantity of pyrolysis products was provided (day 7: 7.5%, day 8: 25%, then 50% until the end of the enrichment phase). Semicontinuous mode between pyrolysis and bioreactor was selected. The pyrolyses were made with the same scheme described in *Chapter 2.2*, WS solution and gases were stored and analyzed as showed in *Figure 15*. Hydraulic retention time (HRT) selected was 10 days, with an organic loading rate (OLR) of 0.4 $gCOD*Day^{-1}$, including the feed solution, medium, extra liquids, and syngas. At the start-up, all the reactors were enriched in biomass, for one week, providing glucose. The pyrolysis products fractions of the OLD were composed of 90% WS and 10% syngas. For the reactors that also included hydrogen, extra COD was provided, starting with an extra 10% COD then gradually increased, to avoid total uptake. For all three sets, hydrogen was produced with a Hoffman's voltameter, filled with 4%wt of Na_2SO_4 solution, stored in a laminated gasbag. Daily, gas samples and 20 mL of liquid samples were taken and analyzed as described in *Figure 15* (analysis methods can be found in *Chapter 2.1*).

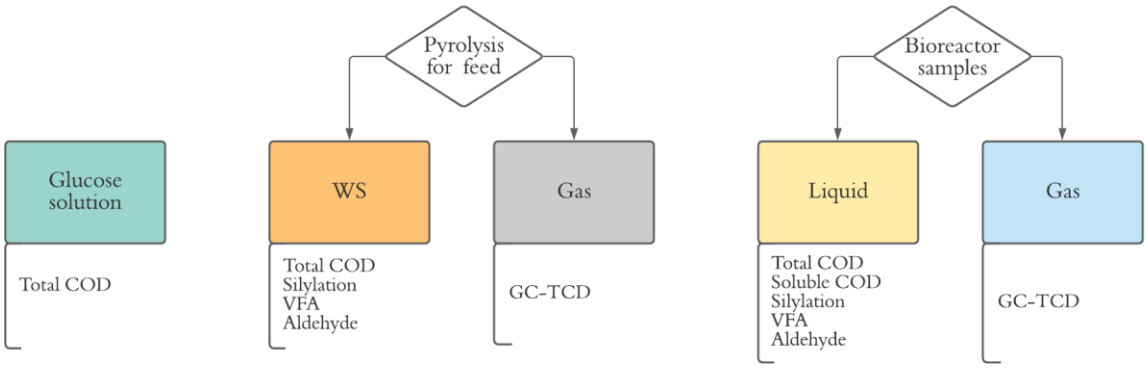

Figure 15. Analysis made during bioreactors experiments. All the analysis method can be founded Chapter 2.1.

For the weekends, on Friday were removed and added three times the volumes. The inoculum selected was a mixed consortium from an anaerobic digestor of agricultural wastes. Between the first and second Set, to avoid the stop of the experiment due to the Christmas pause, an automatic system was developed, with the control of the feeding, and the gas discharge with Arduino. The liquid level inside the reactors was maintained with a U-shape pipe. The scheme of the automatic feeding system is presented in

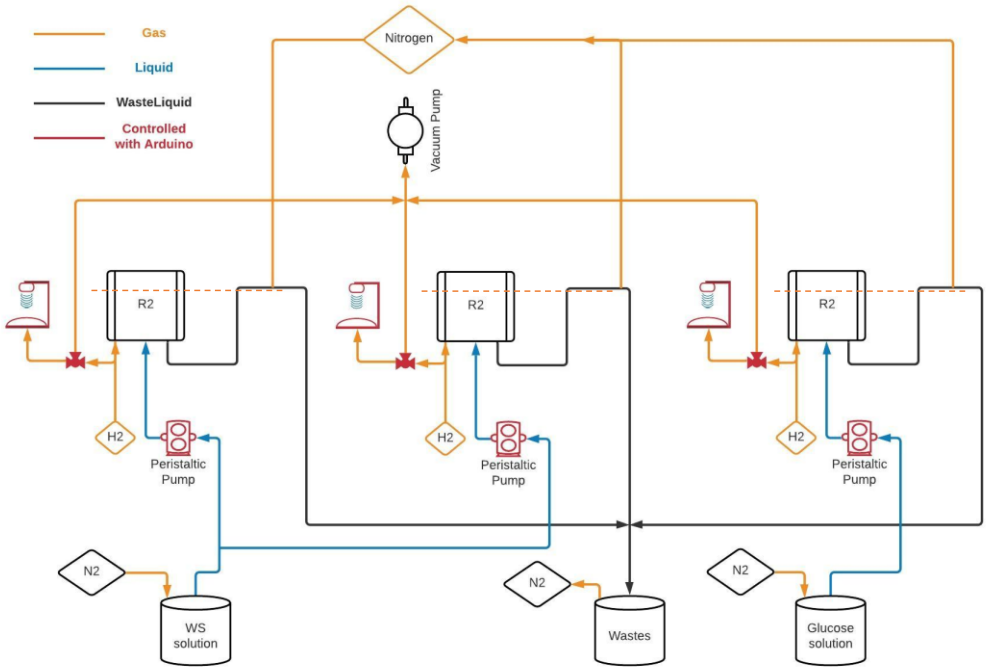

Figure 16, the Arduino script for the control of this system can be found in *Chapter 5.2*.

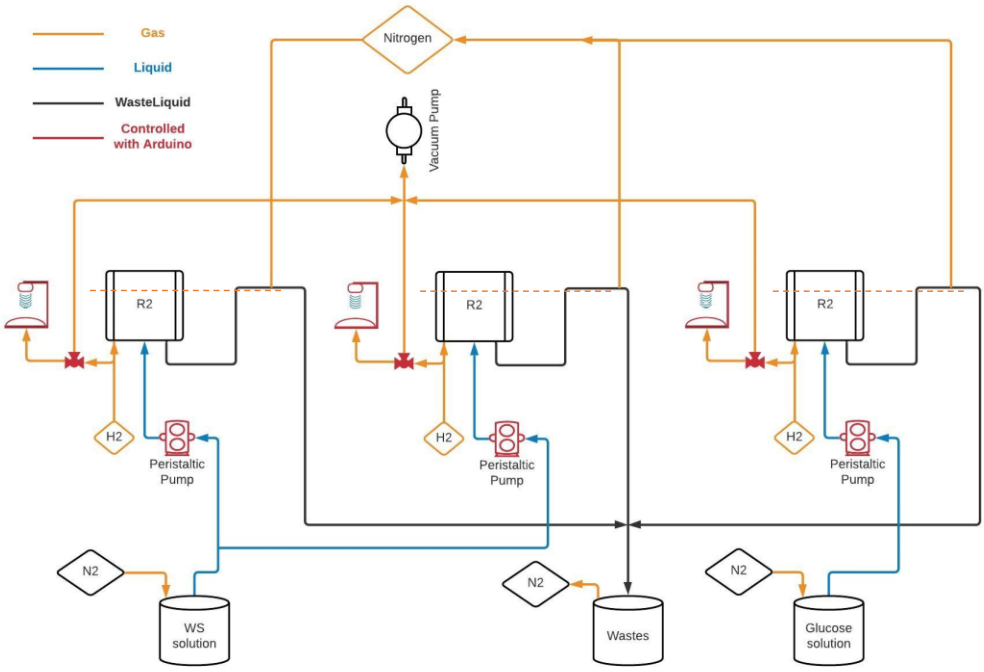

Figure 16. Scheme of the automatic feeding system developed

Set 2 was characterized by the control of pH and methanogens activity, providing 2-bromoethanesulphonate (BES). The first and second reactors were refilled, using an inoculated biochar to evaluate the possible detoxification effect. Biochar from orchard pruning pyrolysis (from Romagna Carbone) was added inside a mixed consortium inoculum sludge for 30 minutes, then filtrated and 100 g were added in the reactors. To prevent the recirculation of the biochar through the liquid pump, two layers of glassballs were added below the char, the first with 4 mm diameter glassballs (325 g) and the second with 7.8 mm diameter glassballs (200 g). The third reactor was left as Set 1 experiment. The liquid recirculation was shifted from continuous mode into a pulsing mode, using Arduino Mega and Elegoo IT-EL-SM-005 8 relay module, with 5 seconds of pumping and 15 of pause, for all the bioreactors (script in *Chapter 5.4*). All the other parameters for the conduction of the experiment were left equal, included the initial procedure of biomass enrichment with glucose. The first reactor, in the last ten days of the experiment was left in a "batch mode", in which no feed was provided, and 1 mL of liquid sample was daily withdrawn for the analysis. Set 3 experiments

lasted nine days. Reactor 2 and 3 were directly shifted into Set3 experiment, without any stop or reinoculation. Also, R1 was directly shifted and fed with only WS solution, providing micro reinoculations (1 $mL*Day^{-1}$) after 10 days. For the methanogens control, lovastatin effect was investigated instead of BES. Target COD was changed to 10 $gCOD*L^{-1}$ only for R1, as well as OLR fixed at 0.2 $gCOD*Day^{-1}$.

For each reactor of each set, a balance of input and output for one RT was done, together with the VFA yield in the output liquid. Daily variation of gases was tracked, considering the input and output of the system. Inside COD for each day was obtained knowing the total input, output, and COD of the previous day. The difference between the expected COD and measured COD of the liquid was daily calculated. pH trend was daily tracked. For Set 3, the analysis available for R1 was investigated to have a more comprehensive understanding of the degradation that occurred.

3 Results

3.1 Review of the pyrolysis products yield

As abovementioned, one of the aims of this thesis is to evaluate pyrolysis as a pretreatment to increase the bioavailability of organic material. Given that chemical oxygen demand (COD) is a direct measure of chemical energy of feedstock, this parameter was specifically targeted for the first time.

In order to define the characteristic of analytical procedure and to have a preliminary broad range for COD yields ($gCOD_{product}/gCOD_{feedstock}$), existing literature about pyrolysis (slow and fast) was used to obtain the characteristic COD partition among bioavailable (water-soluble and gas) and not-bioavailable (water-insoluble and char) pyrolysis products. Large literature available was firstly shortlisted, selecting papers in which both the accurate yield of pyrolysis products and adequate characterization of thereof (e.g. energy content of pyrolysis products) were performed. The selected studies focus on the lignocellulosic biomass, mainly wood sawdust and corn stalk. Both slow and fast pyrolysis were investigated evaluating the effect of temperature, reactor type, biomass, and heating rate. Not all the studies contain a complete mass balance, full energy repartition, nor the COD determination. Where that information where missing, data were back-calculated using:

- The theoretical amount of chemical oxygen demand (gCOD/g) from the other papers and stoichiometric calculation (from elemental analysis).
- Higher Heating Value (HHV, MJ/kg) of feedstock or products, then converted to COD through *Equation 10*.

$$\frac{gCOD}{g} = \frac{HHV\left(\frac{KJ}{g}\right)}{13{,}94\left(\frac{KJ}{gCOD}\right)}$$

Equation 10

3.1.1 Slow pyrolysis yield

Slow pyrolysis is typically associated with a higher mass yield of charcoal, due to the usually lower heating rate and high pyrolysis vapor residence time [4]. Several types of pyrolysis conditions (reactor, temperature, etc.) on similar biomass were considered, to reach wider data and to get a more comprehensive average in the results. The papers considered and the main information on the type of experiment are reported in the following Table 5:

Table 5. Main information of the selected paper for Slow Pyrolysis

Py Type	*Biomass*	*Reactor*	*T (°C)*	*carrier*	*Ref*
SLOW	Betula pendula	Batch reactor	450		[31]
SLOW	Betula pendula	Batch reactor	450		
SLOW	Betula pendula	Batch reactor	450		
SLOW	Corn stover	Horizontal screw-conveyer	450		[32]
SLOW	Corn stover	Horizontal screw-conveyer	450		
SLOW	Corn stover	Horizontal screw-conveyer	450		
SLOW	Corn stover	Horizontal screw-conveyer	550		
SLOW	Corn stover	Horizontal screw-conveyer	550		
SLOW	Corn stover	Horizontal screw-conveyer	550		
SLOW	Corn stover	Horizontal screw-conveyer	650		
SLOW	Corn stover	Horizontal screw-conveyer	650		

SLOW	Corn stover	Horizontal screw-conveyer	650		
SLOW	Beechwood	Updraft reactor	550	N2	[12]
SLOW	Beechwood	Updraft reactor	550	N2	
SLOW	Beechwood	Updraft reactor	650	N2	
SLOW	Cedrus deodara sawdust	Laboratory scale reactor	350	N2	[33]
SLOW	Cedrus deodara sawdust	Laboratory scale reactor	400	N2	
SLOW	Cedrus deodara sawdust	Laboratory scale reactor	450	N2	
SLOW	Cedrus deodara sawdust	Laboratory scale reactor	500	N2	
SLOW	Cedrus deodara sawdust	Laboratory scale reactor	550	N2	
SLOW	Cedrus deodara sawdust	Laboratory scale reactor	600	N2	
SLOW	Cedrus deodara sawdust	Laboratory scale reactor	650	N2	
SLOW	Panicum virgatum L	Laboratory fixed-bed reactor	300	N2	[34]
SLOW	Panicum virgatum L	Laboratory fixed-bed reactor	300	CO 2	
SLOW	Panicum virgatum L	Laboratory fixed-bed reactor	400	N2	
SLOW	Panicum virgatum L	Laboratory fixed-bed reactor	400	CO 2	
SLOW	Panicum virgatum L	Laboratory fixed-bed reactor	500	N2	
SLOW	Panicum virgatum L	Laboratory fixed-bed reactor	500	CO 2	
SLOW	Oak sawdust	Tubular reactor	400	N2	[14]

SLOW	Oak sawdust	Tubular reactor	500	N2	
SLOW	Oak sawdust	Tubular reactor	600	N2	
SLOW	Oak sawdust	Tubular reactor	700	N2	
SLOW	Calophyllum inophyllum wood bark	Fixed bed batch reactor	550		[13]
SLOW	Oak and beech sawdust pellets	Rotary kiln pyrolysis reactor	700		[35]
SLOW	Oak and beech sawdust pellets	Rotary kiln pyrolysis reactor	800		
SLOW	Oak and beech sawdust pellets	Rotary kiln pyrolysis reactor	900		
SLOW	Corn Stalk	Auger reactor	350		[36]
SLOW	Corn Stalk	Auger reactor	400		
SLOW	Corn Stalk	Auger reactor	450		
SLOW	Corn Stalk	Auger reactor	500		
SLOW	Corn Stalk	Auger reactor	550		
SLOW	Corn Stalk	Auger reactor	600		

Most of the studies considered provided an adequate characterization for biochar, gases, Water-Insoluble fraction (e.g. somewhat mentioned as tar), and Water-Soluble fraction. The average COD distribution for the slow pyrolysis is shown in Table 6:

Table 6. % COD Yield of Slow Pyrolysis

Slow Pyrolysis Results				
	Unit	Average	SD	COD Yield
Biomass	gCOD/g	1,29	0,07	-
Char	wt%	33,1%	9,1%	49,8%
	gCOD/g	1,94	0,10	
Liquid	wt%	39,9%	11,0%	32,8%
	gCOD/g	1,06	0,71	

WS	*wt%*	*18,2%*	*3,6%*	*20,0%*
	gCOD/g	*1.42*	*0.10*	
WI	*wt%*	*9,1%*	*1,6%*	*11,2%*
	gCOD/g	*1,60*	*0,17*	
Gas	wt%	27,4%	9,9%	5,0%
	gCOD/g	0,23	0,14	
Other-Loss				12,38%

Looking to COD balance, 50% of the chemical energy is partitioned into biochar, 33% ends up in the condensable liquid (20% into WS and 11% into WI liquid) and just 5% end up in pyrolysis gas (mostly carbon monoxide, hydrogen, and methane). For most of the slow pyrolysis studies a significant part of COD is missing (12%) suggesting that, especially with simple equipment used for slow pyrolysis, there is a significant entrance of oxygen in the system and/or product loss.

This COD partition reveals some interesting features that are not clear when yields are evaluated on a dry mass basis. First, even if analyzed papers reveal a 33% mass yield for biochar (which is in line with general pyrolysis literature [4]), the solids retain roughly half of the chemical energy processed by slow pyrolysis. The remaining part of chemical energy is partitioned into condensable products and, in minimal part, into gas. According to this data, even if slow pyrolysis is the simpler process, bioavailable compounds should be considered a "co-product" of char, which is clearly the main target of slow pyrolysis. Without considering losses, if we look to the relative abundance of bioavailable (WS and gas) and non-bioavailable volatile pyrolysis products (excluding char), the partition generally follows the holocellulose/lignin partition of feedstock. In conclusion, slow pyrolysis favors biochar formation without a significant effect on WS/WI ratio.

3.1.2 Fast pyrolysis yield

Fast pyrolysis is characterized by a higher mass yield of liquid products and a less mass yield of char and gas. For this reason, is widely studied to produce biofuels. According to Bridgewater [4], char and gas products should have an energy yield respectively of 25 and 5 % with an energy loss, due to the process heat requirement, around 15%. The papers considered and the main information on the type of experiment are reported in Table 7:

Table 7. Main information of the selected paper for Fast Pyrolysis

PY TYPE	BIOMASS	REACTOR	T (°C)	carrier	Ref
FAST	Southern pine sawdust	Auger-fed fast pyrolysis reactor	538	N2 or He	[37]
FAST	Southern pine sawdust	Auger-fed fast pyrolysis reactor	593	N2 or He	
FAST	Southern pine sawdust	Auger-fed fast pyrolysis reactor	649	N2 or He	
FAST	Southern pine sawdust	Auger-fed fast pyrolysis reactor	704	N2 or He	
FAST	Southern pine sawdust	Auger-fed fast pyrolysis reactor	760	N2 or He	
FAST	Southern pine sawdust	Auger-fed fast pyrolysis reactor	816	N2 or He	
FAST	Quercus alba	Entrained flow reactor	500	N2	[8]
FAST	Pinus strobus sawdust	Bubbling fluidized-bed reactor	400	N2	[38]
FAST	Pinus strobus sawdust	Bubbling fluidized-bed reactor	500	N2	
FAST	Pinus strobus sawdust	Bubbling fluidized-bed reactor	600	N2	
FAST	Pinewood	Rotating cone reactor	510		[9]

FAST	Arbour pellet	Rotating drum reactor	450		
FAST	Pinewood	Rotating cone reactor	510		
FAST	Arbour pellet	Rotating drum reactor	450		
FAST	Oakwood	Continuous auger reactor	450		[39]
FAST	Pinewood	Continuous auger reactor	450		
FAST	Oak bark	Continuous auger reactor	450		
FAST	Pine bark	Continuous auger reactor	450		
FAST	Oak/maple	Ensyn process Canada			[40]
FAST	Oakwood	NREL vortex reactor	625		[41]
FAST	Maple oak	Ensyn from RTP facility	525		[42]
FAST	Softwood bark	Vacuum pyrolysis	500		[43]
FAST	Softwood bark	Fluidized bed			[44]
FAST	Firwood	Rotating cone reactor			[45]
FAST	Beachwood	Rotating cone reactor			
FAST	General wood	Ensyn transported bed			
FAST	Pine sawdust	Batch induction pyrolysis system e	500	N2	[46]
FAST	Pine sawdust	Batch induction pyrolysis system e	550	N2	
FAST	Pine sawdust	Batch induction pyrolysis system e	600	N2	
FAST	Pine sawdust	Batch induction pyrolysis system e	650	N2	
FAST	Pine sawdust	Batch induction pyrolysis system e	700	N2	
FAST	Beechwood	Fluid bed reactor	500	N2	[47]
FAST	Poplar 2 years	Fluid bed reactor	500	N2	[48]
FAST	Poplar 12 years	Fluid bed reactor	500	N2	

FAST	Douglas Fir Wood	Auger reactor	500		[49]
FAST	Beechwood	Fluidized bed	500	N2	[10]
FAST	Spruce wood	Fluidized bed	500	N2	
FAST	Wheat straw	Fluidized bed	500	N2	

The results are presented in Table 8:

Table 8. % COD Yield of Fast Pyrolysis

Fast Pyrolysis Results				
	Unit	Average	SD	COD Yield
Biomass	gCOD/g	1,30	0,06	-
Char	wt yield	16,6%	4,9%	28,9%
	gCOD/g	2,27	0,15	
Liquid	wt yield	45,0%	15,3%	49,1%
	gCOD/g	1,42	0,29	
WS	*wt yield*	*40,7%*	*11,5%*	*38,2%*
	gCOD/g	*1,21*	*0,38*	
WI	*wt yield*	*16,4%*	*2,6%*	*23,9%*
	gCOD/g	*1,88*	*0,22*	
Gas	wt yield	32,1%	17,9%	5,7%
	gCOD/g	0,23	0,14	
Other-Loss				16,18%

Looking to COD balance, 29% of the chemical energy is partitioned into biochar, 49% ends up in the condensable liquid (38% into WS and 23% into WI liquid) and 6% ends up in pyrolysis gas (mostly carbon monoxide, hydrogen, and methane). As observed for slow pyrolysis, for most of the fast pyrolysis studies a significant part of COD is missing (12%).

For fast pyrolysis, most of COD ends up in the liquid. Merging liquid and gas (whose mass yields are almost identical to that obtained with slow pyrolysis) the overall COD

yield is equal to 60%. Interestingly the WS fraction has an average COD similar to that of anhydro sugars or cellulose (e.g. 1.2 kgO/kg), while the WI part shows an average COD closely similar to that of lignin (more than 2 kgO/kg). This suggests that WS derives mainly from carbohydrates and dehydrated carbohydrates, whereas WI came from lignin. The ratio of bioavailable and non-bioavailable volatile (excluding char) pyrolysis products is close to that observed with slow pyrolysis and, again close to holocellulose/lignin ratio.

3.1.3 Pyrolysis Review Conclusions

As shown by the data collected (Figure 17 and Figure 18), fast pyrolysis is more effective in producing bioavailable substances, since the COD yield of bioavailable products is higher. Fast pyrolysis is selective toward condensable organics. Increasing heat transfer rate has the net effect to decrease char COD yield and increases liquid products, both soluble organics (WS) and insoluble lignin-derived constituents (WI). It is interesting to notice that a variable quantity between 10 and 16 % of the COD yield is missing, probably due to experimental loss and the difficult detection and trapping of all the pyrolysis products. Interestingly, when gases were quantified reveals that COD yield of this fraction is relatively low (usually less than 6%). This suggests that the common practice of evaluating the gas yield by difference is not adequate and tends to provide higher gas yields, which are an artifact of the method used. Given this, a larger effort should be targeted in closing exactly the mass or, at least, the energy balance (or, even better, COD balance) of the pyrolysis.

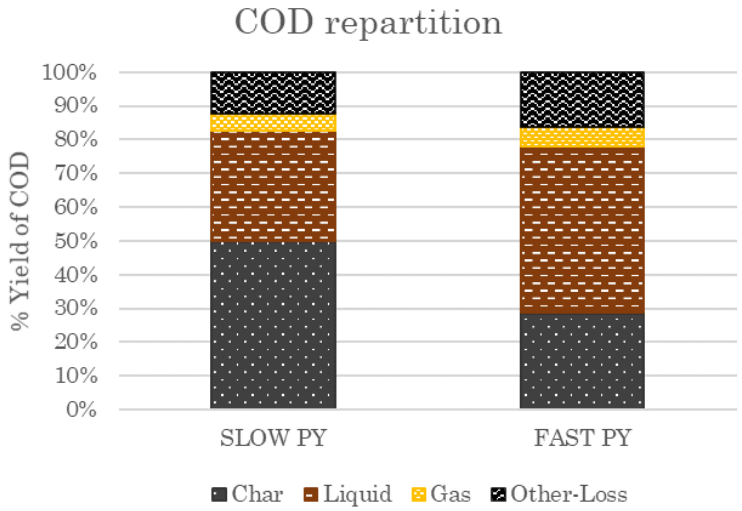

Figure 17. % yield of COD in slow and fast pyrolysis products

Figure 18. % Yield of COD in the liquid fraction of slow and fast pyrolysis

3.2 Results of the pyrolysis products characterization

3.2.1 Ultimate analysis of feedstock and pyrolysis products

In total two biomass samples, five biochar samples, and twelve WI samples were characterized using elemental analysis, ash content, and moisture methods (*Chapter 2.1*). The results are shown in *Table 9*:

Table 9. Biochar and Water-Insoluble Elementary Analysis

	Biomass		*Char*		*WI*	
	Average	±	Average	±	Average	±
*gCOD*g^{-1}*	1.16	0.06	2.28	0.08	1.85	0.20
C	44.8%	1.7%	82.7%	2.5%	61.9%	4.8%
H	5.8%	0.0%	2.6%	0.4%	6.5%	0.3%
O	49.4%	1.7%	12.1%	2.3%	31.4%	5.0%
N	0.0%	0.0%	0.1%	0.1%	0.2%	0.1%
S	0.0%	0.0%	0.0%	0.0%	0.0%	0.0%
Ash	0.30%	0.02%	1.2%	0.2%		
Moisture	8.5%	0.4%				

From elemental composition, biomass had a theoretical oxygen demand (thereafter called COD) content of 1.16 ± 0.04 gCOD*g^{-1} with a typical content of carbon and oxygen close to that of carbohydrates. Biochar shows a higher COD and content of carbon, respectively 2.28 ± 0.02 gCOD*g^{-1} and 82.7% gC/g, with a negligible quantity of nitrogen and sulfur. WI is characterized by a COD of 1.85 ± 0.1 gCOD*g^{-1}, in line with the results of the literature reviewed in *Chapter 3.1*.

3.2.2 COD balance of the different pyrolysis

One of the aims of this thesis was to establish the partition of chemical energy (measured by COD yield) that occurs upon pyrolysis. To provide a description of pyrolysis as pre-treatment a set of pyrolysis experiments were performed, and COD balance, namely COD yield of each pyrolysis product, was established. In total ten pyrolyses experiments were performed: three stepwise pyrolyses (350°C+550°C steps) and N_2 as carrier (A), three pyrolyses with one step and N_2 as carrier in the D50 pyrolizer (B), two pyrolyses with one step in the D20 pyrolyzer (C), and two pyrolyses with one step in D50 pyrolyzer with CO_2 as carrier (D). Molecular composition (for gas), elemental analysis (for char and WI), and direct COD analysis (WS) provided a direct measure of chemical energy partition into different pyrolysis products. COD

yields of various non-bioavailable (Char and CH_4), sparingly fermentable (WI), and fermentable (WS, H_2, and CO) pyrolysis products are shown in *Table 10*.

Table 10. % COD yield from different pyrolysis of sawdust, respect biomass COD:

	A		B		C		D	
	Average	±	*Average*	±	*Average*	±	*Average*	±
Char	46.5%	0.5%	37.0%	2.4%	42.9%	2.1%	36.6%	0.9%
WS	31.7%	5.1%	35.8%	5.0%	37.1%	0.1%	35.6%	1.4%
WI	9.7%	2.0%	15.0%	2.5%	12.9%	2.9%	14.6%	3.4%
H_2	0.2%	0.1%	0.1%	0.0%	0.1%	0.1%	0.5%	0.0%
CH_4	5.0%	1.0%	4.8%	0.3%	2.8%	0.1%	4.1%	1.3%
CO	8.6%	2.7%	8.2%	0.6%	6.8%	0.2%	9.9%	0.1%
Total	101.7%	7.4%	100.9%	0.4%	102.5%	5.2%	101.1%	2.2%
Fermentable	50.2%	9.8%	59.1%	8.2%	56.9%	3.3%	60.5%	4.9%

A first observation is that, once the method was optimized, all the COD balances (Σ $gCOD_{products}/gCOD_{feestock}$) obtained were close to 100%. Two steps pyrolysis showed a significant decrease of fermentable COD yield (more than 5%) in comparison with the other experiments, mainly due to the higher COD yield of char and lower COD yield of WS and WI. One-step pyrolysis, with D50 pyrolizer, didn't highlight any significant difference between the carriers, with a fermentable COD yield of 60% in both cases. The D20 pyrolizer provided a higher COD yield of char than the D50, however, the fermentable COD yield did not change significantly. On the other hand, D20 reactor produces a slightly higher WS yield. This suggests that the main differences between D20 and D50 were related to WI recovery, due to different reactor shapes and pyrolysis chamber size. Even if CO_2 suggests that the composition of pyrolysis gas can be relevant for COD yield, since the use of nitrogen is characterized by procedural advantages, the one-step pyrolysis with nitrogen was chosen as the most suitable model system for the subsequent laboratory experiments. Given the minor differences between DN20 and DN50, the DN20 reactor one was used due to the simplified procedure of pyrolysis products recovery and reactor cleaning.

3.2.3 Analysis of Water-Soluble fraction from pyrolysis: HPLC-SEC

To establish the relative amount of low molecular weight WS (analyzable with GC-MS and more prone di biodegradation) and high molecular weight WS (non GC detectable and with unknown structure), HPLC-SEC was performed on WS fraction. Specifically, a detailed analysis was performed on WS obtained from D50 pyrolizer, one step pyrolysis with N_2 as carrier, and WS faction obtained from D20, and one step pyrolysis with N_2 as carrier. The results, presented %Area of eluted compounds, are shown in *Table 11*.

Table 11. %Area distribution of the WS components

	D50 pyrolizer		D20 pyrolizer	
MW	*Area%*	±	*Area%*	±
<200 Da	60.2%	0.2%	53.4%	0.5%
200-400 Da	6.9%	0.5%	5.9%	0.1%
400-1450 Da	9.9%	1.0%	7.0%	0.3%
1450-3350 Da	3.3%	0.4%	6.4%	0.0%
>3350 Da	19.8%	1.1%	27.2%	0.1%

The results showed that low molecular weight compounds (<200 Da) constitute roughly half of WS, which is in line with the literature concerning detailed WS analysis [50]. Noticeably, D50 pyrolyzer produced a higher amount of low molecular weight compounds than D20. This is probably due to the higher heat transfer achieved or to the improved recovery of high molecular weight compounds with DN20. The remaining part of the WS was formed by compounds with molecular weights between 200-3350 Da, and especially oligomers and high molecular weight (>3350 Da) compounds, which represent more than 20% of WS, with unknown structure. Further investigation, through the use of UV-VIS detector (DAD), was performed in order to provide some clues on the chemical nature of complex higher-weight molecules detected. The results from DAD analysis are presented in *Figure 19*.

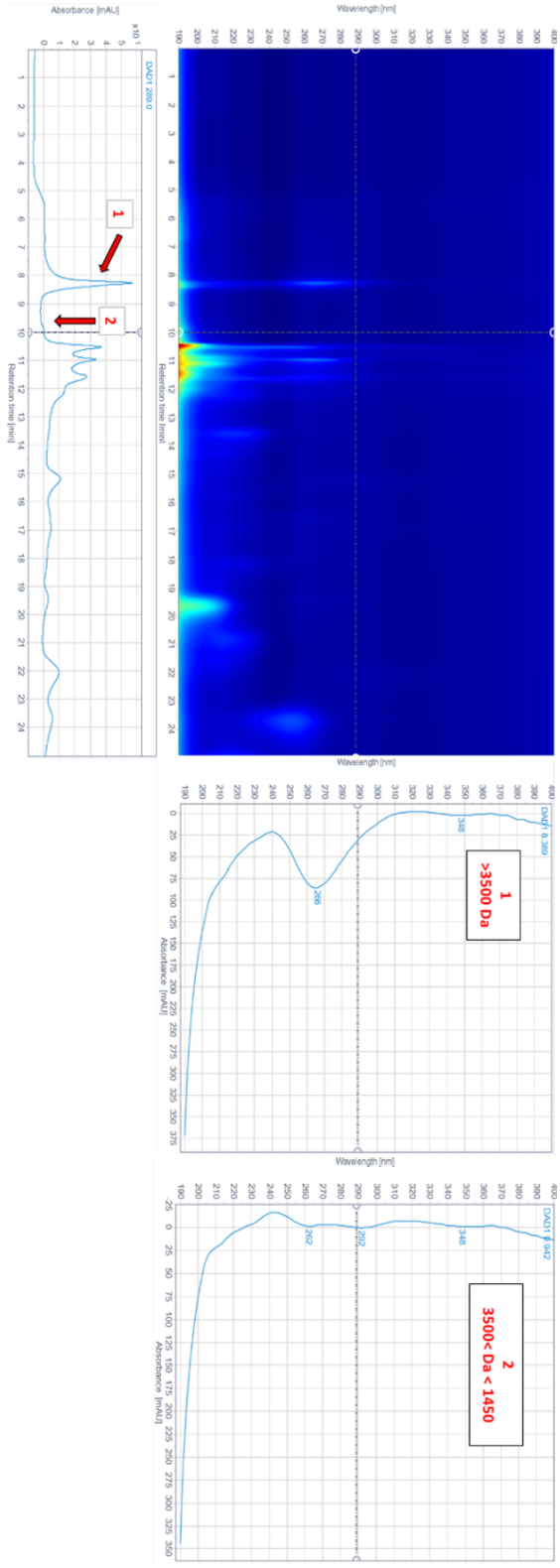

Figure 19. HPLC-SEC RID and DAD (UV-VIS) results for WS sample obtained from one-step pyrolysis with N2, in the D50 pyrolizer

Looking to DAD detector, the fraction with a molecular weight higher than 3350 Da, shows a characteristic peak at 266 nm. This is a typical absorbance of furans, suggesting the presence of dehydrated furanosides or humins-like structures in these high molecular weight constituents [51]. Other peaks were detected at 292 and 348 nm, assigned to carbohydrates-like structure, suggests that this fraction of WS is formed by a complex hybrid polymeric matter which includes polysaccharides and "charred" polysaccharides with some degree of dehydration leading to furanic structure.

3.2.4 Analysis of Water-Soluble fraction from pyrolysis: Volatile Fatty Acids (VFA)

With the VFA method, acetic acid, propionic acid, butyric acid, hexanoic acid, and hydroxy acetone (acetol) were detected and quantified. The response factor (RFs) used were all determined by standard solutions of pure compounds. The theoretical COD (from the molecular structure) of each compound was finally used for the determination of the COD yield. Results are presented as COD yield respect the WS COD content (COD/COD_{WS}), in *Table 12*:

Table 12. % COD yield, respect WS COD, of compounds detected with VFA method

	D50 pyrolizer		D20 pyrolizer	
Compound	*Average*	±	*Average*	±
Acetic Acid	1.5%	0.3%	1.6%	0.1%
Propionic Acid	0.3%	0.0%	0.3%	0.1%
Butyric Acid	0.1%	0.0%	0.1%	0.0%
Hexanoic Acid	0.1%	0.2%	0.0%	0.0%
Acetol	3.0%	1.7%	1.8%	0.0%
Total	5.0%	2.2%	3.9%	0.1%

Although variable, on COD basis, Acetol resulted the major detected compound, corresponding to 1.3 - 4.7% of the COD of WS in D50 pyrolyzer. Acetic acid was the major VFA in WS, and constituted 1.5% and 1.6% ($gCOD/gCOD_{WS}$) of WS respectively with, D50 and D20 pyrolizer. In total, the 5% yield (COD/COD_{WS}) and 3.9%,

respectively for D50 and D20 reactor, were detected using this method. The results, although expressed on COD basis, are in line with those that can be back-calculated from the literature [9], [12], [14].

3.2.5 Analysis of Water-Soluble fraction from pyrolysis: Aldehydes

This method was developed to analyses reactive aldehydes like hydroxy acetaldehyde, which are usually poorly analyzable with direct GC-MS, due to reactivity with other sample constituents. Methoxylation was used to convert hydroxy acetaldehyde into corresponding dimethyl acetal. The response factor (RF) of the compound was obtained from hydroxy acetaldehyde dimer by Sigma-Aldrich. Results, presented as %COD yield from the WS fraction, are summarized in *Table 13*.

Table 13. %COD yield of hydroxy acetaldehyde in WS solution

D50 pyrolizer		D20 pyrolizer	
Average	±	*Average*	±
16.2%	0.1%	13.8%	0.1%

The analysis shows that hydroxy acetaldehyde was a major pyrolysis product of wood pyrolysis, with 16.2% and 13.8% COD yield (COD/COD_{WS}) respectively for DN20 and DN50 reactor. Results are in line with other studies performed with similar methodologies [9]. Then, with an overall $COD/COD_{feedstock}$ of more than 5%, hydroxy acetaldehyde is one of the major compounds obtained from the pyrolysis of fir sawdust.

3.2.6 Analysis of Water-Soluble fraction from pyrolysis: Silylation-GC-MS

Silylation allows the extension of GC-MS analysis to a large amount of highly polar compounds which are present in WS. All the peaks detected were quantified (to have

an overall quantification of GC-MS detectable compounds) and, were possible, the molecules were identified with the support of NIST Mass Spectral 2.0 Searcher, literature [52]–[55], and internal lab databases. A total of 90 peaks were detected/quantified and 29 molecules were identified. For calibration, a mixed standard solution was prepared using m-cresol; resorcinol; p-eugenol; o-eugenol; 2-methoxy,4-methyl phenol; catechol; 2,4-dimethyl phenol; levoglucosan; 2-hydroxy, 1-methyl cyclopenten-3-one; furfuryl alcohol. When the molecule was not identified the RF was set as 1. A hypothetical COD equal to 1.2 gCOD*g^{-1} (equal to that of a generic anhydro hexose) was assigned at all the unknown molecules. *Table 14* show detailed results related to the analysis of WS with Sylilation-GC-MS expressed as COD/COD_{WS}.

Table 14. %COD yield in WS liquid fraction detected with silylation

	DN50 pyrolizer		DN20 pyrolizer	
Compound	*Average*	±	*Average*	±
Levoglucosan	2.9%	0.1%	2.6%	0.2%
Hydroxy acetic acid	1.53%	0.07%	1.82%	0.05%
1,6-anhydro galactofuranose	1.41%	0.07%	1.3%	0.1%
2 hydroxy adipic acid	1.1%	0.1%	0.99%	0.00%
Hydroxyacetaldehyde derivative	1.1%	0.1%	0.93%	0.09%
Furfuryl alcohol	0.88%	0.06%	1.7%	0.2%
2,2-dimethoxy propionic acid	0.50%	0.00%	0.34%	0.00%
Catechol	0.50%	0.01%	0.59%	0.03%
1,2-ethandiol	0.4%	0.1%	0.47%	0.04%
Pyrogallol	0.37%	0.01%	0.26%	0.03%
3 vanil propanol	0.34%	0.04%	0.32%	0.00%
1 propanol	0.34%	0.06%	0.27%	0.04%
2 - Furan methanol	0.17%	0.02%	0.16%	0.05%
2(5H)-Furanone	0.11%	0.01%	0.24%	0.01%
4 propenyl guaiacol	0.11%	0.01%	0.09%	0.01%
Others GC detactable	*14.3%*	*0.2%*	*13.40%*	*0.09%*
Total gCOD/gCODws	*26.0%*	*0.2%*	*25.40%*	*0.09%*

Levoglucosan was found as the major detectable component with this method, with a COD yield of 2.9% gCOD/gCODws; hydroxy acetic acid seems to had a slightly higher COD yield with D20 pyrolizer (1.82%) respect D50 (1.53%); Furfuryl alcohol was produced more in D20 pyrolizer (1.7%) respect D50 (0.88%). The other identified molecules had similar yields in both pyrolizers: 1,6-anhydro galactofuranose 1.35%; 2 hydroxy adipic acid 1%; hydroxyacetaldehyde derivative 1%; Catechol 0.55%; 1,2-ehtandiol 0.44%; Pyrogallol 0.30 %; 3 vanil propanol 0.34%; 1-propanol 0.30%; 2-furan methanol 0.16%; 2-(5H)-furanone 0.15%; 4 propenyl guaiacol 0.10% (COD/COD_{WS}) . The molecules detected had a yield in line with the literature [9], [12], [14]. A total of 26 % WS COD was detected with this method.

3.2.7 Analysis of Water-Soluble fraction from pyrolysis: Silylation-GC-MS

Merging results of all analyses performed a general picture of the analytical profile of WS COD can be obtained (in COD/COD_{ws}, *Table 15).*

Table 15. Final repartition of COD inside WS fraction expressed as COD/CODws

	DN50 pyrolizer		DN20 pyrolizer	
Analysis	*COD yield*	±	*COD yield*	±
Silylation	26.0%	0.2%	25.4%	0.1%
Aldehydes	16.2%	0.1%	13.8%	0.1%
VFA	5.0%	1.2%	3.9%	0.0%
Others 0-200	12.9%	1.0%	10.4%	0.5%
200 - 400 Da	6.9%	0.5%	5.9%	0.1%
400 - 1450 Da	9.9%	1.0%	7.0%	0.3%
1450 - 3500 Da	3.3%	0.4%	6.4%	0.0%
> 3500 Da	19.8%	1.1%	27.2%	0.1%
Total GC detectable	47.3%	1.6%	43.0%	0.2%

Using the sample pretreatment and derivatization methods applied in this thesis an average of 45% on WS can be potentially identified and monitored. Silylation allowed half of the characterization, while the aldehyde method has a key role, due to the high yield of hydroxy acetaldehyde. About half of the WS are not GC-amenable, therefore

further analysis must focus the attention on the possible hydrolysis of the oligomers and humines to have a more comprehensive characterization of high molecular weight contituents.

3.2.8 Analysis of Water-Insoluble fraction from pyrolysis

WI fraction was analyzed with VFA and silylation-GC-MS methods. The RF, when not available was set as 1, assuming a unitary response factor with respect to IS (3-Chlorobenzoic acid). For identified compounds, the COD yield (COD/COD_{WI}) was calculated from mass yield and chemical structure. For unknown compounds, an average COD of 1.85 $gCOD*g^{-1}$ was assumed. The summarized results about composition WI (COD/COD_{WI} for each compound) are shown in Table 16.

*Table 16. Total %COD yield in the identified compounds in WI fraction. *Possible wrong identification*

Compound	COD/CODWS
Levoglucosan	2.14%
Phenol, 2-methoxy-4-(1-propenyl)	2.02%
Catechol	1.51%
Phenol, 2-methoxy-4-methyl	1.25%
2,3-Dimethoxyphenylacetic acid	0.92%
Phenol	0.76%
Methoxy-4-vinylphenol	0.70%
Phenol, 4-ethyl-2-methoxy-	0.66%
4-hydroxy-3-methoxycinnamaldehyde	0.65%
Hydroxy Acetic Acid	0.61%
3-Allyl-6-methoxyphenol	0.55%
1,2,5-pententriol	0.46%
Vanillin	0.42%
Phenol,2-methoxy	0.42%
Furan-2-carboxylic acid, 3-methyl	0.37%
Ethan one, 1-(4-hydroxy-3-methoxyphenyl)	0.36%
4,6-Dioxo heptanoic Acid *	0.34%
3-Vanilpropanol	0.31%
Phenol, 2-methoxy-4-propyl	0.31%
Benzoic acid, 3-methoxy-4-hydroxy	0.31%

2-Propanone, 1-(4-hydroxy-3-methoxyphenyl)-	0.30%
5-hydroxy-2-methoxy-4H-pyran-4-one	0.29%
2-(2-hydroxy ethyl) Phenol	0.28%
2-methoxy-4-propenylphenol	0.23%
Butanoic acid, 4-hydroxy	0.22%
Phenol,2,5-dimethyl-	0.21%
Ethanediol	0.21%
2-methyl Succinic Acid	0.16%
Pyrogallol	0.15%
Phenol,2-methyl-	0.10%
Lactic Acid	0.09%
3-Methyl-1-cyclohexen-1-hydroxy	0.09%
m-Cresol	0.09%
3,5-dimethyl Phenol	0.08%
Furan 3 carboxylic Acid	0.08%
2-Fruan methoxy *	0.08%
p-Cresol	0.08%
o-Cresol	0.08%
2-Pentanone, 4-hydroxy-4-methyl	0.07%
Ethen diol	0.07%
2-Furanmethanol	0.05%
(acetyloxy)-Acetic Acid	0.05%
Others not ID	**17.86%**
Not detected	**64.01%**

Preliminary analysis made on COD basis showed that WI was formed by 36% ($gCOD/gCOD_{WI}$) GC detectable constituents and 64% non-detectable compounds. Interestingly, besides 12% COD/COD_{ws} were phenols and lignols derivatives, a significant portion of GC-MS detectable constituents (around 6% COD/COD_{ws}) consisted of water-soluble substances partitioned into WI fraction (e.g. VFA or levoglucosan). This is probably due to the procedure used for WI obtainment that can concentrate a relatively small portion of WS into the extract obtained after solvent evaporation. In total, GC-MS and silylation-GC-MS allow characterizing more than 35% of WI COD. Noticeably, 2.14% ($gCOD/gCOD_{WI}$) of what is defined as WI is levoglucosan, which is known to be

water-soluble and biodegradable. Further experiments are needed to characterize better this fraction, nonetheless analysis performed suggests a scarce but non-negligible (given the presence of water-soluble substances) bioavailability of WI COD produced by intermediate pyrolysis.

3.3 Results of the pyrolysis products fermentation

Analytical study of COD yield and composition of pyrolysis products provide a detailed description of pyrolysis as targeted pre-treatment to produce bio-available pyrolysis products. Looking into pyrolysis products "from bacterial standpoint" requires establishing the capability of adapted microbial consortia to perform conversion of the large number of chemical functionalities that characterize pyrolysis products. Such measure required the set up of a reliable experimental system, namely a bioreactor, to study such phenomena and to grow the so-called "pyrotrophic MMC consortia", namely microorganisms that can live on pyrolysis products. Preliminary experimental attempts allowed to develop a fairly accurate continuous bio-reactor (section 2.3) which revealed suitable for testing the anaerobic digestion of pyrolysis products, hydrogen, and model compounds (glucose) for production of VFA. As preliminary investigation, each bio-reactor was tested in three different sets, in order to highlight potentials and critical issues of pyrolysis product conversion and capabilities of pyrotrophs.

3.3.1 Set 1

The first set conditions are summarized in *Table 17*:

Table 17. Set 1 configuration

	R1	**R2**	**R3**
Biomass enrichment	First 11 days with glucose	First 11 days with glucose	First 11 days with glucose
Feeding	WS + Syngas + Hydrogen	WS + Syngas	Glucose
Filling material	Glassballs	Glassballs	Glassballs

Input COD concentration (gCOD/L)	20	20	20
RT (Days)	10	10	10
OLR (gCOD/Day)	0.4	0.4	0.4

The goal of the first set was the study of the possible biological degradation of pyrolysis products WS and pyrolysis gases. Initially, all bioreactors were fed with glucose to enhance biofilm formation. R3 was a control reactor, fed with 20 gCOD/L glucose. In R1 and R2 glucose was used as only feed (20 gCOD/L) for 6 days, then in five days an increasing share of pyrolysis (from 7.5% to 25% in days 7-8, from 25% to 50% in 9-13 days and 100% after day 13). Also, R1 was fed with 10% extra COD from hydrogen. Figure 20 shows the daily gas volume production of reactors (missing data corresponds to the days in which gas analysis was not performed, like Saturday or Sunday). The gas analysis showed an average gas uptake of 16.5 mL*Day-1, out of the 60 mL daily provided during the pyrolysis product digestion. CO2 was mainly produced during the initial glucose fermentation, then a huge decrease was noted. CO gas had not a significant uptake. Methane was produced only when reactors were fed with glucose. During the experiment, positive N_2 variation was recorded with an average of 25 mL*Day-1 input. A similar gas trend was obtained in R2, with a progressive decrease in CO_2 production, a low CO uptake, and a slightly positive N_2 input. R3 had an initial high production of H_2. Methane was produced on the first day of the experiment, then was not detected until day 8. After, an average production of methane equal to 30 mL*day^{-1} was detected.

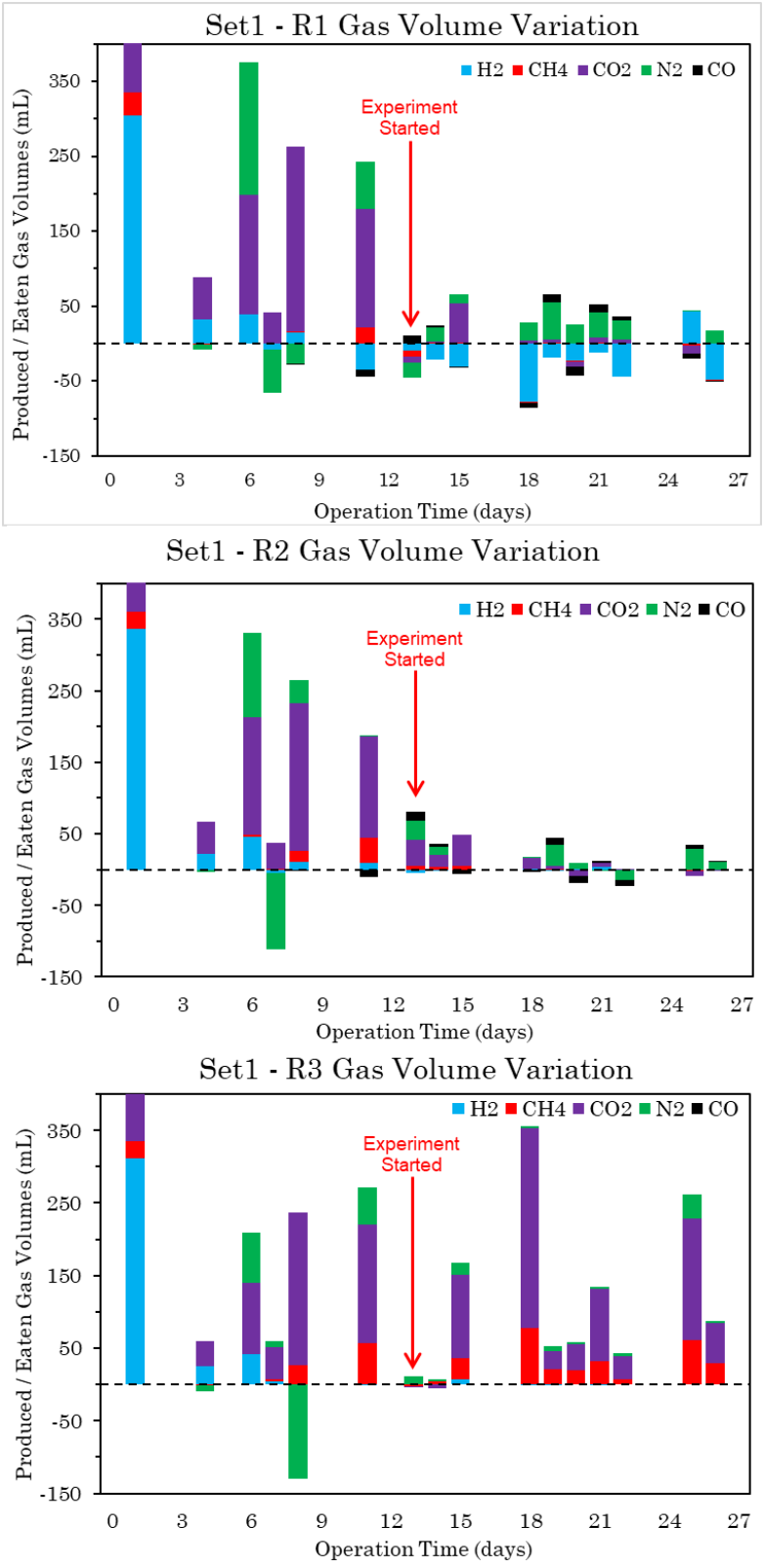

Figure 20. Gas volume variation in Set 1

pH, which measures the degree of acidification showed a large variability during the experiment. The pH was adjusted, using NaOH 1M, when an excessive acidification trend was noted. The trends and the base additions are shown in *Figure 21*. R1 and R2 had a similar trend, with an average pH of 5.19 and 5.14 respectively. R3 recorded a pH of 5.02 on average.

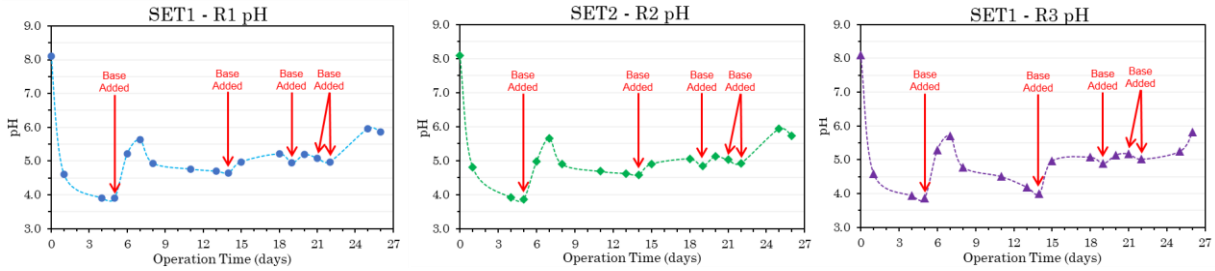

Figure 21. pH trends in Set 1

For all three reactors, the cumulative trend of COD was monitored (*Figure 22*). Knowing the COD inside the reactor and COD input and output, the expected COD of the following day was determined (Expected COD). This value was then compared with the COD calculated the day after (Measured COD). In this way, a possible difference, which is a direct measure of a possible leak, biomass growth, or absorption inside the reactor, was determined (Difference). R1 and R2 had similar trends with a progressive increase of COD difference between measured and expected COD. All the reactors, in the enrichment phase, presented an unstable difference in COD trend. After nine days, in all the reactors, the difference COD reach a positive, quite stable trend.

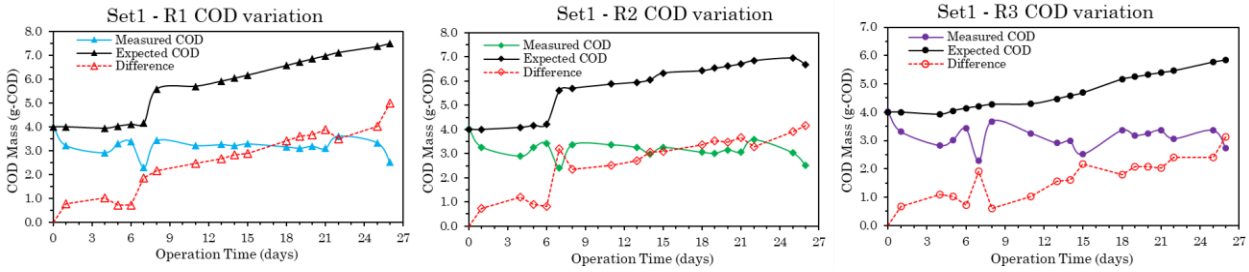

Figure 22. Measured, Expected, and Difference COD in Set 1

VFA daily COD concentrations are shown in *Figure 23*. All reactors had a similar initial trend until day 13. Acetic, propionic, and butyric acids appeared after day four. Propionic acid reaches a maximum amount on day 6 in all the reactors, with a concentration of 3.66 $gCOD*L^{-1}$ in Reactor1, 2.04 $gCOD*L^{-1}$ in Reactor2, and 2.72 $gCOD*L^{-1}$ in Reactor3. Valeric acid was detected on day 6 for R1, day 7 for R2, and day 4 in R3, while caproic acid was founded on day 7 for all the reactors. After day 13, R3 showed an almost constant VFA COD concentration, whereas R1 and R2, which were fed with pyrolysis products, showed a decreasing concentration of all VFA but acetic acid. Such decreasing trend was similar to that expected by simple dilution provided by the daily sampling and addition of the feeding. During the experiment in R3, valeric acid gradually decreases, oppositely caproic acid increases its concentration in time, with a maximum concentration of 6.52 $gCOD*L^{-1}$ on day 26. From day 11, also heptanoic acid was produced and reached a maximum concentration of 0.18 $gCOD*L^{-1}$. Last two days of the R3 experiment, traces of caprylic acid were found (0.01 $gCOD* L^{-1}$).

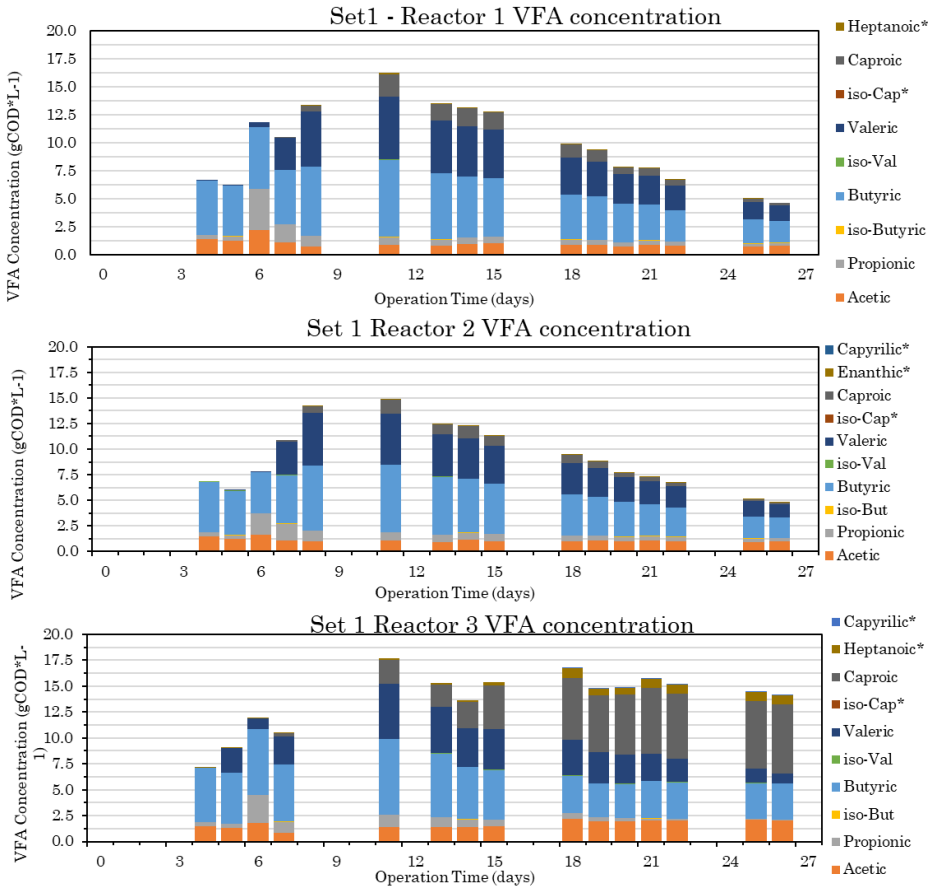

*Figure 23. VFA concentration in SET 1. *Old or Missing Response Factors; Iso-Byu = isobutyric Acid; iso-Val = isovaleric Acid; iso-Cap = isocaproic Acid*

COD input, output, and recovery, together with total gCOD of VFA produced and VFA yield ($gCOD_{VFA}/gCOD_{TOTAL\ OUTPUT\ LIQUID}$) was performed for one Retention Time. Results are shown in *Table 18*.

Table 18. COD balance and VFA yield for Set 1

	R1	**R2**	**R3**	
Period of balance	10	10	10	*Days*
Total input	4.91	4.42	4.40	*gCOD*
Total output	3.58	3.52	3.24	*gCOD*
COD Recovery	72.8%	79.7%	73.6%	*%*
Total VFA	0.41	0.47	2.96	*gCOD*

VFA yield on output liquid	11.4%	13.4%	67.2%	%

R1 and R2 had a similar COD recovery, around 73%, while R2 had a slightly higher COD recovery, 80%. R3, fed with glucose, had the higher yield of VFA, around 67%, while R1 and R2 had similar VFA yield, approximately 12%, with no significant difference provided by hydrogen. VFA yield obtained with R1 and R2 is close to the simple VFA content ($gCOD_{VFA}/gCOD_{\text{pyrolysis products}}$) suggesting that no biological conversion was observed in R1 and R2.

3.3.2 Set 2

The second set conditions are summarized in *Table 19:*

Table 19. Set 2 configuration

	R1	**R2**	**R3**
Biomass enrichment	First 8 days with glucose	First 8 days with glucose	First 8 days with glucose
Methanogens inhibitor	BES	BES	BES
Feeding	WS + Syngas	Glucose + Hydrogen	Glucose+ Hydrogen
Filling material	Biochar and glassballs	Biochar and glassballs	Glassballs
Input COD concentration (gCOD/L)	20	20	20
RT (Days)	10	10	10
OLR (gCOD/Day)	0.4	0.4	0.4

The aim of Set 2 was to evaluate the effect of biochar on pyrotrophic biofilm formation, conversion of pyrolysis products, gas uptake rate, and VFA yield. Moreover, other improvements were targeted to improve the VFA yield, such as the control of methanogenesis through BES addition and pH control (set to 6). Hydrogen uptake rate was studied with and without biochar in glucose fermentation. As in the previous experiment, all bioreactors were initially fed with glucose. After the initial biofilm enrichment phase, R1 (with biochar) was fed with WS and syngas, R2 (with biochar) and R3 (without biochar) with glucose and hydrogen. In R1 glucose was used as only feed for 4 days, then in four days the share of pyrolysis product on COD input (day 5: 6%, day 6: 50%, day7: 50% day 8: 23%) was slowly brought to 100% (day 13). In this Set, R3 was re-inoculated after 21 days, due to the instauration of lactic acid bacteria (LAB) observed during non-monitored time (Christmas holidays). After 23 days Due to the slight decreasing VFAs trend and significant accumulation of pyrolysis markers (levoglucosan) pyrolysis product feed was stopped in R1, and the system was shifted to a batch mode (just following the trend of the reaction without new addition of pyrolysis products. Moreover, R1, which was clearly intoxicated by excessive pyrolysis product load, was provided micro re-inoculation of 5 and 2.5 mL of fresh sewage sludge, respectively, day 28 and 29.

Figure 24 shows the daily gas volume production as well as the main information about the conduction of the experiment course. In R1, initial stage with glucose feeding was characterized by a large production of CO_2, with an average of 250 $mL*day^{-1}$. After the addition of pyrolysis gas, CO uptake was detected, with an average of 23 $mL*day^{-1}$ until the batch mode, when no pyrolysis gases were provided. After switching to 100% of input COD from pyrolysis products, also methane was detected with an average production of 23 $mL*day^{-1}$ until the addition of BES inhibited the methanogens bacteria. Methane was again produced after 13 days of batch mode. R2 was characterized by a good hydrogen uptake during all the experiments, with an average of 35 $mL*day^{-1}$ consumed. In the last three days, there was no uptake, probably due to the shift into continuous recirculation mode, due to

an electrical problem (then fixed for Set 3). Methane was produced for almost all the experiments, although BES addition. On average, 28 $mL*day^{-1}$ of methane was produced during the R2 experiment. R3 in the initial 13 days had an uneven behavior. In the first 16 days, there was no hydrogen uptake, on the contrary, a positive production was detected. After the reinoculation, hydrogen uptake was recorded, with an average uptake of 12 $mL*day^{-1}$.

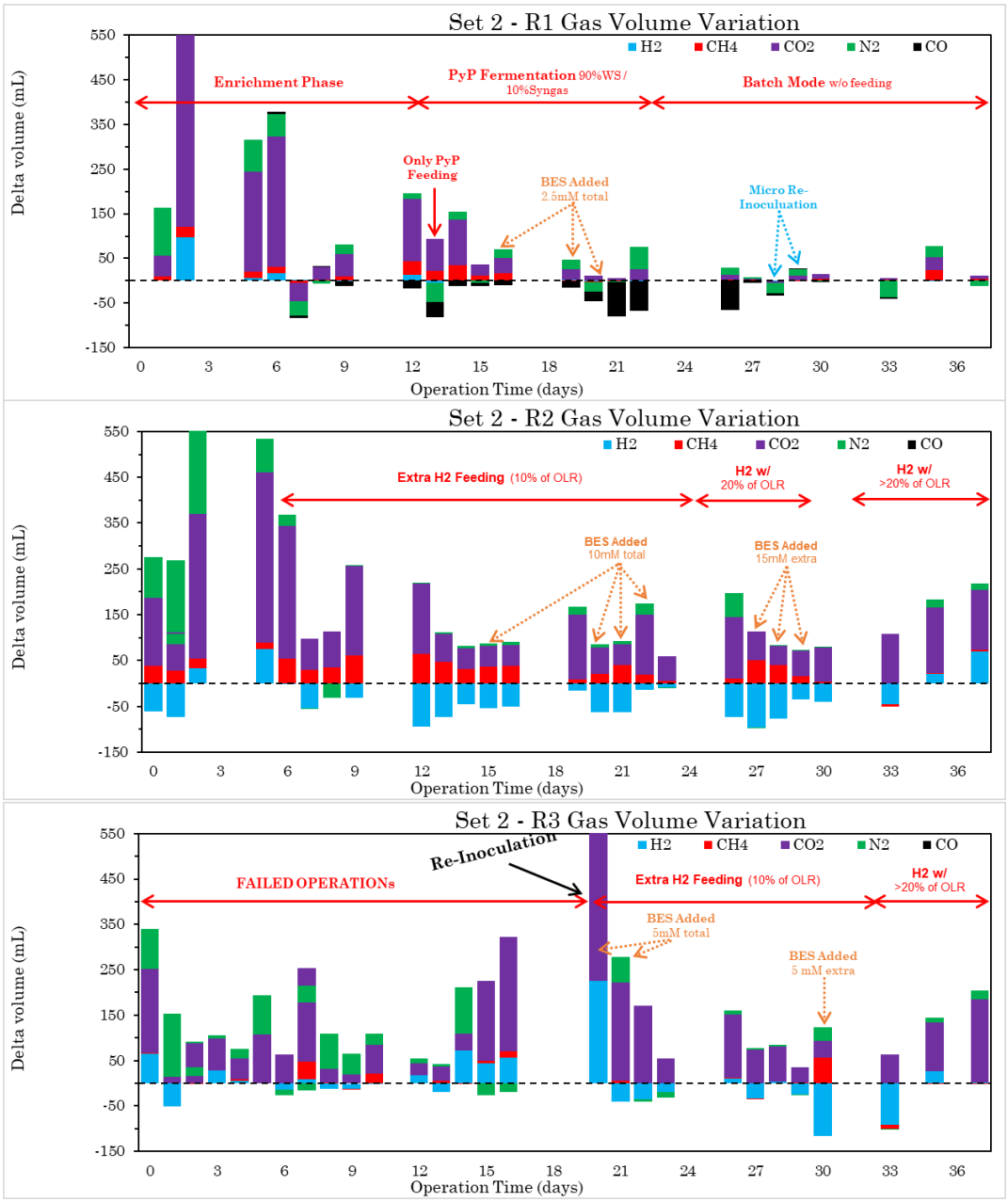

Figure 24. Gas volume variation in Set 2. "Enrichment phase" = initial feeding with glucose to increase the microbial biomass; "Pyp Fermentation" = fed with WS and pyrolysis gas; "Extra H_2 Feeding" = hydrogen daily input as extra COD source.

The pH was daily checked during the weeks, For R1 pH data of the initial days of the batch mode were not detected. The same was for R3 pH data the days before the reinoculation. R1 and R2 had similar trends, and the average pH was, respectively,

5.78 and 5.76, for R3 the average pH before the batch test was 5.43, then during the batch mode, 5.70 was reached as average (*Figure 25*).

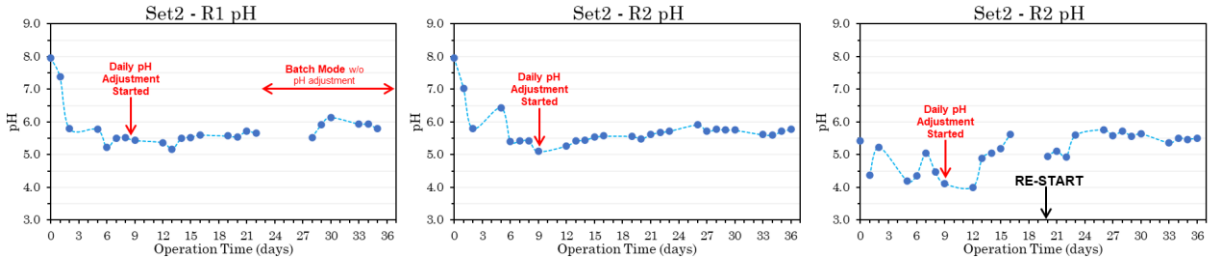

Figure 25. pH trend in Set 2

Input and output COD cumulative trend for Set 2 is shown in *Figure 26*. Knowing the COD inside the reactor and COD input and output, the expected COD of the following day was determined (Expected COD). This value was then compared with the COD calculated the day after (Measured COD). In this way, a possible difference, which is a direct measure of a possible leak, biomass growth, or absorption inside the reactor, was determined (Difference). R1 and R2 had an initial similar trend, with an increasing difference in COD. After day 12 both had a stable COD content, and the difference in COD remained unchanged. R3 maintained a lower difference in COD expected and measured COD for all the Set 2 duration. On day 18 Reactor 3, which was already colonized by bacterial biofilm, had a perfect matching between measured and expected COD.

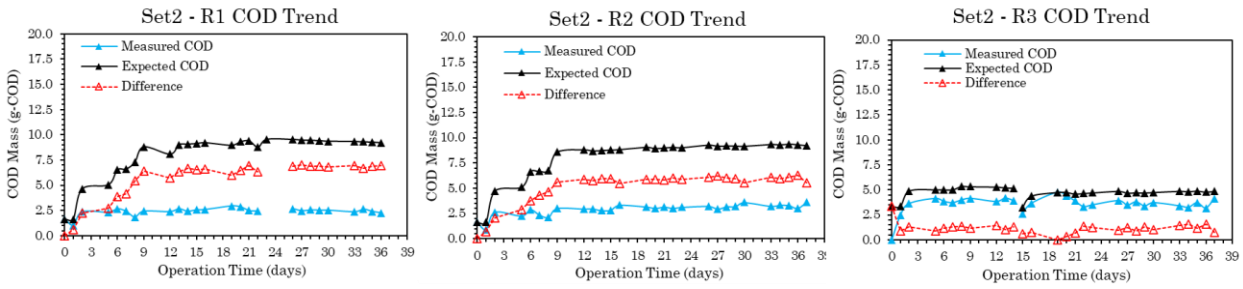

Figure 26.Measured, Expected, and Difference COD in Set 2

In *Figure 27,* VFA COD concentration for Set 2 is shown for the different reactors. Inside R1, in the enrichment phase, the main VFA produced was propionic acid, followed by butyric and acetic acid. After the enrichment period, from day 12 to day

16, the amount of VFA was maintained at 7.5 $gCOD*L^{-1}$, then the concentration dropped, reaching less than 5 $gCOD*L^{-1}$ on day 23. After 6 days of the batch test (day 28), R1 recorded an increased concentration of VFA (from 3.96 to 7.12 $gCOD*L^{-1}$), in particular butyric, valeric, caproic, and heptanoic acid. During the batch mode, caprylic acid (0.01 $gCOD*L^{-1}$) was detected for the first time in R1. In R2 the quantity and types of VFA were constant during almost all the experiments, especially in the last ten days. From day 29 an appreciable amount of heptanoic and caprylic acids were detected, with concentrations around 0.1 $gCOD*L^{-1}$ for both. R3, before the reinoculation, produced mainly acetic acid (on average 3 $gCOD*L^{-1}$). After the reinoculation, the trend was like R2, with the additional production of butyric, valeric, caproic, heptanoic, and caprylic acids. A decreasing trend for butyric acid and an increase of caproic acid was detected.

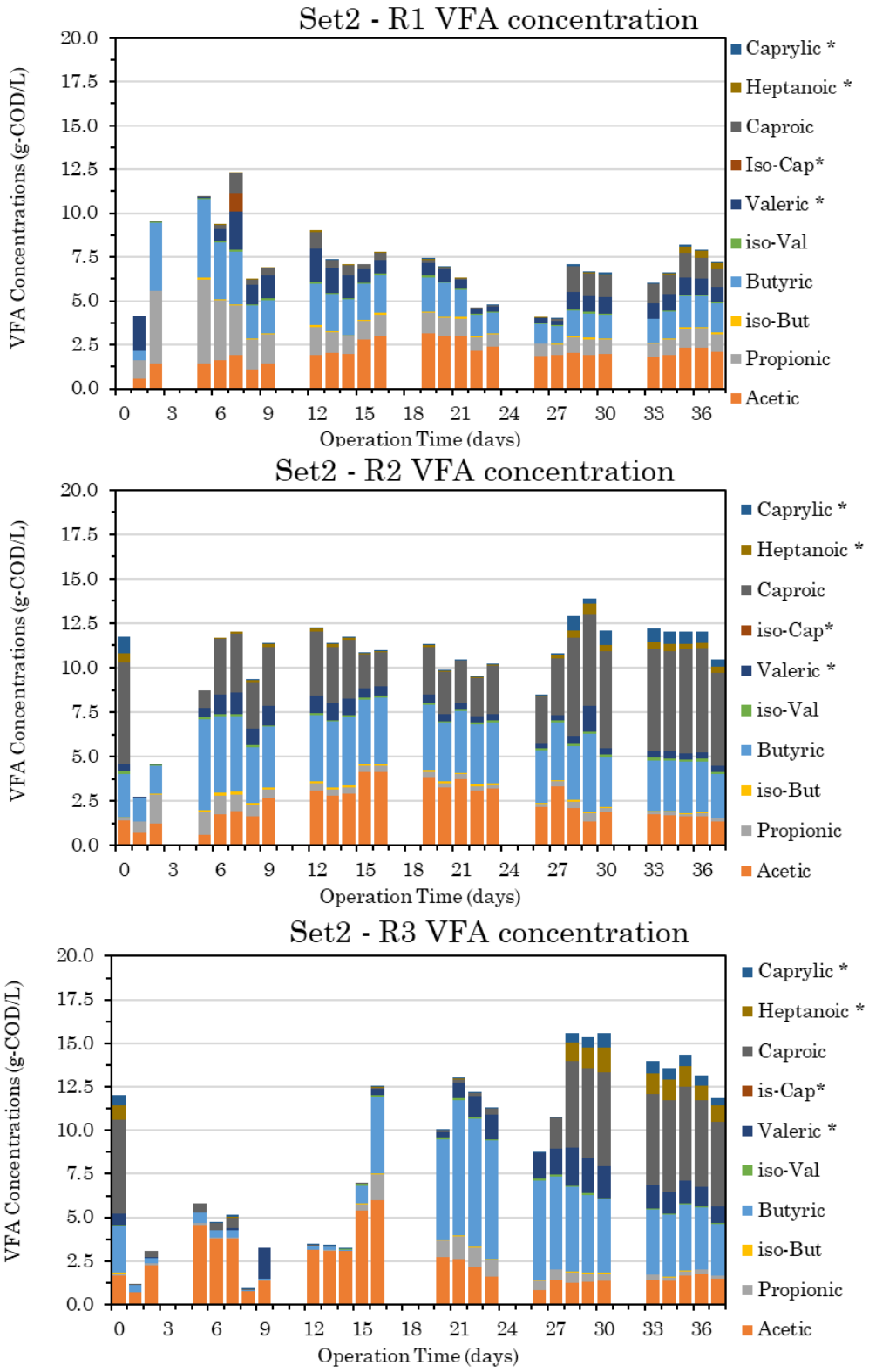

*Figure 27. VFA concentration in Set 2. *Old or Missing Response Factors; Iso-Byu = isobutyric Acid; iso-Val = isovaleric Acid; iso-Cap = isocaproic Acid*

The first reactor, in the last two weeks of the experiment, was left in a "batch mode", in which no feed was provided, and 1 mL of liquid sample was daily withdrew for the analysis. Also, on day 27 and 28 micro re-inoculations were provided, respectively of 5 and 2.5 mL. In *Figure 28* a detailed VFA COD variation of R1 liquid in batch mode is presented. On days 23, 28, 34, and 35 there was a net production of VFA, meanwhile on days 26, 33, 36, and 37 a net decrease of VFA concentration was detected. While on day 23 mainly acetic acid was produced, on days 28 and 35 longer VFAs dominated, with the production of butyric, valeric, and caproic acids mainly. In total, a net variation of +4 gCOD/L of VFA was recorded in this period, with a final yield of 50% VFA_{COD}/Total $_{OUTPUT\ LIQUID\ COD}$.

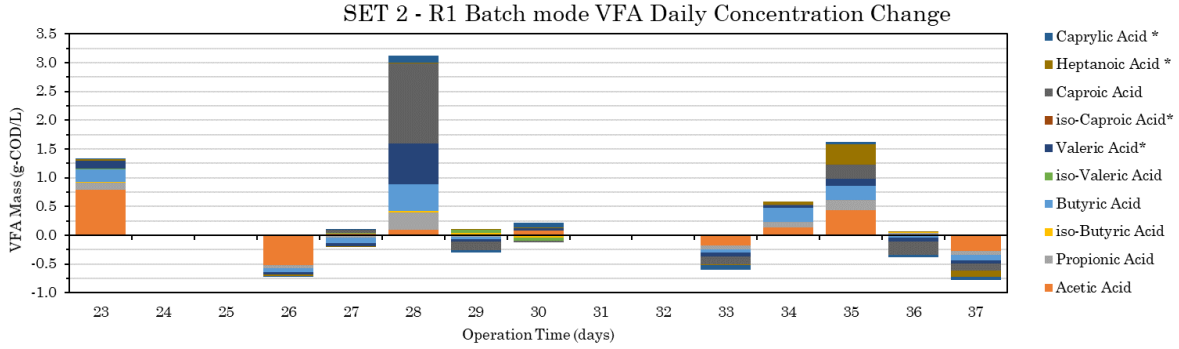

*Figure 28. VFA daily concentration variation in Batch test, Set2 R1. *Missing Response Factors.*

COD input, output, and recovery, together with total gCOD of VFA produced and VFA yield ($gCOD_{VFA}$/$gCOD_{TOTAL\ OUTPUT\ LIQUID}$) was performed for one RT for R2 and R3, while for R1 the balance was performed only for 8 days, due to the further conversion in batch mode. Results are shown in *Table 20*.

Table 20. COD balance and VFA yield for Set 2

	R1	**R2**	**R3**	
Period of balance	8	10	10	*Days*
Total input	4.04	5.45	5.00	*gCOD*
Total output	3.24	4.95	4.72	*gCOD*
COD Recovery	80.1%	90.9%	94.5%	*%*
Total VFA	0.98	3.22	3.89	*gCOD*

VFA yield on output liquid	30.1%	65.03%	82.3%	%

R2 had around 91% of COD recovery and R3 had almost 100% of COD recovery, which confirms the ability of "tetrapod" reactor to prevent leaks. R1 had a COD closure equal to 80 %, significantly lower than the others. However, during the batch test, the COD of the liquid was constant, this excludes leaks in R1. An option can be found in a possible change of the WS feeding solution with the time (formation of precipitate was observed when WS is left settling for a long time), and therefore an error in the amount theoretical COD provided. For the VFA COD yield, R3 showed a higher yield than Set1, probably due to complete biofilm formation and adaptation of microorganisms. R2 had a lower yield compared to R3, which cannot be explained just by absorption on biochar, since an equilibrium should have already been reached during the first part of the experiment, neither with methane production that recorded only 0.07 gCOD for the period considered. VFA yield in R1 reaches 30%, significantly higher than Set1. However, the initial enrichment of biomass with glucose could have saturated biochar with VFA, which had released them later, after the feed with pyrolysis products (*Figure 29*). In R2, despite a conspicuous amount of BES provided, the methanogenesis activity continued for a long period. BES added were 0.11 g, 1.06 g, and 0.44 g respectively to R1, R2, and R3. Those results support the thesis of a detoxification effect of biochar [56], [57], but represent a problematic issue for the systems that use BES as methanogenic inhibitors. Hydrogen uptake seems higher in R2 amended with biochar, but probably a strong effect was produced by the pulsing recirculation of the liquids, which increased the exchange between gas and liquid phases. Nonetheless, R2 converted most of the hydrogen into methane due to the aforementioned BES de-toxification by biochar. In R3 hydrogen uptake, was initially lower than R2, but after the reinoculation, the difference between R2 and R3 decreased. Interestingly, R1 and R2 had, initially, a growing gap between Expected and measured COD inside the reactor until the tenth day, while R3 has not such difference (*Figure 29*). This initial gap is probably due to the biochar absorption of

relatively hydrophobic chemicals, such as phenols and longer VFA (e.g. butyric acid) [56].

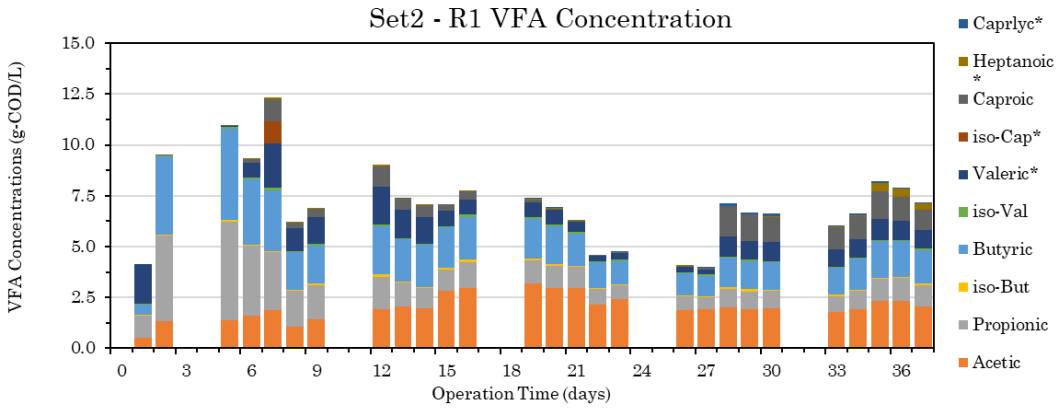

*Figure 29. VFA concentration in Set2 R. *Old or Missing Response Factors; Iso-Byu = isobutyric Acid; iso-Val = isovaleric Acid; iso-Cap = isocaproic Acid*

3.3.3 Set 3

The third set conditions are summarized in *Table 21*:

Table 21. Set 3 configuration

	R1	**R2**	**R3**
Feeding	WS	Glucose	Glucose
Filling material	Biochar and glassballs	Biochar and glassballs	Glassballs
Input COD concentration (gCOD/L)	10	20	20
RT (Days)	10	10	10
OLR (gCOD/Day)	0.2	0.2	0.2

Set 2 highlighted a difficult conversion of pyrolysis products at 20 gCOD/L concentration, even in presence of biochar. The target of Set 3 experiment was the evaluation of possible degradation of pyrolysis products at lower concentrations, mainly to address toxicity issues. Besides R1, R2 and R3 were used again with glucose to provide a control and to evaluate the effect of hydrogen in the previous experiment. Then the R1 inlet COD concentration was halved to 10 $gCOD*L^{-1}$ with an OLR of 0.2 $gCOD*day^{-1}$. R1 was fed only with WS solution, and pyrolysis gases were not provided. R2 and R3 were directly shifted, without any stop or reinoculation, into Set3, to evaluate the possible changes from hydrogen remotion. *Figure 30* shows the gas volume variation for all the reactors in Set3. In R1, an average of 14 $mL*day^{-1}$ input of nitrogen was detected. Hydrogen was produced only on day 1. CO_2 was produced almost all days, with an average of 4 $mL*day^{-1}$. Both R2 and R3 showed an uptake o H_2 on day 0, probably remained from Set2. R2 recorded each day's methane production, with an average of 36 $mL*day^{-1}$, together with CO_2 production (68 $mL*day^{-1}$), while R3 started methane production on day 7.

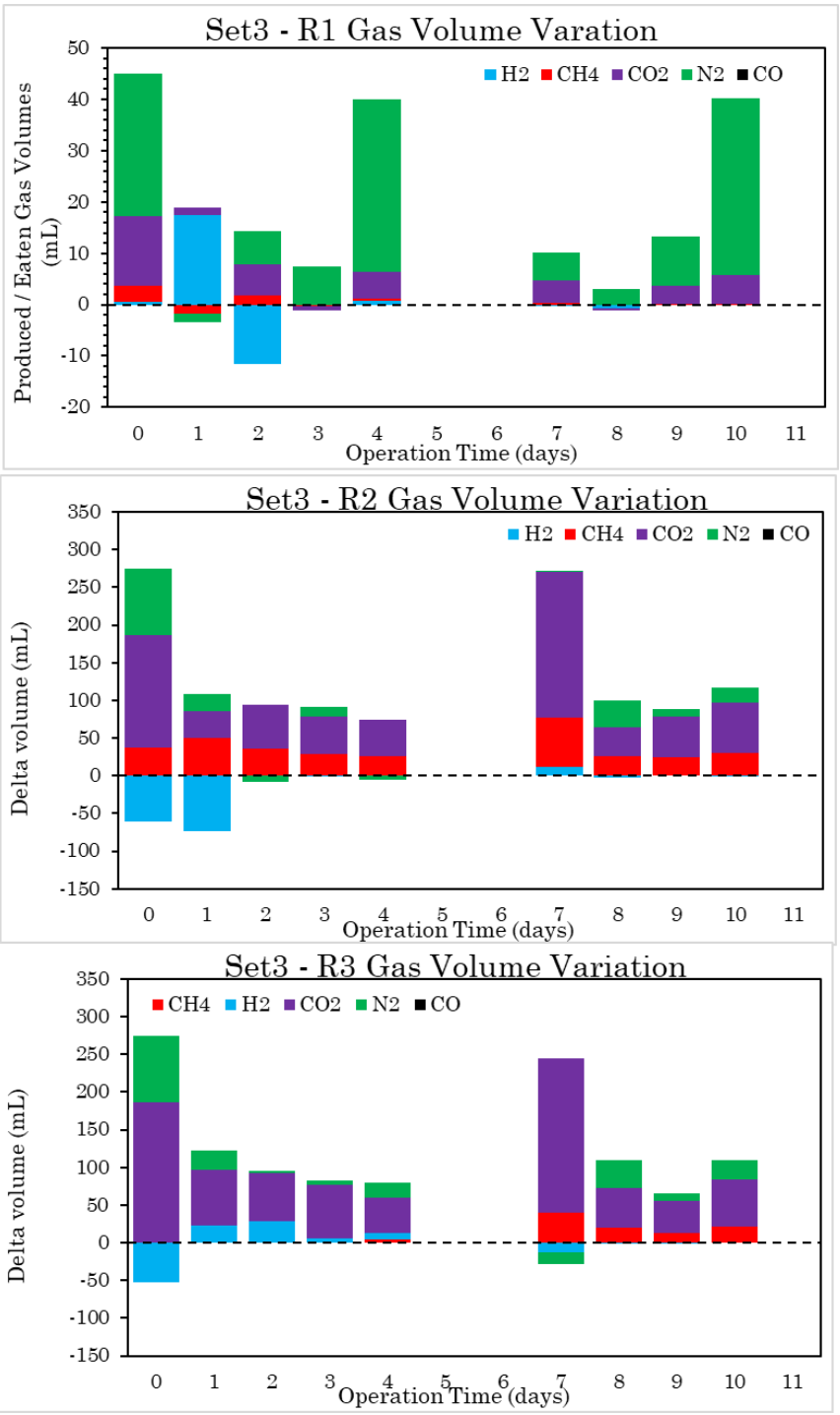

Figure 30. Gas volume variation in Set 3

Figure 31 shows the pH trend of Set3. All the reactors had a similar trend, which tends to acidification if not basified. On average reactor 1, 2, and 3 had a pH of 5.87, 5.66, and 5.70 respectively.

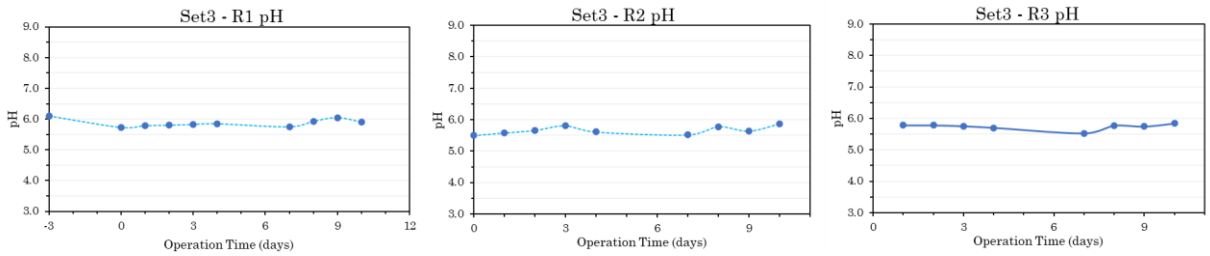

Figure 31. pH trend in Set 3

Input and output COD cumulative trend for Set3 is shown in *Figure 32*. Knowing the COD inside the reactor and COD input and output, the expected COD of the following day was determined (Expected COD). This value was then compared with the COD calculated the day after (Measured COD). In this way, a possible difference, which is a direct measure of a possible leak, biomass growth, or absorption inside the reactor, was determined (Difference). Initially, R1 had slightly a negative COD difference that changed into positive only on day 10. R2 and R3 had a similar trend, with a difference in COD that increased after day 7.

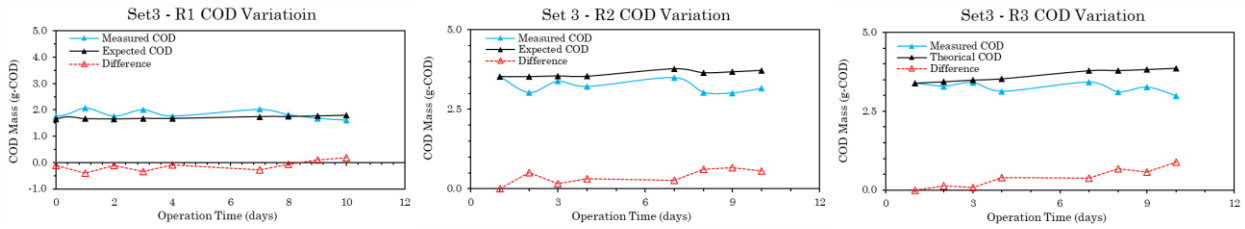

Figure 32. Measured, Expected, and Difference COD in Set 3

In *Figure 33* VFA concentration during Set 3 is presented. Initially, in all three reactors, acetic, propionic, iso-butyric, butyric, valeric, capric, heptanoic, and caprylic acids were present. At the end of the experiment, VFA composition of R1 mainly included acetic, propionic, and butyric acids. In fact, R1 had a negative trend of VFA concentration, with exceptions on days 1, 3 and 8. Concentrations of VFA in R2 were constant during the experiment, except for heptanoic and caprylic acid, which almost

disappeared at the end of set 3. VFA content of R3 was equal for the duration of the experiment. VFA's concentration in R2 and R2 were stably around, 12 $gCOD*L^{-1}$. Instead, VFA concentration in R1 decreased from 4 $gCOD*L^{-1}$ to 1.5 $gCOD*L^{-1}$.

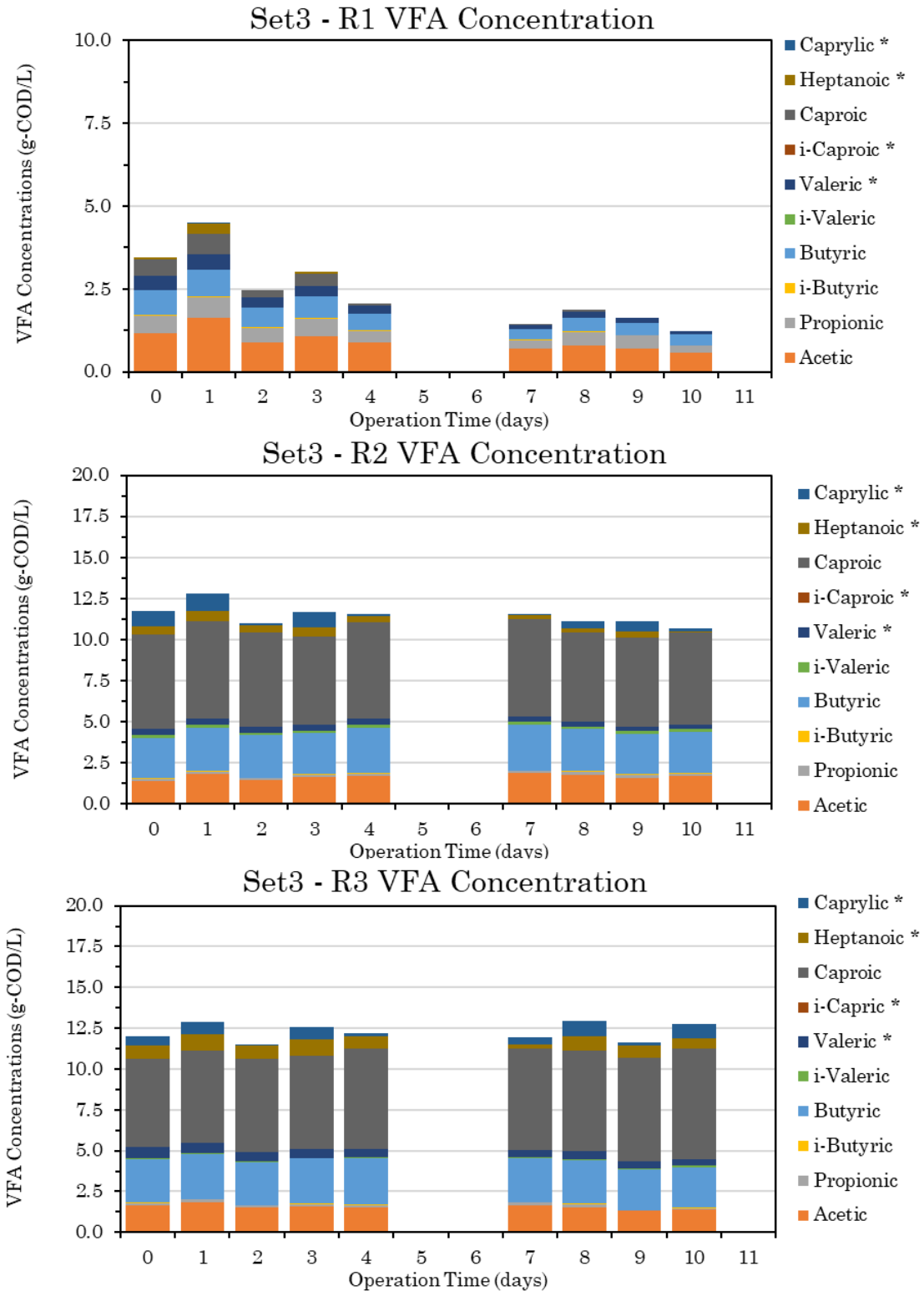

*Figure 33. VFA concentration in Set 3. *Old or Missing Response Factors; Iso-Byu = isobutyric Acid; iso-Val = isovaleric Acid; iso-Cap = isocaproic Acid*

COD input, output, and recovery, together with total gCOD of VFA produced and VFA yield ($gCOD_{VFA}/gCOD_{TOTAL\ OUTPUT\ LIQUID}$) was performed for 9 days, due to the limited time remaining. Results are shown in *Table 22*

Table 22. COD balance and VFA yield for Set 3

	R1	**R2**	**R3**	
Biomass enrichment	None	None	None	
Period of balance	9	9	9	*Days*
Total input	1.99	4.60	4.60	*gCOD*
Total output	1.83	3.40	3.11	*gCOD*
COD Recovery	92.1%	73.8%	67.5%	*%*
Total VFA	0.61	1.65	2.17	*gCOD*
VFA yield on output liquid	33.5%	48.5%	69.9%	*%*

The COD recovery for R1 was higher for all three Sets, 92.1%. Overall Pyrolysis product-to-VFA yield of R1 was 33.5%. This value, although close to that of previous experiments is remarkable considering that during set 3 no glucose was administered to R1. Nonetheless, it should be pointed out that those achievements could have been made by a partial underestimation of the input COD of the liquid, or the biochar could have released extra COD (possibly VFAs) from the previous experiments (*Figure 34*). However, the first consideration seems more adequate, in reason of prolonged monitoring of the system that should have provided the re-absorption of eventually VFAs.

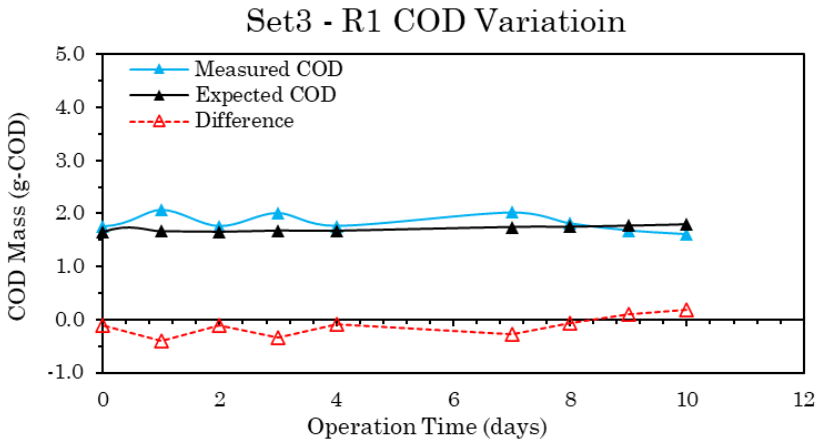

Figure 34. Negative COD balance in Set 3 R1

R2 and R3 had drastically decreased the COD recovery, from 95% to 70% after quitting the hydrogen supply. However, R2 recorded a significant increase in VFA COD yield, meanwhile, R3 had a decrease of 13% of VFA recovery. Both R2 and R3 produced methane in Set 3 experiment. Since for R2 and R3 there is a continuity between Set2 and Set3, in Figure 35 the two sets were combined to form a single picture in which the COD yields the main VFA are presented (in $gCOD/gCOD_{VFA}$). Both the reactors, after day 30, had a stable trend. R2 presents a higher quantity of acetic (about 15%), butyric (22%), and caproic acid (50%), meanwhile R3 provided a similar relative amount of acetic, valeric, and heptanoic acid (about 8-12%), with also butyric (28%) and caproic (40%). Seems that biochar enhances the production of VFA with an equal number of carbons. After the remotion of hydrogen, both reactors registered an unstable trend, especially for caproic and caprylic acid.

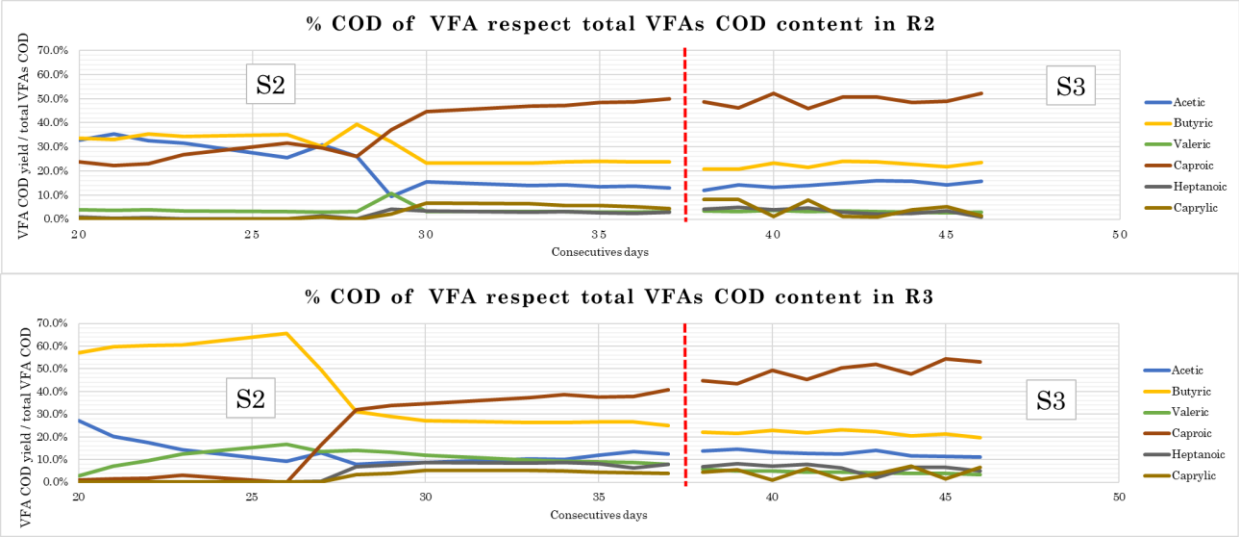

Figure 35. gCOD/gCOD$_{VFA}$. Comparison between R2 and R3 with and without hydrogen in Set2 and Set3. Redline divide Set2 and Set3

R1 was further investigated with silylation-GC.MS, to evaluate the degradation kinetic of WS pyrolysis products. The main degraded molecules founded are shown in *Table 23*.

Table 23. Molecules degraded in Set 3 R1 during the first 3 days. Data expressed as input and output concentration

	Total added	Total decrease	% degradation
	gCOD/L	gCOD/L	%COD
Levoglucosan	1.79	1.14	63.7%
3,4 -dihydroxy pentenoic acid	2.06	1.10	53.4%
Cyclooctane 1,2 dihydroxy	1.27	0.99	77.9%
Ethanediol	1.88	0.93	49.7%
Catechol	1.51	0.90	59.6%
2,5-hydroxy 1,4 dioxane	0.88	0.67	76.5%
1,6-anhydro galactofuranose	0.80	0.50	62.5%
2 Hydroxy Adipic Acid	0.82	0.46	56.6%
Hydroxy Acetic Acid	1.12	0.40	36.1%
Lactic Acid	0.27	0.10	36.7%

During the 3 days monitoring, the results suggested a degradation of levoglucosan equal to 1.14 gCOD*L^{-1} (63.7% of degradation), 3,4-dihydroxy pentenoic acid 1.10

gCOD*L^{-1} (53.4 % of degradation), Cyclooctane 1,2 dihydroxy 0.99 gCOD*L^{-1} (77.9% of degradation), Ethanediol 0.93 gCOD*L^{-1} (49.7 % of degradation), Catechol 0.90 gCOD*L^{-1} (% of degradation), 2,5-hydroxy 1,4 dioxane 0.67 gCOD*L^{-1} (76.5% of degradation), 1,6-anhydro galactofuranose 0.50 gCOD*L^{-1} (62.5% of degradation), 2 Hydroxy Adipic Acid 0.40 gCOD*L^{-1} (56.6% of degradation), Hydroxy Acetic Acid 0.40 gCOD*L^{-1} (36.1% of degradation), Lactic Acid 0.10 gCOD*L^{-1} (36.7% of degradation).

4 Conclusions

Pyrolysis has demonstrated the ability to convert more than the 50% of the biomass's COD into smaller molecules that are potentially fermentable. The yield of fermentable compounds increases with increasing heating rates, with up to 60-70% yield obtainable with optimized fast pyrolysis. Intermediate pyrolysis experiments allowed to reach an almost complete closure of COD balance. Results show that about half of biomass COD is converted into WS and gas approximately 35-45% of COD is retained into the biochar, and 10-15% of COD is converted into WI substances. Water-Insoluble fraction, which collects 13% of COD, had a poor degradation (10%), but the ability of the culture medium to solubilize it, opens the possibility of novel biotic and abiotic experiments. WS and gas, selected as candidates for biological conversion through MMC, retained 45% of the initial COD. The development of the biotrickling bed reactors in preliminary experiments highlight some critical issue in small-scale fermentation, namely leaks and losses that become relevant below the liter scale. Such issues were fixed through the sequential improvement of the reactor and methods, achieving an adequate COD balance of a validated system. This can be considered an experimental tool for reliable determination of yield and conversion of pyrolysis products. Within an acidogenic reactor (treated with BES as methanogen inhibitor) 20 gCOD/L of Wood derived WS was revealed unsuitable for the production of VFA even in presence of biochar. Slow adaptation with 10 gCOD/L shows a 30% conversion to VFA, and the final optimized experiments, performed with biochar and 10 gCOD/L of WS as input, showed a promising bioconversion, with a production of a significant amount of VFA and negligible methane production. Analysis of GC-MS detectable highlight main issue of WS conversions and suggest an important role of slow adaptation of microbial consortia to pyrothropic conditions. WS pyrolysis confirmed to be a challenging substrate, which requires slow adaptation of the

microbial consortia, and low concentration to allow faster conversions. On the other hand, hydrogen influenced the VFA production, stabilizing the concentrations of longer VFA. This ability can be used as an easy way to shift the type and yield of product in a biorefinery, potentially channeling the peaks of renewable energy (through electrolysis) into chemicals.

Although preliminary, work performed in this thesis provided the base for further investigations, which can pursue the optimization in order to increase the yields and productivities of pyrotrophic MMC. In conclusion, the anaerobic digestion of pyrolysis products is feasible but challenging. The methods developed in this thesis open up the potential to study the bioconversion of pyrolysis products and could be the first step of wider investigation. Several aspects could be investigated in future:

- The fate of each pyrolysis products and identification of most relevant toxic compounds (targeted detoxification)
- Effect of biomass type on pyrolysis product fermentation
- Pre-treatment of the biomass, in order to increase the yield of less toxic compounds
- Effect of pyrolysis conditions or catalyst in order to produce bioavailable pyrolysis products.

5 Annex

5.1 Water-Insolubles biodegradation tests

5.1.1 Water-Insolubles biodegradation test Methods

To evaluate the degradability of WI, batch tests were planned for a total duration of 20 days. 25 mL glass vials were used with rubber stoppers. 10 mL syringes were used to collect the gas. The experimental design and set-up are presented in *Figure 36* and *Table 24*.

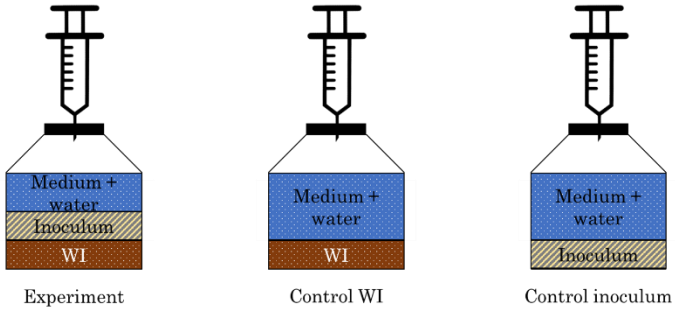

Figure 36. Experimental design of the WI experiments

Table 24. Set-up of the experiment

Component	WI Experiment	Control WI	Control inoculum
WI	0.1 g	0.1 g	0 g
Inoculum	10 mL	0 mL	10 mL
Medium	4 mL	4 mL	4 mL
Water	6 mL	16 mL	10 mL
Total volume	20 mL	20 mL	20 mL

For the Experiment and the Control WI, five vials in double were prepared and analyzed after 0, 5, 10, 15, and 20 days. For the Control inoculum, only one vial was left for the duration of the experiment, to evaluate the amount of gas produced. Initially the WI used was analyzed with silylation and VFA methods. Approximately 0.1 g of WI, were added to the vials. Inoculum, medium, and water were provided and, before the sealing with the rubber stopper, the vials were flushed under nitrogen to remove oxygen. All the vials were kept at 45 °C. The gases were analyzed with the GC-TCD method, liquid's COD, both total and soluble, was determined. Also, the liquid was analyzed with VFA and Silylation method (all the analysis can be found in Chapter 2.1). The samples taken at 5 and 20 days were further investigated, the liquid solution was mixed with a magnetic bar to disperse all the WI and both total and soluble COD were detected.

5.1.2 Water-Insolubles biodegradation test Results

As shown in this thesis WI pyrolysis products retain a significant portion of the chemical energy of the feedstock. Within preliminary experiments, all pyrolysis products (including WI) were provided to biological reactors, nonetheless, a clear indication of biodegradability of that fraction was not obtained due to several parameters involved (e.g. toxicity of WI and consequential interaction between WI and WS biodegradation). To understand the exact bioavailability of WI, anaerobic digestion of isolated WI was performed as shown in Figure 37. 9.25 gCOD/L of WI were mixed with inoculum and nutrients. Total COD values are extremely variable. In all the vials a negligible or null amount of biogas was produced. During the experiment, gradual solubilization of the WI was observed. Further experiments highlight the ability of the medium to solubilize and disperse the WI in water. In fact, the soluble COD for both the control and WI experiment was increased on an average of 3.5 gCOD/L respect to the initial soluble COD (*Figure 37*).

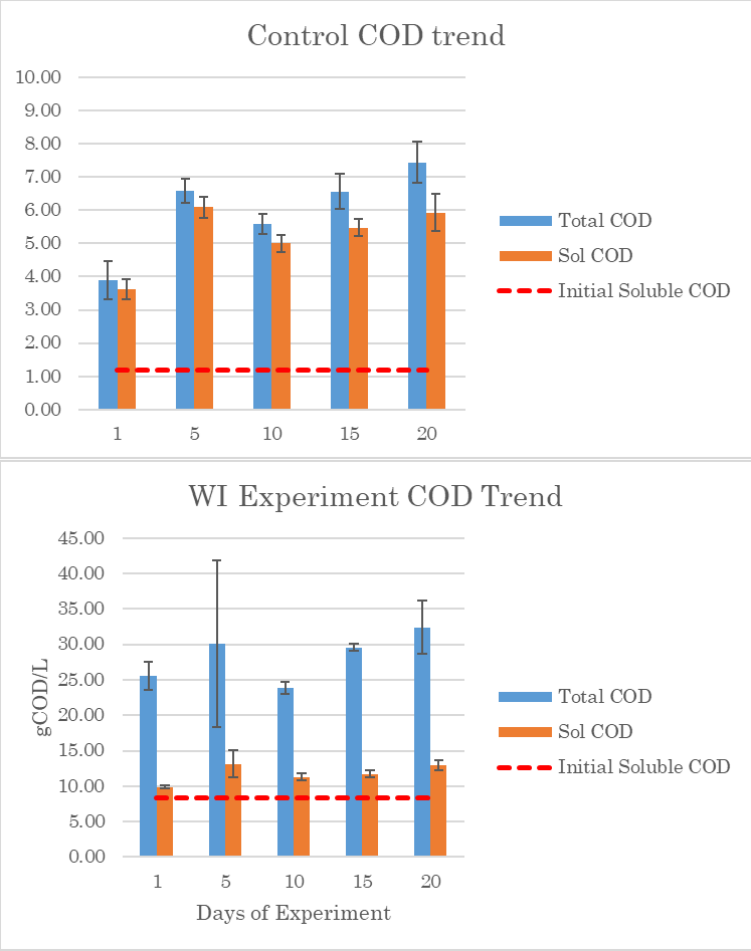

Figure 37. COD trend in the batch experiments

Two samples were further investigated to collect a total balance of inputs and outputs. In both experiments, a negative balance was detected for the total COD, while an increase of soluble COD was found (*Figure 38*).

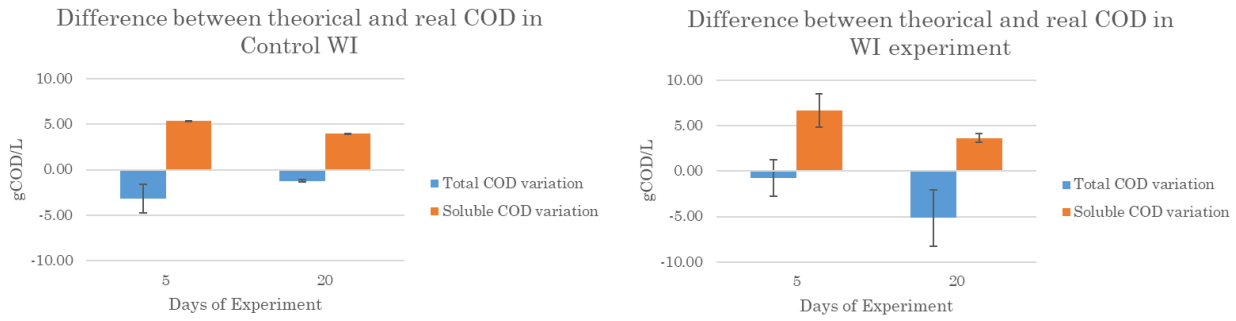

Figure 38. COD variation, respect the theorical, at day 5 and day 20

From the analysis result a decrease of levoglucosan in the vials with WI and bacteria, but an accumulation in the ones with only WI, probably for the solubilization of this compound (*Figure 39*).

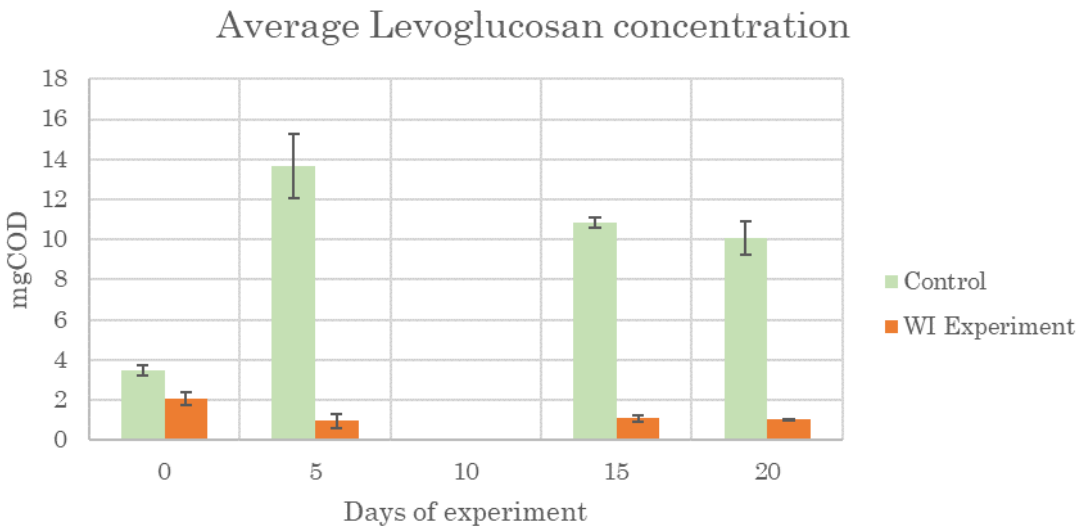

Figure 39. Average levoglucosan concentration during the experiments

A decrease of levoglucosan was noted also in the control. This suggests a possible aerobic degradation for the instauration of a slight bacterial activity in the control. At the same time, a major amount of 2,5-dimethyl Phenol was detected in the WI experiment but not in the control, this can be a possible product of the fermentation or the solubilization of it could be increased by the bacteria. A reverse situation was found for the 2-methoxy-4-methyl Phenol, which seems to be present only in the control (*Figure 40*).

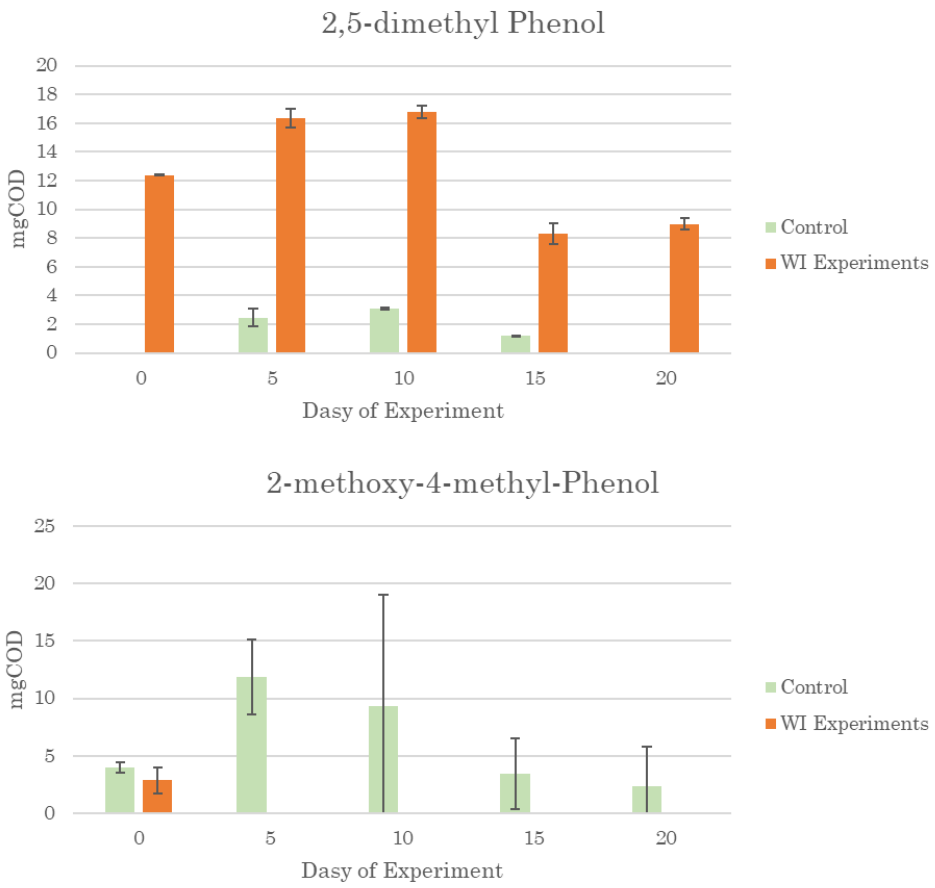

Figure 40. Two main compounds that differ in the WI experiment and the Control

Probably aerobic conditions establish in the vials during the experiments, with the consequent loss of total COD. However, the solubilization and dispersion of the WI could allow future tests on the degradation and procedural ways for the analysis and characterization.

5.2 Multiple gasometers script

```
const int totreading = 50;
float sample1[totreading];
int readnum = 0;
float total1 = 0;
float average1 = 0;
float volume11 = 0;
float volume12 = 0;


float sample2[totreading];
float total2 = 0;
float average2 = 0;
float volume21 = 0;
float volume22 = 0;


float sample3[totreading];
float total3 = 0;
float average3 = 0;
float volume31 = 0;
float volume32 = 0;


const int trigPin1 = 22;//pin connectretted to trig of ultrasound measurer
const int echoPin1 = 23;//pin connected to echo of ultrasound measurer

const int trigPin2 = 32;//pin connectretted to trig of ultrasound measurer
const int echoPin2 = 33;//pin connected to echo of ultrasound measurer

const int trigPin3 = 42;//pin connectretted to trig of ultrasound measurer
const int echoPin3 = 43;//pin connected to echo of ultrasound measurer

float duration1, cm1, duration2, cm2, duration3, cm3;



void setup() {
  // initialize serial communication:
  Serial.begin(9600);
  pinMode(trigPin1, OUTPUT);
  pinMode(echoPin1, INPUT);
  pinMode(trigPin2, OUTPUT);
  pinMode(echoPin2, INPUT);
  pinMode(trigPin3, OUTPUT);
  pinMode(echoPin3, INPUT);

}


void loop() {
```

```
  USDM1(); // measurement of gas amount in reactor 1


}


void USDM1() {
  // establish variables for duration of the ping,
  // and the distance result in inches and centimeters:

  if (readnum <= (totreading - 1)) {


    pinMode(trigPin1, OUTPUT);  //measuring another volume in the first
reactor
    digitalWrite(trigPin1, LOW);
    delayMicroseconds(2);
    digitalWrite(trigPin1, HIGH);
    delayMicroseconds(10);
    digitalWrite(trigPin1, LOW);


    pinMode(echoPin1, INPUT);
    duration1 = pulseIn(echoPin1, HIGH);
    cm1 = duration1 / 29 / 2;

    sample1[readnum] = cm1;
    total1 = total1 + sample1[readnum];



    pinMode(trigPin2, OUTPUT); //measuring another volume in the second
reactor
    digitalWrite(trigPin2, LOW);
    delayMicroseconds(2);
    digitalWrite(trigPin2, HIGH);
    delayMicroseconds(10);
    digitalWrite(trigPin2, LOW);


    pinMode(echoPin2, INPUT);
    duration2 = pulseIn(echoPin2, HIGH);
    cm2 = duration2 / 29 / 2;

    sample2[readnum] = cm2;
    total2 = total2 + sample2[readnum];



   pinMode(trigPin3, OUTPUT);  //measuring another volume in the third
reactor
    digitalWrite(trigPin3, LOW);
    delayMicroseconds(2);
    digitalWrite(trigPin3, HIGH);
    delayMicroseconds(10);
```

```
    digitalWrite(trigPin3, LOW);


    pinMode(echoPin3, INPUT);
    duration3 = pulseIn(echoPin3, HIGH);
    cm3 = duration3 / 29 / 2;

    sample3[readnum] = cm3;
    total3 = total3 + sample3[readnum];



    readnum = readnum + 1; //adding 1 to the if cycle
    delay (100);
  }

  else {

    average1 = total1 / totreading;
    average2 = total2 / totreading;
    average3 = total3 / totreading;


//In this section double calibrations are provided

    volume11 = (-267.44*average1+2323.3); //R_square of 0.9991
    volume21 = (-264*average2+2169.6); //R_square of 0.9966
    volume31 = (-226.42*average3+2102.9); //R_square of 0.9963



   volume12 = ((0.0003*volume11*volume11)+(0.8905*volume11)-(0.3104));
//R_square of 0.9997
   volume22 = ((0.0004*volume21*volume21)+(0.8751*volume11)+(22.836));
//R_square of 0.9982
   volume32 = ((0.0002*volume31*volume21)+(0.8900*volume11)+(6.0714));
//R_square of 0.9878



   if(volume12<0){
    volume12=0;
   }

   if(volume22<0){
    volume22=0;
   }

   if(volume32<0){
    volume32=0;
   }



    Serial.print(volume12, 0);
    Serial.print("   ");
```

```
Serial.print(volume22, 0);
Serial.print("    ");
Serial.print(volume32, 0);
Serial.print("\r");


  readnum = 0;

  total1 = 0;
  total2 = 0;
  total3 = 0;

  average1 = 0;
  average2 = 0;
  average3 = 0;

  volume11 = 0;
  volume21 = 0;
  volume31 = 0;

  volume12 = 0;
  volume22 = 0;
  volume32 = 0;

  //delay(100);

  delay(55100);
   }

}
```

5.3 Automatic feeding system script

```
/*_____________VARABLES DECLARATION_________*/
const int totreading = 50;
int readnum = 0;
float total = 0;

float duration, cm;
int Vdischarge = 0; //used for the switch function


float average1 = 0;
float volume11 = 0;
float volume12 = 0;


float average2 = 0;
float volume21 = 0;
float volume22 = 0;


float average3 = 0;
float volume31 = 0;
float volume32 = 0;


/*_____________________________TIME FUNCTIONS_____________________________*/
unsigned long int tgas;
unsigned long int tliquid;
const unsigned long int liquid_feeding_time_1 = 12700 ; //L determine the
duration, in millisecond, of the liquid feeding for PUMP1
const unsigned long int liquid_feeding_time_2 = 14114 ; //L determine the
duration, in millisecond, of the liquid feeding for PUMP2
const unsigned long int liquid_feeding_time_3 = 12200 ; //L determine the
duration, in millisecond, of the liquid feeding for PUMP3
const unsigned long int gas_control_time = 86360986; //G   determine, in
milliseconds, the time of normal activity and gas check 23h 59min 20s 986ms
unsigned long int liquid_check;
unsigned long int gas_check;
const unsigned long int pause_period = 300000 ; //P  pause for the gas check
of 5 min
unsigned long int pause_check;


/* _____________________PIN    DECLARATION_________*/

const int trigPin1 = 22;//pin connectretted to trig of ultrasound measurer
const int echoPin1 = 23;//pin connected to echo of ultrasound measurer

const int trigPin2 = 32; //pin connectretted to trig of ultrasound measurer
const int echoPin2 = 33;//pin connected to echo of ultrasound measurer

const int trigPin3 = 42;//pin connectretted to trig of ultrasound measurer
const int echoPin3 = 43;//pin connected to echo of ultrasound measurer
```

```
const int valvegas1 = 8;
const int valvegas2 = 5;
const int valvegas3 = 2;

const int pump1 = 9;
const int pump2 = 6;
const int pump3 = 3;


/*____________FUNCTION DECLARATION___________*/


/*_____________________________first react_____________________________________*/

float R1VOLUME() {
  /*FUNCTION THAT MEASURE THE VOLUME IN THE FIRST GASBAG AND RETURN THE
VOLUME MEASURE*/
  // establish variables for duration of the ping,
  // and the distance result in inches and centimeters:

  while (readnum < totreading) {


    digitalWrite(trigPin1, LOW);
    delayMicroseconds(2);
    digitalWrite(trigPin1, HIGH);
    delayMicroseconds(10);
    digitalWrite(trigPin1, LOW);



    duration = pulseIn(echoPin1, HIGH);

    cm = duration / 29 / 2;

    total = total + cm;

    readnum += 1;

    average1 = total / totreading;
    delay(10);
  }


  volume11 = (-267.44 * average1 + 2323.3); //R_square of 0.9991
  volume12 = ((0.0003 * volume11 * volume11) + (0.8905 * volume11) -
(0.3104)); //R_square of 0.9997

  if (volume12 < 0) {
    volume12 = 0;
  }

  readnum = 0;
  total = 0;
  average1 = 0;
```

```
  volume11 = 0;
  //Serial.print("Volume1 is:___");
  //Serial.println(volume12, 0);
  return volume12;
}



/*_____________________second reactor_____________________*/

float R2VOLUME() {
  /*FUNCTION THAT MEASURE THE VOLUME IN THE SECOND GASBAG AND RETURN THE
VOLUME MEASURE*/
  // establish variables for duration of the ping,
  // and the distance result in inches and centimeters:

  while (readnum < (totreading)) {

    digitalWrite(trigPin2, LOW);
    delayMicroseconds(2);
    digitalWrite(trigPin2, HIGH);
    delayMicroseconds(10);
    digitalWrite(trigPin2, LOW);



    duration = pulseIn(echoPin2, HIGH);

    cm = duration / 29 / 2;

    total = total + cm;

    readnum += 1;
    average2 = total / totreading;
    delay(10);

  }

  volume21 = (-236.7 * average2 + 1899.1); //R_square of 0.9975
  volume22 = ((-0.0002 * volume21 * volume21) + (1.1111 * volume21) -
(16.113)); //R_square of 0.9994


  if (volume22 < 0) {
    volume22 = 0;
  }

  readnum = 0;
  total = 0;
  average2 = 0;
  volume21 = 0;

  //Serial.print("Volume2 is:___");
  //Serial.println(volume22, 0);
  return volume22;
}
```

```
/*_____________________third reactor_____________________________________*/
float R3VOLUME() {
  /*FUNCTION THAT MEASURE THE VOLUME IN THE THIRD GASBAG AND RETURN THE
VOLUME MEASURE*/
  // establish variables for duration of the ping,
  // and the distance result in inches and centimeters:

  while (readnum < (totreading ))
{                                                                    //L
'ERRORE è IN QUEDTI CILCI WHILE :(


    digitalWrite(trigPin3, LOW);
    delayMicroseconds(2);
    digitalWrite(trigPin3, HIGH);
    delayMicroseconds(10);
    digitalWrite(trigPin3, LOW);



    duration = pulseIn(echoPin3, HIGH);

    cm = duration / 29 / 2;

    total = total + cm;

    readnum += 1;
    average3 = total / totreading;
    delay(10);

  }

  volume31 = (-226.42 * average3 + 2102.9); //R_square of 0.9963
  volume32 = ((0.0002 * volume31 * volume31) + (0.8900 * volume31) +
(6.0714)); //R_square of 0.9889


  if (volume32 < 0) {
    volume32 = 0;
  }

  readnum = 0;
  total = 0;
  average3 = 0;
  volume31 = 0;
  //Serial.print("Volume3 is:___");
  //Serial.println(volume32, 0);
  return volume32;
}


/*____________________dischargin gas funcions_____________________________*/

void discharge1() {
  Serial.println("Reactor 1 Gas Dircharging");
```

```
  R1VOLUME();
  while (volume12 > 400) {
    digitalWrite(valvegas1, LOW);
    R1VOLUME();
  }
}


void discharge2() {
  Serial.println("Reactor 2 Gas Dircharging");
  R2VOLUME();
  while (volume22 > 400) {
    digitalWrite(valvegas2, LOW);
    R2VOLUME();
  }
}


void discharge3() {
  Serial.println("Reactor 3 Gas Dircharging");
  R3VOLUME();
  while (volume32 > 400) {
    digitalWrite(valvegas3, LOW);
    R3VOLUME();
  }
}



/*_____________________MAIN FUNCTIONS DECLARATION_____________*/


void setup() {
  // initialize serial communication:

  Serial.begin(9600);
  pinMode(trigPin1, OUTPUT);
  pinMode(trigPin2, OUTPUT);
  pinMode(trigPin3, OUTPUT);
  pinMode(echoPin1, INPUT);
  pinMode(echoPin2, INPUT);
  pinMode(echoPin3, INPUT);


  pinMode(valvegas1, OUTPUT);
  pinMode(valvegas2, OUTPUT);
  pinMode(valvegas3, OUTPUT);

  pinMode(pump1, OUTPUT);
  pinMode(pump2, OUTPUT);
  pinMode(pump3, OUTPUT);
  Serial.println("I start");



}
```

```
void loop() {
  digitalWrite(valvegas1, HIGH);
  digitalWrite(valvegas2, HIGH);
  digitalWrite(valvegas3, HIGH);

  digitalWrite(pump1, HIGH);
  digitalWrite(pump2, HIGH);
  digitalWrite(pump3, HIGH);



  /*____________________gas check_____________________________*/

  Serial.println("Gas cycle begin");

  tgas = millis();
  //Serial.print("tgas is___");
  //Serial.println(tgas);
  //Serial.print("gas_control_time is___");
  //Serial.println(gas_control_time);
  gas_check = tgas + gas_control_time;
  //Serial.print("gas_check is___");
  //Serial.println(gas_check, 0);

  while (tgas < gas_check) {

  /*_____________________Pause for 5 mins_____________________*/
  Serial.println("Pause");
  tgas = millis();
  pause_check = tgas + pause_period;
  while (tgas < pause_check) {
    tgas = millis();
  }
  Serial.println("End pause");



    R1VOLUME();
    //Serial.println("I read R1");
    if (volume12 > 500) {
      Vdischarge += 1;
      //Serial.println("Vdisch +1");

    }

    R2VOLUME();
    if (volume22 > 500) {
      Vdischarge += 3;
      //Serial.println("Vdisch +3");
    }
    //Serial.println("I read R2");

    R3VOLUME();
```

```
    if (volume32 > 500) {
      Vdischarge += 5;
      //Serial.println("Vdisch +5");
    }

    //Serial.println("I read R3");

    //Serial.print("Vdischarge is__");
    //Serial.println(Vdischarge);

    //temporany restitution of the volumes

    Serial.print(volume12, 0);
    Serial.print("           ");
    Serial.print(volume22, 0);
    Serial.print("           ");
    Serial.println(volume32, 0);

    //now each case has only one Vdischarge value, ex Vdischarge=8 gasbag 2
and gasbag 3 are full, Vdischarge=4 gasbag 1 and 3 are full,
    //Vdischarge=9 all to be empty!


    switch (Vdischarge) { //find what to do with the gas

      case 1: //fisrt reactor full
        //Serial.println("switch case 1");
        discharge1();
        digitalWrite(valvegas1, HIGH);


        break;

      case 3: //second reactor full
        //Serial.println("switch case 3");
        discharge2();
        digitalWrite(valvegas2, HIGH);

        break;

      case 5: //third reactor full
        //Serial.println("switch case 5");
        discharge3();
        digitalWrite(valvegas3, HIGH);

        break;

      case 4: //first and second full
        //Serial.println("switch case 4");
        discharge1();
        digitalWrite(valvegas1, HIGH);
        discharge2();
        digitalWrite(valvegas2, HIGH);
        break;

      case 6: //first and third full
        //Serial.println("switch case 6");
```

```
      discharge1();
      digitalWrite(valvegas1, HIGH);
      discharge3();
      digitalWrite(valvegas3, HIGH);

      break;

    case 8: //second and third full
      //Serial.println("switch case 8");
      discharge2();
      digitalWrite(valvegas2, HIGH);
      discharge3();
      digitalWrite(valvegas3, HIGH);
      break;

    case 9: //all full
      //Serial.println("switch case 9");
      discharge1();
      digitalWrite(valvegas1, HIGH);
      discharge2();
      digitalWrite(valvegas2, HIGH);
      discharge3();
      digitalWrite(valvegas3, HIGH);
      break;
  }

  Vdischarge = 0;
  delay(500);
  tgas = millis();
  //Serial.print("New tgas is___");
  //Serial.println(tgas);
}


/*_____________________liquid change_____________________________*/

Serial.println("Reactor 1 Feeding");

tliquid = millis();
liquid_check = tliquid + liquid_feeding_time_1;

while (tliquid < liquid_check) {

  digitalWrite(pump1, LOW);
  tliquid = millis();
}

digitalWrite(pump1, HIGH);


Serial.println("Reactor 2 Feeding");
tliquid = millis();
liquid_check = tliquid + liquid_feeding_time_2;
while (tliquid < liquid_check) {

  digitalWrite(pump2, LOW);
```

```
    tliquid = millis();
  }

  digitalWrite(pump2, HIGH);


  Serial.println("Reactor 3 Feeding");
  tliquid = millis();
  liquid_check = tliquid + liquid_feeding_time_3;
  while (tliquid < liquid_check) {

    digitalWrite(pump3, LOW);

    tliquid = millis();
  }

  digitalWrite(pump3, HIGH);



  // Serial.print("I've finish to pump the liquids and the time is:     ");
  //Serial.println(millis());

  /* Serial.print(volume12, 0);
    Serial.print("   ");

    Serial.print(volume22, 0);
    Serial.print("   ");

    Serial.println(volume32, 0); */


  volume12 = 0;

  volume22 = 0;

  volume32 = 0;

  Vdischarge = 0;

  tgas = 0;

  tliquid = 0;

  gas_check = 0;

  liquid_check = 0;

  delay(500);
}
```

5.4 Pulsing recirculation script

```
/*_____________VARABLES DECLARATION_________*/
const int totreading = 50;
int readnum = 0;
float total = 0;

float duration, cm;
int Vdischarge = 0; //used for the switch function


float average1 = 0;
float volume11 = 0;
float volume12 = 0;


float average2 = 0;
float volume21 = 0;
float volume22 = 0;


float average3 = 0;
float volume31 = 0;
float volume32 = 0;


/*_____________________________TIME FUNCTIONS_____________________________*/
unsigned long int pause = 0; //used  as timer for the pause
unsigned long int flow = 0; //used as timer for the flow
unsigned long int pause_check = 0; //used for the while cycle
unsigned long int flow_check = 0; //used for the while cycle
const unsigned long int pause_duration = 15000 ; //duration of the pause, 15
s
const unsigned long int flow_duration = 5000 ; //pump flowing time, 5s



/* _____________________PIN    DECLARATION_________*/

const int trigPin1 = 22;//pin connectretted to trig of ultrasound measurer
const int echoPin1 = 23;//pin connected to echo of ultrasound measurer

const int trigPin2 = 32; //pin connectretted to trig of ultrasound measurer
const int echoPin2 = 33;//pin connected to echo of ultrasound measurer

const int trigPin3 = 42;//pin connectretted to trig of ultrasound measurer
const int echoPin3 = 43;//pin connected to echo of ultrasound measurer

const int pumppin = 8;



/*_____________FUNCTION DECLARATION___________*/



/*_____________________________first react_____________________________*/
```

```
float R1VOLUME() {
  /*FUNCTION THAT MEASURE THE VOLUME IN THE FIRST GASBAG AND RETURN THE
VOLUME MEASURE*/
  // establish variables for duration of the ping,
  // and the distance result in inches and centimeters:

  while (readnum < totreading) {


    digitalWrite(trigPin1, LOW);
    delayMicroseconds(2);
    digitalWrite(trigPin1, HIGH);
    delayMicroseconds(10);
    digitalWrite(trigPin1, LOW);



    duration = pulseIn(echoPin1, HIGH);

    cm = duration / 29 / 2;

    total = total + cm;

    readnum += 1;

    average1 = total / totreading;
    delay(10);
  }


  volume11 = (-267.44 * average1 + 2323.3); //R_square of 0.9991
  volume12 = ((0.0003 * volume11 * volume11) + (0.8905 * volume11) -
(0.3104)); //R_square of 0.9997

  if (volume12 < 0) {
    volume12 = 0;
  }

  readnum = 0;
  total = 0;
  //Serial.print("Volume1 is:___");
  //Serial.println(volume12, 0);
  return volume12;
}



/*____________________second reactor____________________*/

float R2VOLUME() {
  /*FUNCTION THAT MEASURE THE VOLUME IN THE SECOND GASBAG AND RETURN THE
VOLUME MEASURE*/
  // establish variables for duration of the ping,
  // and the distance result in inches and centimeters:

  while (readnum < (totreading)) {
```

```
    digitalWrite(trigPin2, LOW);
    delayMicroseconds(2);
    digitalWrite(trigPin2, HIGH);
    delayMicroseconds(10);
    digitalWrite(trigPin2, LOW);



    duration = pulseIn(echoPin2, HIGH);

    cm = duration / 29 / 2;

    total = total + cm;

    readnum += 1;
    average2 = total / totreading;
    delay(10);

  }

  volume21 = (-236.7 * average2 + 1899.1); //R_square of 0.9975
  volume22 = ((-0.0002 * volume21 * volume21) + (1.1111 * volume21) -
(16.113)); //R_square of 0.9994


  if (volume22 < 0) {
    volume22 = 0;
  }

  readnum = 0;
  total = 0;

  //Serial.print("Volume2 is:___");
  //Serial.println(volume22, 0);
  return volume22;
}



/*_____________________third reactor_____________________________________*/
float R3VOLUME() {
  /*FUNCTION THAT MEASURE THE VOLUME IN THE THIRD GASBAG AND RETURN THE
VOLUME MEASURE*/
  // establish variables for duration of the ping,
  // and the distance result in inches and centimeters:

  while (readnum < (totreading ))
{                                                                          //L
'ERRORE è IN QUEDTI CILCI WHILE :(


    digitalWrite(trigPin3, LOW);
    delayMicroseconds(2);
    digitalWrite(trigPin3, HIGH);
    delayMicroseconds(10);
    digitalWrite(trigPin3, LOW);
```

```
    duration = pulseIn(echoPin3, HIGH);

    cm = duration / 29 / 2;

    total = total + cm;

    readnum += 1;
    average3 = total / totreading;
    delay(10);

  }

  volume31 = (-226.42 * average3 + 2102.9); //R_square of 0.9963
  volume32 = ((0.0002 * volume31 * volume31) + (0.8900 * volume31) +
(6.0714)); //R_square of 0.9889


  if (volume32 < 0) {
    volume32 = 0;
  }

  readnum = 0;
  total = 0;

  //Serial.print("Volume3 is:___");
  //Serial.println(volume32, 0);

  return volume32;
}



/*_____________________________MAIN FUNCTIONS
DECLARATION_____________________________________________*/


void setup() {
  // initialize serial communication:

  Serial.begin(9600);
  pinMode(trigPin1, OUTPUT);
  pinMode(trigPin2, OUTPUT);
  pinMode(trigPin3, OUTPUT);
  pinMode(echoPin1, INPUT);
  pinMode(echoPin2, INPUT);
  pinMode(echoPin3, INPUT);


  pinMode(pumppin, OUTPUT);


}
```

```
void loop() {
  digitalWrite(pumppin, HIGH);


  //Activating for 5 seconds the pump
  flow = millis();
  flow_check = flow + flow_duration;

  while (flow < flow_check) {
    digitalWrite(pumppin, LOW);
    flow = millis();
  }

  //turn off for 15 seconds the pumps
  digitalWrite(pumppin, HIGH);

  pause = millis();
  pause_check = pause + pause_duration;

  while (pause < pause_check) {
    pause = millis();
  }


  R1VOLUME();
  R2VOLUME();
  R3VOLUME();

  Serial.print(volume12, 0);
  Serial.print("      ");
  Serial.print(volume22, 0);
  Serial.print("      ");
  Serial.println(volume32, 0);
  //Serial.print(volume32, 0);
  //Serial.print("\r");

}
```

Bibliography

[1] S. Fernando, S. Adhikari, C. Chandrapal, and N. Murali, "Biorefineries: Current status, challenges, and future direction," *Energy and Fuels*, vol. 20, no. 4. American Chemical Society , pp. 1727–1737, Jul-2006, doi: 10.1021/ef060097w.

[2] D. L. Van Dyne, M. G. Blase, and L. D. Clements, "A Strategy for Returning Agriculture and Rural America to Long-Term Full Employment Using Biomass Refineries." https://hort.purdue.edu/newcrop/proceedings1999/v4-114.html (accessed Dec. 31, 2020).

[3] M. T. Agler, B. A. Wrenn, S. H. Zinder, and L. T. Angenent, "Waste to bioproduct conversion with undefined mixed cultures: The carboxylate platform," *Trends in Biotechnology*, vol. 29, no. 2. Elsevier Current Trends, pp. 70–78, 01-Feb-2011, doi: 10.1016/j.tibtech.2010.11.006.

[4] A. V. Bridgwater, "Review of fast pyrolysis of biomass and product upgrading," *Biomass and Bioenergy*, vol. 38, pp. 68–94, 2012, doi: 10.1016/j.biombioe.2011.01.048.

[5] D. Mohan, C. U. Pittman, and P. H. Steele, "Pyrolysis of wood/biomass for bio-oil: A critical review," *Energy and Fuels*, vol. 20, no. 3. American Chemical Society , pp. 848–889, May-2006, doi: 10.1021/ef0502397.

[6] F. X. Collard and J. Blin, "A review on pyrolysis of biomass constituents: Mechanisms and composition of the products obtained from the conversion of cellulose, hemicelluloses and lignin," *Renewable and Sustainable Energy Reviews*, vol. 38. Elsevier Ltd, pp. 594–608, 01-Oct-2014, doi: 10.1016/j.rser.2014.06.013.

[7] A. P. Pinheiro Pires *et al.*, "Challenges and opportunities for bio-oil refining: A review," *Energy and Fuels*, vol. 33, no. 6. American Chemical Society, pp. 4683–4720, 20-Jun-2019, doi: 10.1021/acs.energyfuels.9b00039.

[8] B. A. Black *et al.*, "Aqueous Stream Characterization from Biomass Fast Pyrolysis and Catalytic Fast Pyrolysis," *ACS Sustain. Chem. Eng.*, vol. 4, no. 12, pp. 6815–6827, Dec. 2016, doi: 10.1021/acssuschemeng.6b01766.

[9] F. Stankovikj, A. G. McDonald, G. L. Helms, M. V. Olarte, and M. Garcia-Perez, "Characterization of the Water-Soluble Fraction of Woody Biomass Pyrolysis Oils," *Energy and Fuels*, vol. 31, no. 2, pp. 1650–1664, Feb. 2017, doi: 10.1021/acs.energyfuels.6b02950.

[10] N. Charon *et al.*, "Multi-technique characterization of fast pyrolysis oils," *J. Anal. Appl. Pyrolysis*, vol. 116, pp. 18–26, Nov. 2015, doi: 10.1016/j.jaap.2015.10.012.

[11] M. Garcia-Perez, A. Chaala, H. Pakdel, D. Kretschmer, and C. Roy, "Characterization of bio-oils in chemical families," *Biomass and Bioenergy*, vol. 31, no. 4, pp. 222–242, Apr. 2007, doi: 10.1016/j.biombioe.2006.02.006.

[12] C. Branca, P. Giudicianni, and C. Di Blasi, "GC/MS characterization of liquids generated from low-temperature pyrolysis of wood," *Ind. Eng. Chem. Res.*, vol. 42, no. 14, pp. 3190–3202, Jul. 2003, doi: 10.1021/ie030066d.

[13] R. Sakthivel, K. Ramesh, P. M. Shameer, and R. Purnachandran, "A Complete Analytical Characterization of Products Obtained from Pyrolysis of Wood Barks of Calophyllum inophyllum," *Waste and Biomass Valorization*, vol. 10, no. 8, pp. 2319–2333, Aug. 2019, doi: 10.1007/s12649-018-0236-7.

[14] A. Sına, B. in Uskan, and S. Gülbay, "Detailed characterization of the pyrolytic liquids obtained by pyrolysis of sawdust," *J. Anal. Appl. Pyrolysis*, vol. 90, pp. 48–52, 2011, doi: 10.1016/j.jaap.2010.10.003.

[15] D. Ravelli and C. Samori, "Biomass Valorization: Sustainable Methods for the Production of Chemicals," *iI press*, 2021. .

[16] R. Kleerebezem and M. C. van Loosdrecht, "Mixed culture biotechnology for bioenergy production," *Current Opinion in Biotechnology*, vol. 18, no. 3. Elsevier Current Trends, pp. 207–212, 01-Jun-2007, doi: 10.1016/j.copbio.2007.05.001.

[17] R. Kleerebezem and M. C. van Loosdrecht, "Mixed culture biotechnology for bioenergy production," *Curr. Opin. Biotechnol.*, vol. 18, no. 3, pp. 207–212, 2007, doi: 10.1016/j.copbio.2007.05.001.

[18] K. W. Hanselmann, "Microbial energetics applied to waste repositories," *Experientia*, vol. 47, no. 7. Birkhäuser-Verlag, pp. 645–687, Jul-1991, doi: 10.1007/BF01958816.

[19] R. Kleerebezem, B. Joosse, R. Rozendal, and M. C. M. Van Loosdrecht, "Anaerobic digestion without biogas?," *Reviews in Environmental Science and Biotechnology*, vol. 14, no. 4. Springer Netherlands, pp. 787–801, 01-Dec-2015, doi: 10.1007/s11157-015-9374-6.

[20] R. C. Brown, "Hybrid thermochemical/biological processing: Putting the cart before the horse?," in *Applied Biochemistry and Biotechnology*, 2007, vol. 137–140, no. 1–12, pp. 947–956, doi: 10.1007/s12010-007-9110-y.

[21] C. Torri and D. Fabbri, "Biochar enables anaerobic digestion of aqueous phase from intermediate pyrolysis of biomass," *Bioresour. Technol.*, vol. 172, pp. 335–341, Sep. 2014, doi: 10.1016/j.biortech.2014.09.021.

[22] Y. Shen, L. Jarboe, R. Brown, and Z. Wen, "A thermochemical-biochemical hybrid processing of lignocellulosic biomass for producing fuels and chemicals," *Biotechnology Advances*, vol. 33, no. 8. Elsevier Inc., pp. 1799–1813, 01-Dec-2015, doi: 10.1016/j.biotechadv.2015.10.006.

[23] C. Torri, G. Pambieri, C. Gualandi, M. Piraccini, A. G. Rombolà, and D. Fabbri, "Evaluation of the potential performance of hyphenated pyrolysis-anaerobic digestion (Py-AD) process for carbon negative fuels from woody biomass," *Renew. Energy*, vol. 148, pp. 1190–1199, Apr. 2020, doi: 10.1016/j.renene.2019.10.025.

[24] S. S. Liaw, V. H. Perez, R. J. M. Westerhof, G. F. David, C. Frear, and M. Garcia-Perez, "Biomethane Production from Pyrolytic Aqueous Phase: Biomass Acid Washing and Condensation Temperature Effect on the Bio-oil and Aqueous Phase Composition," *Bioenergy Res.*, vol. 13, no. 3, pp. 878–886, Sep. 2020, doi: 10.1007/s12155-020-10100-3.

[25] S. S. Liaw, C. Frear, W. Lei, S. Zhang, and M. Garcia-Perez, "Anaerobic digestion of C1-C4 light oxygenated organic compounds derived from the torrefaction of lignocellulosic materials," *Fuel Process. Technol.*, vol. 131, pp. 150–158, Mar. 2015, doi: 10.1016/j.fuproc.2014.11.012.

[26] V. De Groof, M. Coma, T. Arnot, D. J. Leak, and A. B. Lanham, "Medium Chain Carboxylic Acids from Complex Organic Feedstocks by Mixed Culture Fermentation," *Molecules*, vol. 24, no. 3, p. 398, Jan. 2019, doi: 10.3390/molecules24030398.

[27] D. Arslan, K. J. J. Steinbusch, L. Diels, H. De Wever, C. J. N. Buisman, and H. V. M. Hamelers, "Effect of hydrogen and carbon dioxide on carboxylic acids patterns in mixed culture fermentation," *Bioresour. Technol.*, vol. 118, pp. 227–234, 2012, doi: 10.1016/j.biortech.2012.05.003.

[28] S. A. Channiwala and P. P. Parikh, "A unified correlation for estimating HHV of solid, liquid and gaseous fuels," *Fuel*, vol. 81, no. 8, pp. 1051–1063, 2002, doi: 10.1016/S0016-2361(01)00131-4.

[29] M. Ghidotti, D. Fabbri, C. Torri, and S. Piccinini, "Determination of volatile fatty acids in digestate by solvent extraction with dimethyl carbonate and gas chromatography-mass spectrometry," *Anal. Chim. Acta*, vol. 1034, pp. 92–101, Nov. 2018, doi: 10.1016/j.aca.2018.06.082.

[30] L. Busetto, D. Fabbri, R. Mazzoni, M. Salmi, C. Torri, and V. Zanotti, "Application of the Shvo catalyst in homogeneous hydrogenation of bio-oil obtained from pyrolysis of white poplar: New mild upgrading conditions," *Fuel*, vol. 90, no. 3, pp. 1197–1207, Mar. 2011, doi: 10.1016/j.fuel.2010.10.036.

[31] L. Fagernäs, E. Kuoppala, K. Tiilikkala, and A. Oasmaa, "Chemical composition of birch wood slow pyrolysis products," *Energy and Fuels*, vol. 26,

no. 2, pp. 1275–1283, Feb. 2012, doi: 10.1021/ef2018836.

[32] H. Cong *et al.*, "Slow Pyrolysis Performance and Energy Balance of Corn Stover in Continuous Pyrolysis-Based Poly-Generation Systems," *Energy and Fuels*, vol. 32, no. 3, pp. 3743–3750, Mar. 2018, doi: 10.1021/acs.energyfuels.7b03175.

[33] A. K. Varma, L. S. Thakur, R. Shankar, and P. Mondal, "Pyrolysis of wood sawdust: Effects of process parameters on products yield and characterization of products," *Waste Manag.*, vol. 89, pp. 224–235, Apr. 2019, doi: 10.1016/j.wasman.2019.04.016.

[34] G. Pilon and J.-M. Lavoie, "CHARACTERIZATION OF SWITCHGRASS CHAR PRODUCED IN TORREFACTION AND PYROLYSIS CONDITIONS." Accessed: 06-May-2020. [Online]. Available: http://ojs.cnr.ncsu.edu/index.php/BioRes/article/view/BioRes_06_4_4824_Pilon_Lavoi_Switchgrass_Char_Torrefaction_Pyrolysis.

[35] T. S. Tanoh, A. Ait Oumeziane, J. Lemonon, F. J. Escudero Sanz, and S. Salvador, "Green Waste/Wood Pellet Pyrolysis in a Pilot-Scale Rotary Kiln: Effect of Temperature on Product Distribution and Characteristics," *Energy & Fuels*, vol. 34, no. 3, pp. 3336–3345, Mar. 2020, doi: 10.1021/acs.energyfuels.9b04365.

[36] Y. Yu, Y. W. Chua, and H. Wu, "Characterization of Pyrolytic Sugars in Bio-Oil Produced from Biomass Fast Pyrolysis," *Energy and Fuels*, vol. 30, no. 5, pp. 4145–4149, May 2016, doi: 10.1021/acs.energyfuels.6b00464.

[37] J. Zhang, H. Toghiani, D. Mohan, C. U. Pittman, and R. K. Toghiani, "Product analysis and thermodynamic simulations from the pyrolysis of several biomass feedstocks," *Energy and Fuels*, vol. 21, no. 4, pp. 2373–2385, Jul. 2007, doi: 10.1021/ef0606557.

[38] W. J. DeSisto *et al.*, "Fast pyrolysis of pine sawdust in a fluidized-bed reactor," in *Energy and Fuels*, 2010, vol. 24, no. 4, pp. 2642–2651, doi: 10.1021/ef901120h.

[39] L. Ingram *et al.*, "Pyrolysis of wood and bark in an auger reactor: Physical properties and chemical analysis of the produced bio-oils," *Energy and Fuels*, vol. 22, no. 1, pp. 614–625, Jan. 2008, doi: 10.1021/ef700335k.

[40] K. Sipilä, E. Kuoppala, L. Fagernäs, and A. Oasmaa, "Characterization of biomass-based flash pyrolysis oils," *Biomass and Bioenergy*, vol. 14, no. 2, pp. 103–113, Mar. 1998, doi: 10.1016/S0961-9534(97)10024-1.

[41] S. Czernik, D. K. Johnson, and S. Black, "Stability of wood fast pyrolysis oil," *Biomass and Bioenergy*, vol. 7, no. 1–6, pp. 187–192, Jan. 1994, doi: 10.1016/0961-9534(94)00058-2.

[42] R. Maggi and B. Delmon, "Comparison between 'slow' and 'flash' pyrolysis oils from biomass," *Fuel*, vol. 73, no. 5, pp. 671–677, May 1994, doi: 10.1016/0016-2361(94)90007-8.

[43] T. Ba, A. Chaala, M. Garcia-Perez, and C. Roy, "Colloidal properties of bio-oils obtained by vacuum pyrolysis of softwood bark. Storage stability," *Energy and Fuels*, vol. 18, no. 1, pp. 188–201, Jan. 2004, doi: 10.1021/ef0301250.

[44] D. Meier and O. Faix, "State of the art of applied fast pyrolysis of lignocellulosic materials - A review," *Bioresource Technology*, vol. 68, no. 1. Elsevier Sci Ltd, pp. 71–77, 01-Apr-1999, doi: 10.1016/S0960-8524(98)00086-8.

[45] C. A. Mullen, A. A. Boateng, K. B. Hicks, N. M. Goldberg, and R. A. Moreau, "Analysis and comparison of bio-oil produced by fast pyrolysis from three barley biomass/byproduct streams," in *Energy and Fuels*, 2010, vol. 24, no. 1, pp. 699–706, doi: 10.1021/ef900912s.

[46] P. D. Muley, C. Henkel, K. K. Abdollahi, C. Marculescu, and D. Boldor, "A critical comparison of pyrolysis of cellulose, lignin, and pine sawdust using an induction heating reactor," *Energy Convers. Manag.*, vol. 117, pp. 273–280, Jun. 2016, doi: 10.1016/j.enconman.2016.03.041.

[47] K. Atsonios, K. D. Panopoulos, A. V Bridgwater, and E. Kakaras, "Biomass fast pyrolysis energy balance of a 1kg/h test rig," *Int. J. Thermodyn.*, vol. 18, no. 4, p. 267, Dec. 2015, doi: 10.5541/ijot.5000147483.

[48] C. Dou, D. S. Chandler, F. L. P. Resende, and R. Bura, "Fast Pyrolysis of Short Rotation Coppice Poplar: An Investigation in Thermochemical Conversion of a Realistic Feedstock for the Biorefinery," *ACS Sustain. Chem. Eng.*, vol. 5, no. 8, pp. 6746–6755, Aug. 2017, doi: 10.1021/acssuschemeng.7b01000.

[49] S. S. Liaw, V. H. Perez, R. J. M. Westerhof, G. F. David, C. Frear, and M. Garcia-Perez, "Biomethane Production from Pyrolytic Aqueous Phase: Biomass Acid Washing and Condensation Temperature Effect on the Bio-oil and Aqueous Phase Composition," *Bioenergy Res.*, pp. 1–9, Feb. 2020, doi: 10.1007/s12155-020-10100-3.

[50] X. Fu, Q. Li, and C. Hu, "Identification and structural characterization of oligomers formed from the pyrolysis of biomass," 2019, doi: 10.1016/j.jaap.2019.104696.

[51] A. Martinez, M. E. Rodriguez, S. W. York, J. F. Preston, and L. O. Ingram, "Use of UV Absorbance To Monitor Furans in Dilute Acid Hydrolysates of Biomass," *Biotechnol. Prog.*, vol. 16, no. 4, pp. 637–641, Aug. 2000, doi: 10.1021/bp0000508.

[52] C. Torri, E. Soragni, S. Prati, and D. Fabbri, "Py-SPME-GC-MS with on-fiber derivatization as a new solvent-less technique for the study of polar

macromolecules: Application to natural gums," *Microchem. J.*, vol. 110, pp. 719–725, Sep. 2013, doi: 10.1016/j.microc.2013.08.006.

[53] D. Fabbri, G. Chiavari, S. Prati, I. Vassura, and M. Vangelista, "Gas chromatography/mass spectrometric characterisation of pyrolysis/silylation products of glucose and cellulose," *Rapid Commun. Mass Spectrom.*, vol. 16, no. 24, pp. 2349–2355, Dec. 2002, doi: 10.1002/rcm.856.

[54] M. B. Figueirêdo, R. H. Venderbosch, H. J. Heeres, and P. J. Deuss, "In-depth structural characterization of the lignin fraction of a pine-derived pyrolysis oil," *J. Anal. Appl. Pyrolysis*, vol. 149, p. 104837, Aug. 2020, doi: 10.1016/j.jaap.2020.104837.

[55] K. I. Kuroda, "Pyrolysis-trimethylsilylation analysis of lignin: Preferential formation of cinnamyl alcohol derivatives," *J. Anal. Appl. Pyrolysis*, vol. 56, no. 1, pp. 79–87, 2000, doi: 10.1016/S0165-2370(00)00085-1.

[56] M. O. Fagbohungbe *et al.*, "The challenges of anaerobic digestion and the role of biochar in optimizing anaerobic digestion," *Waste Management*, vol. 61. Elsevier Ltd, pp. 236–249, 01-Mar-2017, doi: 10.1016/j.wasman.2016.11.028.

[57] J. Pan, J. Ma, L. Zhai, T. Luo, Z. Mei, and H. Liu, "Achievements of biochar application for enhanced anaerobic digestion: A review," *Bioresource Technology*, vol. 292. Elsevier Ltd, p. 122058, 01-Nov-2019, doi: 10.1016/j.biortech.2019.122058.